Regulation, transport aspects and degeneration of penicillin biosynthesis in *Penicillium chrysogenum*

Rutger Douma

Regulation, transport aspects and degeneration of penicillin biosynthesis in *Penicillium chrysogenum*

Proefschrift

ter verkrijging van de graad van doctor
aan de Technische Universiteit Delft
op gezag van Rector Magnificus prof.ir. K.C.A.M Luyben,
voorzitter van het College voor Promoties
in het openbaar te verdedigen op dinsdag 14 december 2010 om 10:00 uur

door

Rutger Dirk DOUMA

ingenieur in de biotechnologie
geboren te Sittard

Dit proefschrift is goedgekeurd door de promotor:
Prof.dr.ir. J.J. Heijnen

Copromotor: Dr. W.M. van Gulik

Samenstelling promotiecommissie:

Rector Magnificus	voorzitter
Prof. dr. ir. J.J. Heijnen	Technische Universiteit Delft, promotor
Dr. W.M. van Gulik	Technische Universiteit Delft, copromotor
Prof. dr. C. Wittmann	Technische Universität Braunschweig, Germany
Prof. dr. I.J. van der Klei	Rijksuniversiteit Groningen
Prof. dr. A.J.M. Driessen	Rijksuniversiteit Groningen
Prof. dr. J.T. Pronk	Technische Universiteit Delft
Dr. ir. W.A. van Winden	DSM Biotechnology Center, Delft
Prof. dr. J.H. de Winde	Technische Universiteit Delft, reservelid

This project is financially supported by the Netherlands Ministry of Economic Affairs and the B-Basic partner organizations (www.b-basic.nl) through B-Basic, a public private NWO-ACTS programme (ACTS: Advanced Chemical Technologies for Sustainability). This project was carried out within the research programme of the Kluyver Centre for Genomics of Industrial Fermentation which is part of the Netherlands Genomics Initiative / Netherlands Organization for Scientific Research.

Cover design by Joris Schaap.

Summary

Penicillin has been produced on an industrial scale for several decades. The improvements in its production process, in terms of product yields and production rates, present an unprecedented success in fermentation technology. However, the obtained product yields still remain far from their theoretical maximum. More insight in the regulation of the penicillin biosynthesis pathway and connected central metabolic pathways, as well as in the mechanisms of penicillin and side chain precursor transport, which are still incompletely understood, could provide leads for further improvement. As has been observed for other high producing organisms, industrial *Penicillium chrysogenum* strains appear to loose their high productivity in extended fermentations (degeneration), making the implementation of a continuous fermentation process impossible. The recent sequencing of its genome and advancements in analytical techniques enable researchers to get more insights in these issues using a systems biology approach, which is the topic of this thesis.

In general there is a relation between the rate of product formation of a micro organism and its growth rate under substrate limiting conditions. In case of catabolic products, that is, compounds which are an end product of a catabolic pathway, e.g. alcohol as an end product of the fermentation of sugars, the rate of product formation is proportional to the growth rate. If product formation is not coupled to catabolism, any relation between growth and product formation may exist. Such a non-linear relation has also been determined for penicillin production in *P. chrysogenum*. However, if such a relation is determined under certain specific cultivation conditions, e.g. in steady state chemostat cultures, it does not automatically hold under dynamical (non steady state) conditions, e.g. in a fed-batch cultivation were the growth rate changes in time. To be able to describe the relation between growth and penicillin production under different (steady state as well as dynamic) conditions a mathematical model is required in which the genetic regulation of enzymes levels of the penicillin biosynthesis pathway is taken into account. In **Chapter 2** an analysis is performed of enzyme activities in the penicillin production pathway at different growth rates which indicated that IPNS has a rate-limiting role for penicillin production. A model based on the regulation of the gene encoding for such a rate-limiting enzyme in the

penicillin pathway, describing the dynamics of penicillin production from gene to flux, was developed and showed a significantly improved description of the specific production rate during steady state and dynamic phases of penicillin fermentations.

In general, not only enzyme levels but also intracellular penicillin pathway metabolites and transport steps can control productivity. To study these aspects an accurate method is needed to measure intracellular metabolite levels. The traditional cold methanol quenching method with subsequent washing by centrifugation was found to be inappropriate to measure intracellular penicillin and phenylacetic acid levels, because their extracellular amount was too high. In **chapter 3** the development of a new sample quenching and filtration based washing method for quantification of intracellular metabolites was described. This method was found to have a superior washing efficiency compared with the standard centrifugation based washing method, making it possible to measure intracellular levels of metabolites which are extracellularly abundant. Such measurements are especially useful in transport studies. The method was validated by successfully measuring the intracellular levels of metabolites related to penicillin biosynthesis, including the transported PAA and PenG metabolites.

Chapter 4 describes the successful application of the method developed in **chapter 3**, in a study on transport mechanisms and transport kinetics of phenylacetic acids (PAA) and penicillin-G (PenG) in *P. chrysogenum*. PAA was found to be taken up rapidly by passive diffusion and simultaneously exported by an energy consuming ABC transporter. The PenG anion was found to be reversibly transported over the cell membrane by a facilitated transporter, driven by the negative electrochemical potential difference. The estimate capacity of the PenG transporter was found to be larger than the penicillin flux, but not much larger.

It has been observed that upon prolonged cultivation, *P. chrysogenum* gradually looses its capacity to produce penicillin. This phenomenon, called degeneration, was studied in ethanol limited chemostats at a systems level (from gene to flux), of which the results are presented in **chapter 5**. Degeneration was found to be a reproducible phenomenon leading to a 10-fold reduction in the biomass specific penicillin production rate after about 30 generations of growth in chemostat culture. No indications were found that the observed massive decrease in penicillin production was caused by a decrease in the number of copies of the penicillin gene cluster, a decrease in the number of peroxisomes (in which part of the penicillin pathway is located) or changes in metabolite levels in central metabolism. The

expression levels of genes related to sulfur and nitrogen metabolism decreased significantly during degeneration, which corresponds with the decreased demand for the precursor amino acids cysteine and valine. Also energy charge and changed concentrations of penicillin pathway precursors (valine, cysteine, α-aminoadipic acid and PAA) could be ruled out as causes for degeneration. In contrast, the enzyme amounts of IPNS and ACVS and the transport PenG capacity decreased significantly and the IPNS amount and PenG export capacity correlated well with the decrease in the specific penicillin production rate, which is in agreement with the results from **chapter 2**. This indicates that degeneration is due to decreased amount of penicillin pathway related protein levels (enzymes, transporters). The reason of this decrease is most probably a changed regulation (translation efficiency, post-translational modification efficiency) and/or a higher protein degradation rate of these penicillin pathway enzymes.

Samenvatting

Penicilline wordt al een aantal decennia op industriële schaal geproduceerd. De verbeteringen in het productieproces van penicilline, in termen van productierendement en productiesnelheid, zijn een ongekend succes in de fermentatietechnologie. Het verkregen productierendement blijft echter nog ver verwijderd van het theoretische maximum. Meer inzicht in zowel de regulatie van de metabole route van penicillineproductie en de aangesloten centrale metabole routes, als in de mechanismen van penicilline- en zijketenprecursortransport, waarvan het mechanisme nog steeds niet compleet bekend is, zou aanknopingspunten kunnen bieden voor toekomstige verbeteringen. Zoals is waargenomen bij andere hoog producerende organismen lijken industriële *Penicillium chrysogenum* stammen na verloop van tijd hun hoge productiviteit te verliezen in lange fermentaties, wat degeneratie wordt genoemd. Dit zorgt ervoor dat penicilline niet in continucultures geproduceerd kan worden. De recente sequentiebepaling van het genoom en de vooruitgang in analytische technieken stellen onderzoekers in staat om meer inzicht te

krijgen in deze zaken via een systeembiologische benadering, wat het onderwerp van dit proefschrift is.

In het algemeen is er onder substraat beperkte condities een relatie tussen de productvormingssnelheid van een micro-organisme en zijn groeisnelheid. In het geval van katabole producten - dat wil zeggen stoffen die een eindproduct van een katabole route zijn, zoals alcohol als een eindproduct van de fermentatie van suikers - is er een lineaire relatie tussen de productvormingssnelheid en de groeisnelheid. Als productvorming niet gekoppeld is aan katabolisme, kan elke non-lineaire relatie tussen groei en productvorming bestaan. Zo'n niet-lineaire relatie is ook bepaald voor penicillineproductie in *P. chrysogenum*. Als een dergelijke relatie echter bepaald wordt onder specifieke groeicondities, bijvoorbeeld in steady state chemostaat culturen, betekent het niet dat deze ook toepasbaar is onder dynamische (non-steady state) groeicondities, zoals fed-batch processen waarin de groeisnelheid verandert in de tijd. Om de relatie tussen groei en penicillineproductie te kunnen beschrijven onder verschillende (steady state en dynamische) omstandigheden, is een wiskundig model nodig, waarin rekening wordt gehouden met genetische regulatie van enzymniveaus in de penicilline biosyntheseroute. In **hoofdstuk 2** wordt een analyse uitgevoerd van enzymactiviteiten in de penicilline biosyntheseroute tijdens verschillende groeisnelheden, waaruit bleek dat IPNS een beperkende rol speelt voor penicillineproductie. Een model gebaseerd op de regulatie van het gen dat codeert voor een dergelijk snelheidsbeperkend enzym in de penicilline biosyntheseroute, waarmee de dynamiek van penicillineproductie van gen tot flux wordt bepaald, is ontwikkeld en toonde een significant verbeterde beschrijving van de specifieke productvormingssnelheid in steady state en dynamische fasen van penicillinefermentaties.

In het algemeen kunnen niet alleen enzymniveaus de productiviteit bepalen, maar ook intracellulaire metabolieten in de metabole route van penicillineproductie en transportstappen. Om deze aspecten te bestuderen is een nauwkeurige methode nodig om intracellulaire metabolietniveaus te meten. De traditionele methode waarin met koude methanol het metabolisme stilgelegd wordt en daaropvolgend de cellen gewassen worden met centrifugatie bleek ongeschikt om intracellulair penicilline en fenylazijnzuur te meten, omdat hun extracellulaire hoeveelheden te hoog waren. In **hoofdstuk 3** wordt de ontwikkeling van een nieuwe methode beschreven om de intracellulaire metabolietniveaus te bepalen waarin gelijktijdig het metabolisme stil wordt gelegd en de cellen gewassen worden middels filtratie. Deze methode bleek een superieur wasrendement te hebben vergeleken met de standaard wasmethode gebaseerd op centrifugatie. Dit maakt het

mogelijk om intracellulaire metabolietniveaus te meten die extracellulair in overvloed aanwezig zijn. Dit soort metingen is vooral nuttig voor transportstudies. De methode werd gevalideerd door de intracellulaire metabolietniveaus in de penicilline biosyntheseroute succesvol te meten, inclusief PAA en PenG, stoffen die onderhevig zijn aan transport.

In **hoofdstuk 4** wordt een succesvolle toepassing van de ontwikkelde methode uit **hoofdstuk 3** beschreven in een studie naar transportmechanismen en –kinetiek van fenylazijnzuur (PAA) en penicilline-G (PenG) in *P. chrysogenum*. PAA werd snel opgenomen door passieve diffusie en tegelijkertijd geëxporteerd door een energie consumerende ABC transporter. Het anion van PenG werd reversibel over het membraan getransporteerd door een gefaciliteerde transporter, gedreven door het negatieve electrochemische potentiaalverschil. De geschatte capaciteit van het PenG transport was groter dan de penicillineflux, maar niet veel groter.

Het is waargenomen dat bij langdurige kweek *P. chrysogenum* geleidelijk aan zijn capaciteit verliest om penicilline te produceren. Dit fenomeen, dat degeneratie genoemd wordt, is bestudeerd in ethanol gelimiteerde chemostaten op systeemniveau (van gen tot flux). De resultaten hiervan worden gepresenteerd in **hoofdstuk 5**. Degeneratie bleek een reproduceerbaar fenomeen dat leidt tot een 10-voudige afname van de biomassa specifieke penicillineproductiesnelheid na ongeveer 30 generaties van groei in chemostaatcultuur. Er werden geen aanwijzingen gevonden dat de waargenomen sterke daling van de penicillineproductie werd veroorzaakt door een daling van het aantal penicilline genclusters of een daling van het aantal peroxisomen (waarin de penicillineroute gedeeltelijk plaatsvindt) of door veranderingen in de metabolietniveaus in het centrale metabolisme. De expressieniveaus van genen betrokken bij zwavel- en stikstofmetabolisme daalden aanzienlijk tijdens degeneratie, wat correspondeert met de verminderde vraag naar de precursoraminozuren cysteïne en valine. De energielading en veranderde concentraties van penicillineroute precursors (valine, cysteïne, α-aminoadipinezuur en PAA) konden worden uitgesloten als oorzaken voor degeneratie. De enzymhoeveelheden van IPNS, ACVS en de transportcapaciteit van PenG daalden echter aanzienlijk en dezen correleerden goed met de daling in de specifieke penicillineproductiesnelheid, wat in overeenstemming is met de resultaten uit **hoofdstuk 2**. Dit duidt erop dat degeneratie het gevolg is van verminderde penicillineroute gerelateerde eiwitniveaus (enzymen, transporters). De reden van deze daling ligt vermoedelijk in de veranderde regulatie (translatie-efficiëntie, post-translationele modificatie-efficiëntie) en/of een verhoogde afbraaksnelheid van deze penicillineroute enzymen.

Table of contents

List of abbreviations

The following abbreviations have been used throughout this thesis.

2PG	2-phosphoglycerate
3PG	3-phosphoglycerate
6-APA	6-aminopenicillanic acid
6PG	6-phosphogluconate
8-HPA	8-hydroxypenicillic acid
AAA	L-α -aminoadipic acid
AcCoA	acetyl-Coenzyme A
ActAld	Acetaldehyde
ACV	L-α-(δ-aminoadipyl)-L-α-cystenyl-D-α-valine
ACVS	L-α-(δ-aminoadipyl)-L-α -cystenyl-D-α-valine synthetase
ADP	adenosine diposphate
Ala	L-Alanine
Alfa-KG	α-ketogluterate
AMP	adenosine monoposphate
Arg	L-Arginine
Asp	L-Aspartic acid
Asn	L-Asparagine
AT	acyl coenzyme A: Isopenicillin-N acyltransferase
ATP	adenosine triposphate
Cys	L-cysteine
DHAP	dihydroxyacetone phosphate
E4P	erythrose-4-phosphate
F6P	fructose-6-phosphate
FAD(H)	flavin adenine dinucleotide
FBP	fructose-1,6-bisphophate
G1P	glucose-1-phosphate
G3P	glycerol-3-phosphate

G6P	glucose-6-phosphate
GAP	glyceraldehyde-3-phosphate
Gln	L-Glutamine
Glu	L-Glutamic acid
Gly	Glycine
His	L-Histidine
Ile	L-Isoleucine
IPN	isopenicillin-N
IPNS	isopenicillin-N synthase
Leu	L-Leucine
Lys	L-Lysine
M1P	mannose-1-phophate
M6P	mannose-6-phosphate
Met	L-Methionine
NAD(H)	nicotinamide dinucleotide
NADP(H)	nicotinamide dinucleotide phosphate
o-OH-PAA	ortho-hydroxyphenylacetic acid
OPC	6-oxopiperidine-2-carboxylic acid
PEP	phosphoenolpyruvate
PenG	penicillin-G
Phe	L-Phenylalanine
Pi	phosphate
PIO	penicilloic acid
Pro	L-Proline
R5P	ribose-5-phosphate
Ru5P	ribulose-5-phosphate
S7P	sedoheptulose-7-phosphate
Ser	L-Serine
SucCoA	Succinyl-CoA
T6P	trehalose-6-phosphate
Thr	L-Threonine
Trp	L-Tryptophan
Tyr	L-Tyrosine
UDP-G	Uridine Diphosphate-glucose
X5P	xylulose-5-phosphate
Val	L-valine

CHAPTER 1

General introduction

History of penicillin production

In 1928 Alexander Fleming set a number of *Staphylococcus* culture-plates aside and noticed that around a contaminating mold a halo of lyzed cells was formed (Fleming, 1928). Although this contamination was by accident and not in the interest of his work, Fleming recognized the potential of the antimicrobial agent produced by this mold. The mold was later identified as *Penicillium notatum* and the antimicrobial agent was named penicillin (Clutterbuck et al., 1932).

Fleming continued to work on penicillin for a while, but found it difficult to extract the compound in sufficient quantities and had problems with the compound's stability. For about a decade Fleming's work remained relatively unknown outside of his own group and was rather seen as a scientific curiosity than a scientific breakthrough (Nielsen, 1997).

About a decade later Howard Florey and Ernst Chain recommenced working on penicillin. A newly developed extraction procedure enabled them to extract enough penicillin to perform clinical trials on mice, which showed positive results (Chain et al., 1940). In 1941 the first dose on a human was administered showing that the antibiotic could cure infectious diseases (Abraham et al., 1941). The outbreak of the Second World War with its many victims proved to be a catalyst for the further development of an industrial production process for penicillin.

In 1941 Florey and Heatley went to the United States to evoke interest from industrial parties to produce penicillin on large scale. However, many companies felt hesitant to develop a fermentative production process for penicillin, because they feared that the chemical structure of penicillin would soon be elucidated and a chemical production process would outcompete a fermentative process. Still Merck & Co., E.R. Squibb & Sons, Chas. Pfizer & Co and Abbott Laboratories picked up the challenge and started work on the development of an industrial production process of penicillin. In 1944 Pfizer was the first to open a commercial production plant (Nielsen, 1997). Further research on cultivation methods was performed in the Northern Regional Research Laboratory in Peoria, Illinois (Moyer and Coghill, 1946a; Moyer and Coghill, 1946b; Moyer and Coghill, 1947).

Although under German occupation, also in the Netherlands a group of scientists at the Nederlandsche Gist- en Spritusfabriek (NG&FS, Netherlands Yeast and Spirit factory, renamed Gist-Brocades in 1968 and currently part of DSM) secretly worked on the

development of an industrial penicillin production during the Second World War. This work was complicated by the severely restricted conditions during wartime, but nevertheless NG&FS managed to introduce penicillin on the market by January 1946 and by 1948 the production met the total demands of the Dutch market (Burns and van Dijck, 2002). Research on penicillin production is continued at the site in Delft by DSM up to date.

Although initially only administered to soldiers, penicillin soon became a standard cure for infectious diseases, saving millions of lives worldwide and is probably the most successful drug development up to date. While Fleming was not the first to observe antimicrobial activity of microbiologically produced substances, he was the first to recognize their potential, a feat for which he later was awarded the Nobel price for medicine in 1945 together with Chain and Florey.

Strain and process development

Strain

Fleming's original isolate was a *P. notatum* strain with a maximal production of 1-2 mg/L, which is too low for commercial production. During World War 2 the Army Transport Command initiated a worldwide quest for better producing *Penicillium* strains. A particularly high penicillin producing *P. chrysogenum* strain was isolated from a cantaloupe from a local market in Peoria, Illinois (Raper et al., 1944; Nielsen, 1997). This strain, named *P. chrysogenum* NRRL 1951, is the parent strain of all worldwide industrially used *P. chrysogenum* strains nowadays (Raper et al., 1944; van den Berg et al., 2008).

The University of Wisconsin, Madison initiated a strain improvement program on *P. chrysogenum* NRRL 1951 based on random mutagenesis (by radiation or chemical agents) and selection for better producing strains. A famous strain of this program was *P. chrysogenum* Wisc. 54-1255, with a greatly improved penicillin yield (Elander, 1983). Several commercial companies initiated their own programs to improve product yields and strain properties like robustness and morphology for industrial fermentation (Lein, 1986).

Although strain development by random mutagenesis and selection proved to be a powerful tool, it also has disadvantages. As implied by the term, the mutagenesis has a random nature and will also bring undesired genetic modifications. Furthermore it led to an undefined genome with multiple gene copies. From the 80's of the previous century

onwards penicillin yields have also been improved by DNA modification techniques (Miller and Ingolia, 1989; Veenstra et al., 1991; Martin, 1992).

Degeneration

With the greatly improved penicillin production by evolved strains new challenges on strain development arise. Already in 1932 Clutterbuck noticed that penicillin yields reduced upon subcultivation of penicillin producing strain (Clutterbuck et al., 1932). It is known that a lot of extra metabolic energy consumption is associated with penicillin production (van Gulik et al., 2001) and cells producing less penicillin easily outcompete cells which produce penicillin. Therefore, the phenomenon of reduced penicillin yields upon extended cultivation or transfer, called degeneration, becomes even more apparent in industrial high penicillin producing strains, where non-producers have an even higher competitive advantage over highly producing cells (Righelato, 1976; Christensen et al., 1995; van Gulik et al., 2000). Degeneration is very ill-understood and has a major consequence that a continuous production process, which has great economic advantages for a bulk product such as penicillin, is not possible.

Process

Until the 1940's the only industrial fermentative production processes were anaerobic like the acetone butanol ethanol (ABE) process and ethanol fermentations. Penicillin production, which is an aerobic process, poses major challenges in oxygen supply and sterility. Throughout the years oxygen supply and nutrient requirements were studied and optimized (Lein, 1986), leading to the fed-batch cultivation under glucose limited conditions because a continuous production process is prohibited by the above mentioned degeneration phenomenon.

With improvements in calculating power by computers, mathematical models were developed from the 1970's onwards to identify targets to further improve production yields (Heijnen et al., 1979; Bajpai and Reuss, 1980; Bajpai and Reuss, 1981). These models were black-box kinetic models based on balancing methods and on conservation of elements and energy. Application and validation of these models have shown that rationally designing feed schemes can improve product yields considerably (Heijnen et al., 1979; Bajpai and Reuss, 1981).

In fed-batch processes the production was improved by aiming at high cell density conditions. Together with the improvement of the strain this led to drastic economic

improvement of the overall process. The current final penicillin concentration in industrial production is estimated to be 50 g/L (Nielsen, 1997), which is an unprecedented improvement of microbial production of commercially interesting compounds. Lessons learned from the development of this process are nowadays applied on improvement of other fermentative production processes.

Microorganism

Penicillium chrysogenum is a genus of filamentous fungi belonging to the division of ascomycota. Filamentous fungi are multicellular and grow in hyphae. It is known there is a relation between penicillin production and morphology. While *P. chrysogenum* strains early on in the lineage form long unbranched hyphae, high producing strains are highly branched and penicillin is believed to be produced in subapical cells, the cells after the tip (Zangirolami et al., 1997).

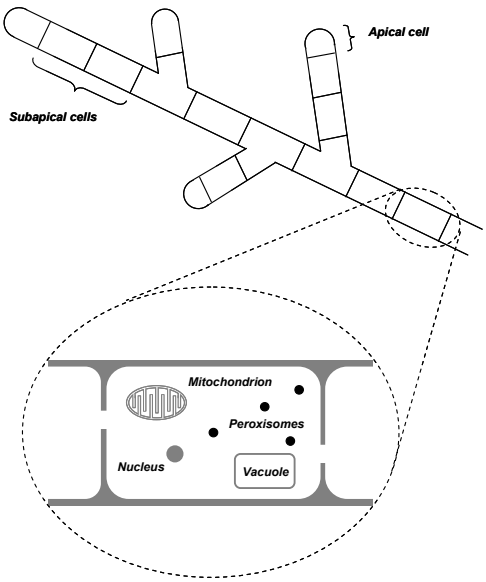

Figure 1.1 Schematic overview of a hypha and a single cell and its components.

Being a eukaryote, *P. chrysogenum* is highly compartmentalized as shown in figure 1.1. Substrates are taken up into the cytosol and metabolites are trafficking among the different compartments. Most oxidative steps in metabolism take place in mitochondria, making them the primary compartment for energy supply. Vacuoles are versatile organelles,

involved in many aspects of protein turnover, cellular homeostasis, membrane trafficking, signaling and nutrition (Veses et al., 2008). Peroxisomes are small microbodies which mainly serve to detoxify the organism by removing reactive oxygen species (van der Klei and Veenhuis, 2002).

Penicillium chrysogenum DS17690 is a high producing strain which has been developed by Gist-Brocades, recently part of DSM, and used for industrial scale penicillin production in the 1980's. This strain was used for the work presented in this thesis. It is a direct continued cultivation strain of *Penicillium chrysogenum* DS12975 (van Gulik et al., 2000; van Gulik et al., 2001; Thykaer et al., 2008). This strain has been extensively used for research on industrial penicillin production over the last decade (Kleijn et al., 2006; Nasution et al., 2008; van den Berg et al., 2008; Harris et al., 2009; Kiel et al., 2009).

As a result of the strain improvement program *Penicillium chrysogenum* DS17690 contains multiple copies of various genes. Most notably it contains 10-12 copies of the penicillin gene cluster (personal communication, DSM). The penicillin gene cluster is the set of genes which codes for the enzymes needed to produce penicillin (Fierro et al., 1995).

Metabolism

Penicillin pathway

In the 1980's the production pathway of penicillin was elucidated (figure 1.2). The first step is the condensation of the three precursor amino acids AAA, Val and Cys into the tripeptide ACV by the non-ribosomal protein complex ACVS. ACV can be oxidized into bis-ACV, which can be reduced back into ACV consuming 1 molecule of NADPH (Theilgaard and Nielsen, 1999). The enzyme IPNS catalyzes the oxidative ring closure of ACV into IPN consuming 3 molecules of ATP. Another enzyme is the carboxylic acid-CoA ligase which converts imported PAA in their CoA-ester. These CoA esters are used by acyl-CoA transferase (AT) to convert IPN into PenG in the peroxisomes. AT is a promiscuous enzyme; when phenylacetic acid (PAA) is added to the cultivation medium PenG is produced, but addition of phenoxyacetic acid results in PenV production. Next to the mentioned intermediates, several byproducts are formed in PenG biosynthesis; OPC, bis-ACV, 8-HPA, PIO and o-OH-PAA. The genes *pcbAB* (coding for ACVS), *pcbC* (coding for IPNS) and *pcbD* (coding for AT) make up the penicillin gene cluster (Fierro et al., 1995). The gene for the transporter of PenG is not known.

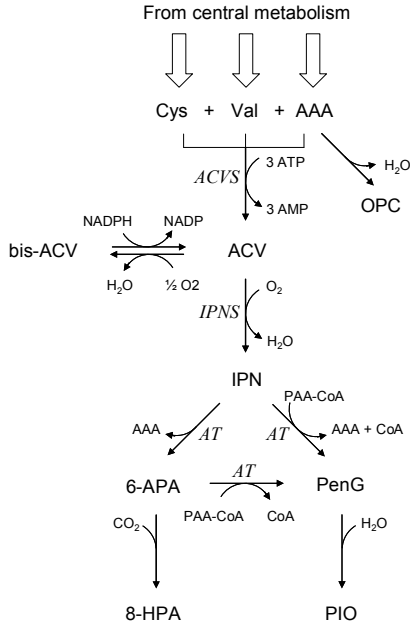

Figure 1.2 Penicillin pathway. Enzyme names catalyzing the reactions are indicated next to the reaction arrows.

Central carbon and amino acid metabolism

Central carbon metabolism and amino acid metabolism of *P. chrysogenum* is schematically depicted in figure 1.3. When cultivated on glucose, the glycolysis is used for production of pyruvate, ATP and NADH. Pyruvate is further oxidized in the TCA cycle towards carbon dioxide, again yielding ATP and NADH. PenG production is associated with a significant extra ATP drain, making ATP synthesis a potential bottleneck for PenG production (van Gulik et al., 2001). Production of cysteine, one of the precursor amino acids for penicillin production, requires for SO_4^{2-} reduction large quantities of NADPH, which is mainly produced in the pentose phosphate pathway. Efficient penicillin production requires a considerable part of the glucose to be channeled into the pentose phosphate pathway (Kleijn et al., 2007). Some intermediates of glycolysis and the TCA cycle, Pyr, alfa-KG and Oxaloacetate are used to produce the amino acid precursors for penicillin production, Val, AAA and Cys respectively. Furthermore many intermediates of glycolysis and the TCA cycle are necessary to produce biomass. When ethanol is used as sole carbon source, carbon enters central metabolism via AcCoA. In this case gluconeogenesis is necessary to supply glycolytic intermediates for biomass, penicillin and amino acid production.

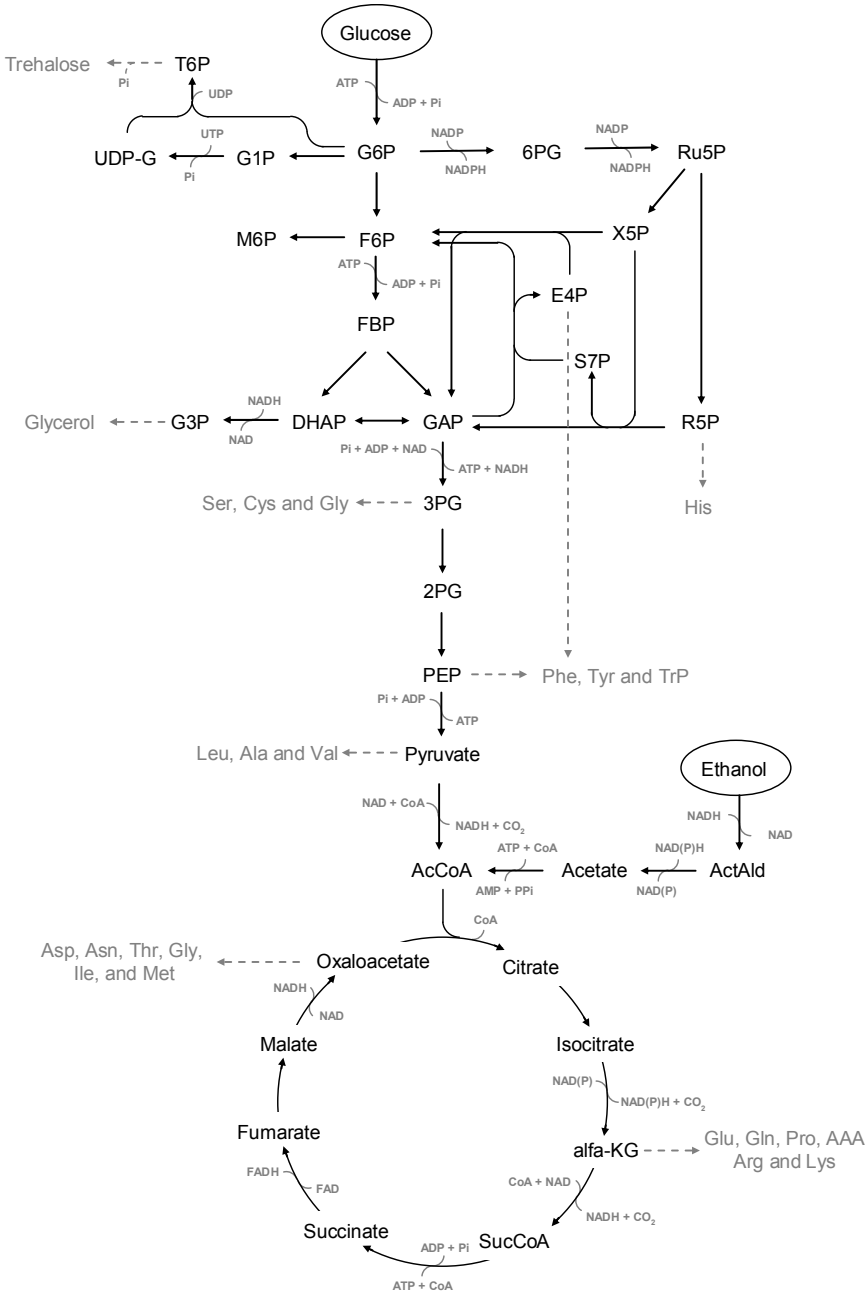

Figure 1.3 Central carbon and amino acid metabolism. Dashed grey lines indicate pathways towards amino acids from central carbon metabolism precursors. Carbon substrates used in this thesis are encircled.

The increased knowledge on stoichiometry enabled the development of stoichiometric models allowing flux analysis. These types of models are based on the conservation of mass in a defined stoichiometric network and were explained previously (Savinell and Palsson, 1992; Vallino and Stephanopoulos, 1993; van Gulik and Heijnen, 1995). Flux and metabolite analysis in an industrial high producing *P. chrysogenum* strain showed that central carbon metabolism is not likely to contain bottlenecks for penicillin production, because for the same biomass specific penicillin production rate q_p, with ethanol or glucose as sole limiting carbon source, very different amino acids metabolite levels, including the pen pathway precursors Val, Cys and AAA, were measured (Nasution, 2007). Supply of NADPH and ATP more likely seems to be a bottleneck for penicillin production (van Gulik et al., 2000).

Transport

Important and possibly rate-limiting steps in penicillin production are formed by transport processes. Compounds which are supplied to the cultivation medium have to be imported into the cell. The transport mechanism of many substrates has been elucidated over the years and are reviewed for filamentous fungi (Burgstaller, 1997) and *Saccharomyces cerevisiae* (van der Rest et al., 1995) amongst others. Specific studies with *Penicillium chrysogenum* showed that sulfate is taken up with symport of two protons (Hillenga et al., 1996b) and that the basic amino acid permease is a H^+ symporter (Hillenga et al., 1996a). However, the transport mechanism of some important compounds is still under debate or unknown. Prominent examples are the transport mechanism of the precursor PAA (Fernández-Cañón et al., 1989b; Fernández-Cañón et al., 1989a; Martínez-Blanco et al., 1989; Tan et al., 1993; Hillenga et al., 1995) and the product PenG (Andrade et al., 2000; van den Berg et al., 2001a; Martín et al., 2005).

Biological systems

DNA sequencing and developments in transcriptome and proteome analysis

An organism's hereditary information is located in its DNA, which contains all genes necessary for the development and functioning of the organism. Genes are transcribed to produce mRNA, which subsequently can be translated into proteins. These different levels are respectively called genome, transcriptome and proteome and are depicted in figure 1.4. Improved analytical techniques have enabled researchers to analyze the full chain from genome to metabolome and fluxome in recent years.

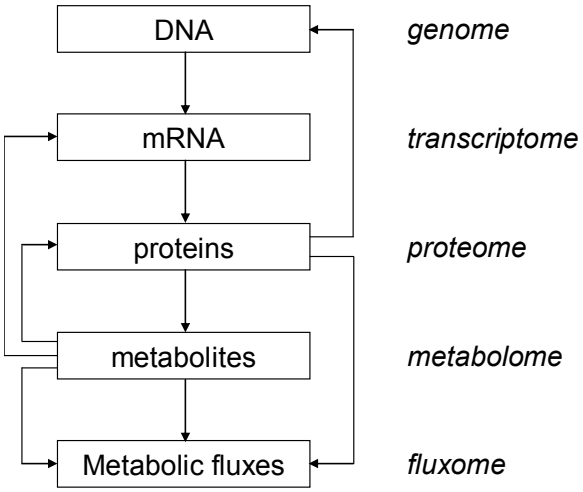

Figure 1.4 Hierarchical levels of control in biological systems.

The study of the genetic information in a cell, the genome, has taken a flight with the development of DNA sequencing techniques. The first fully sequenced genome was of *Haemophilus influenzae* (Fleischmann et al., 1995) and by 2003 the human genome project was finished. In the last decade the number of sequenced microbial genomes increased exponentially (Benson et al., 2009). In 2008 the genome of *P. chrysogenum* Wisc. 54-1255 was published (van den Berg et al., 2008).

Knowing the DNA sequence of *P. chrysogenum*, it became possible to study the mRNA transcribed in cells, the transcriptome. This development enabled researchers to get an understanding of how microorganisms react to their environment through genetic regulation. For *P. chrysogenum* several transcriptome studies have been performed in the recent years revealing genes which are upregulated under penicillin-producing conditions and candidate genes for transport proteins (van den Berg et al., 2008; Harris et al., 2009).

The DNA sequence can also be used to study the total amount of translated proteins in microorganisms, the proteome, using mass spectrometry (MS). Although it proved to be difficult to find reliable analysis techniques for proteome studies, recent developments in mass spectrometry allowed the first proteome studies on *P. chrysogenum* (Kiel et al., 2009; Jami et al., 2010).

Metabolome

Intracellular metabolites have a major impact on fluxes and regulation at metabolic and genetic levels (figure 1.4) and the study of metabolites is independent of knowing any kind of DNA sequence and has a longer history. Although gas chromatography (GC) and High-performance liquid chromatography (HPLC) techniques exist for a few decades, it proved difficult to determine very low (10^{-6} – 10^{-4} M) intracellular concentrations accurately. Furthermore the very fast turnover times (< 1 second) of central metabolite pools poses even more challenges for accurate quantification requiring special sampling/quenching methods. De Koning and Van Dam came with a breakthrough in metabolomics by developing a methodology to arrest metabolism while keeping cells intact, allowing washing by quenching them in cold (-40°C) aqueous methanol (De Koning and Van Dam, 1992). Integration of this quenching/washing technique with efficient extraction (Gonzalez et al., 1997; Canelas et al., 2009) and MS-based analysis (Mashego et al., 2005; Villas-Bôas et al., 2005b) allowed accurate intracellular metabolite determination. A recent metabolome study in *P. chrysogenum* revealed that with different intracellular concentrations of amino acid precursors for penicillin production (Cys, Val, AAA) the same biomass specific penicillin production rate can be achieved (Nasution et al., 2008). This shows that q_p mostly depends on other factors such as energy/redox supply and/or levels of enzymes/transporters, all of which are unknown at present.

The increased accuracy of MS-analysis revealed that during methanol quenching considerable amounts of metabolites leaked out of the cells, posing new challenges to find organism specific solutions to obtain accurate intracellular metabolite concentrations (Wittmann et al., 2004; Bolten et al., 2007; Canelas et al., 2008a; Taymaz-Nikerel et al., 2009). Furthermore, so far only metabolites which are predominantly intracellular were measured. For measurement of metabolites which also have large extracellular fractions such as PenG and PAA, washing of cells to discard these extracellular metabolites becomes very important.

Toward systems biology

With the improved understanding of the behavior of different –omics and their interrelation attempts have been made to come to a systems understanding of microbial cells. This new integrative field is usually referred to as systems biology (Kitano, 2002; Barrett et al., 2006). Although there are still many challenges ahead to get to a complete understanding of cellular processes, more and more of integrative –omics approaches are appearing (Ideker et al., 2001; Kresnowati et al., 2006).

Aim and outline of this thesis

The past strain development of *P. chrysogenum* was performed via random mutagenesis and selection. Current industrial strains have a tremendously increased penicillin production compared to Fleming's original isolate. Still, it is expected that yields of penicillin production can be improved (Nielsen, 1997; van Gulik et al., 2000). The above mentioned recent developments in analytical techniques allow a systems analysis of penicillin biosynthesis to identify possible genetic engineering targets to enhance production and especially to shed light on degeneration.

In **chapter 2** an experimental analysis of enzyme activities within the penicillin pathway was made under different conditions to trace whether any of these enzymes plays a rate-limiting role. Parameters for black box mathematical models derived from chemostat experiments are known to show discrepancies when applied on dynamic fed-batch fermentations due to large time constants (>> 10 hour) of changes in enzyme level. Results of the penicillin pathway enzyme activity assays were used to get an understanding of rate-limiting steps in the penicillin pathway and were used to construct a simple penicillin production mathematical model based on gene regulation of the rate limiting enzyme. Model parameters were derived from steady state and dynamic chemostat experiments and the model structure was validated by testing it on the dynamic start-up of chemostat runs and fed-batch fermentations.

Improved MS-based metabolite analysis and better sampling and sample processing techniques were developed recently to obtain more reliable intracellular metabolite concentrations (Canelas et al., 2008a). However, so far only metabolite concentrations of central carbon metabolism, nucleotides and amino acids were measured. Measurement of intracellular precursor substrate (PAA) and product (PenG) concentrations poses extra challenges, mainly on the efficiency of the absolute essential removal of extracellularly present metabolites, which are usually abundant for such precursors and products. In **chapter 3** a conventional washing method based on centrifugation is compared with a new one based on rapid cold filtration leading to a new method which allows accurate measurement of intracellular PAA and PenG concentrations, which can also be applied on other systems where efficient washing is required to discard extracellular metabolites.

A practical application of the developed sampling and sample processing method is given in **chapter 4**, in which the method is applied to study transport of PAA and PenG over the

plasma membrane in *P. chrysogenum*. This is done by performing stimulus response experiments at different time scales with PAA and PenG and analyzing the intracellular accumulation of those compounds and analyzing oxygen consumption to distinguish energy requirements for transport. Concentration ratios between intra- and extracellular PAA and PenG, together with energy requirements, are used to get insights in the transport mechanisms and kinetics of PAA and PenG.

Industrial penicillin production fermentations have to be terminated when penicillin productivity decreases due to degeneration of product formation. In **chapter 5** a systems biology approach is performed to analyze the mechanisms which contribute to degeneration of penicillin production. Genome, transcriptome, proteome, metabolome and fluxome were monitored in a degenerating system to analyze this phenomenon. As a model system an ethanol limited chemostat was used, because degeneration of penicillin production is known to be more pronounced with ethanol as the sole limiting carbon source.

CHAPTER 2

Dynamic gene expression regulation model for growth and penicillin production in *Penicillium chrysogenum*

Abstract - As is often the case for microbial product formation, the penicillin production rate of Penicillium chrysogenum has been observed to be a function of the growth rate of the organism. The relation between the biomass specific rate of penicillin formation (q_p) and growth rate (μ) has been measured under steady state conditions in carbon limited chemostats resulting in a steady state $q_p(\mu)$ relation. Direct application of such a relation to predict the rate of product formation during dynamic conditions, as they occur e.g. in fed-batch experiments, leads to errors in the prediction, because q_p is not an instantaneous function of the growth rate but rather lags behind because of adaptational and regulatory processes. In this paper a dynamic gene regulation model is presented, in which the specific rate of penicillin production is assumed to be a linear function of the amount of a rate-limiting enzyme in the penicillin production pathway. Enzyme activity assays were performed and strongly indicated that isopenicillin-N synthase (IPNS) was the main rate-limiting enzyme for penicillin-G biosynthesis in our strain. The developed gene regulation model predicts the expression of this rate limiting enzyme based on glucose repression, fast decay of the mRNA encoding for the enzyme as well as the decay of the enzyme itself. The gene regulation model was combined with a stoichiometric model and appeared to accurately describe the biomass and penicillin concentrations for both chemostat steady-state as well as the dynamics during chemostat start-up and fed-batch cultivation.

Douma RD, Verheijen PJ, de Laat WM, Heijnen JJ, van Gulik WM. 2010. Dynamic gene expression regulation model for growth and penicillin production in *Penicillium chrysogenum*. *Biotechnology and Bioengineering* **106** (4): 608-618.

Introduction

Industrial fermentation processes, in which micro organisms are used to produce pharmaceuticals and fine and bulk chemicals from renewable feed stocks, are increasingly used. An example of such a process, which is being performed for a long time already, is the production of β-lactam antibiotics by the fungus *Penicillium chrysogenum*. The total worldwide market of β-lactam compounds amounted to $5 billion in 1999 (Demain and Elander, 1999).

For the development, optimization and control of industrial fermentation processes mathematical modeling is indispensible. Several attempts have been undertaken to develop mathematical models to describe the growth and the penicillin production during cultivations of *P. chrysogenum* (Heijnen et al., 1979; Menezes et al., 1994; Birol et al., 2002; Roa Engel et al., 2009; Bajpai and Reuss, 1980). It has been found from steady state carbon limited chemostat cultivations carried out at different dilution rates that the specific penicillin production rate (q_p) is strongly dependent on the growth rate (μ) of the organism (van Gulik et al., 2000). Also for product formation in other microorganisms such behavior is observed, e.g. tylosin production in *Streptomyces fradiae* (Gray and Bhuwapathanapun, 1980) and erythromycine production in *Saccharopolyspora erythraea* (Lynch and Bushell, 1995). However, the obtained steady state $q_p(\mu)$ relations are not suited to apply to dynamic fed-batch cultivations where the growth rate is changing in time. This is caused by adaptation of the concentrations of the enzymes in the penicillin biosynthesis pathway, a phenomenon called relaxation (Roels, 1983).

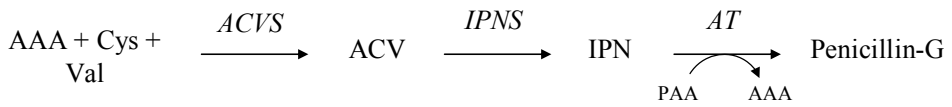

Figure 2.1 Schematic pathway towards penicillin-G from the three precursor amino acids. Abbreviations of all compounds can be found in the nomenclature section.

The stoichiometry of the penicillin biosynthesis pathway in *Penicillium chrysogenum* is well understood and the metabolites and enzymes participating in this pathway are schematically depicted in figure 2.1 (Martín and Gutiérrez, 1995; Nielsen, 1997; Brakhage, 1998). Much less is known about the regulation of the flux through the pathway, which can be controlled hierarchically, i.e. by transcriptional regulation of enzyme levels and/or on a

metabolic level by interactions of enzymes with substrates, products, or allosteric effectors. Clearly these different levels of regulation occur on different time scales. Changes in metabolite concentrations occur on a time scale of seconds to minutes thus metabolite concentrations can be considered as pseudo steady state in fermentation processes where changes occur on a time scale of hours. Changes in enzyme levels occur on a time scale of minutes to hours and thus enzyme levels might lag behind in dynamic fed-batch processes.

It is well known that in general the control of the enzyme level on the flux through a biochemical pathway is distributed amongst all enzymes of the pathway. However, not every enzyme in the pathway exerts the same control on the flux and in some cases the flux is dominated by the activity of a single enzyme, the so-called rate-limiting enzyme (Gunnarsson et al., 2004). Nielsen and Jørgensen (1995) concluded from a metabolic control analysis of the penicillin biosynthesis pathway in a high producing strain of *P. chrysogenum* that the rate-limiting step resides either at ACVS or at IPNS (Nielsen and Jørgensen, 1995).

In this paper a dynamic model for penicillin production based on gene regulation of a rate-limiting enzyme is described with which q_p can be predicted throughout dynamic conditions such as chemostat start-up, dynamic fed-batch experiments as well as steady state conditions in a chemostat. In this model the presence of glucose represses the expression of the gene encoding for this rate-limiting enzyme in penicillin biosynthesis (Brakhage et al., 1992; Feng et al., 1994; Gutierrez et al., 1999; Litzka et al., 1999; Martín et al., 1999; Revilla et al., 1986). q_p is then a linear function of the amount of this rate-limiting enzyme. Decay of mRNA and enzyme are also taken into account.

A dynamic gene regulation model for penicillin production

Assumptions

In a previous study (van Gulik et al., 2000) it was observed that the relation between the specific growth rate and the specific rate of penicillin production in carbon limited chemostat cultures was very similar for different carbon sources (i.e. glucose, ethanol and acetate). So in spite of the fact that central metabolism functions very differently during growth on these three carbon sources, leading to very different concentrations of intracellular metabolites (Nasution et al., 2006b). This had apparently no effect on the penicillin production rate. This is a strong indication that metabolic control is absent.

The basis of our model is therefore the assumption that penicillin production is exclusively controlled hierarchically, i.e. metabolic control is considered negligible, and is determined by a single rate-limiting enzyme, i.e. one of the three enzymes in the penicillin biosynthesis pathway as shown in figure 2.1.

Several groups have found that transcription of the genes encoding for the enzymes in the penicillin biosynthesis pathway is repressed by glucose (Brakhage et al., 1992; Feng et al., 1994; Gutierrez et al., 1999; Litzka et al., 1999; Martín et al., 1999; Revilla et al., 1986). Therefore the assumption is made that the transcription of the gene encoding for the rate-limiting enzyme is repressed by glucose. Herewith the synthesis rate of the rate-limiting enzyme becomes a function of the glucose concentration only and the assumption can be made that q_p is proportional to the concentration of the limiting enzyme. Furthermore degradation of this enzyme is assumed to be according to first order kinetics.

The glucose-uptake rate is assumed to follow hyperbolic uptake kinetics. Glucose is consumed according to the linear equation for substrate consumption (Herbert-Pirt relation) for growth, product formation and maintenance (Pirt, 1965; van Gulik et al., 2001). The value of q_p in this relation will follow from the gene regulation model.

Model structure

For all relevant extracellular components (i) in the bioreactor a mass balance can be constructed:

$$\frac{dC_i M}{dt} = \Phi_{in} C_{i,in} - \Phi_{out} C_i + q_i M C_x \qquad (2.1)$$

The substrate consumption by *P. chrysogenum* in the model can be described by the well-known Herbert-Pirt relation (Pirt, 1965; van Gulik et al., 2001).

$$q_s = \frac{\mu}{Y_{sx}^{\max}} + \frac{q_p}{Y_{sp}^{\max}} + m_s \qquad (2.2)$$

The parameters of the Herbert-Pirt equation, Y_{sx}^{max}, Y_{sp}^{max} and m_s, were previously determined by Van Gulik et al.(van Gulik et al., 2001) for the high producing strain of *P. chrysogenum* used. Substrate consumption is considered to be a hyperbolic function of the substrate concentration.

$$q_s = q_s^{\max} \frac{C_s}{K_s + C_s} \tag{2.3}$$

To design a complete model the relation between q_p and C_s (or μ) is needed. This relation will be based on the assumptions mentioned above. Transcriptional repression of the gene encoding for the rate-limting enzyme is accounted for in the model by the formation of an active glucose-repressor complex (G_mR) by the binding of m molecules of glucose (G) to the inactive repressor protein (R).

$$mG + R \rightleftarrows G_m R \tag{2.4}$$

The effector-repressor complex binds to the operator of the gene coding for the limiting enzyme and blocks expression of this gene.

$$O + G_m R \rightleftarrows OG_m R \tag{2.5}$$

Assuming that the intracellular concentration of glucose is proportional to the extracellular concentration C_s, the equilibrium constants for these reactions can now be written, as:

$$K_1 = \frac{X_{G_m R}}{(C_s)^m \cdot X_R} \tag{2.6}$$

$$K_2 = \frac{X_{OG_m R}}{X_O \cdot X_{G_m R}} \tag{2.7}$$

In this relation X_j is the intracellular concentration of compound j. With the assumption that X_{OGmR} is small compared to $(X_R)_t$ the mass balance for the repressor protein can be simplified to:

$$(X_R)_t = X_R + X_{G_m R} \tag{2.8}$$

The mass balance for the operator can be written as:

$$(X_O)_t = X_O + X_{OG_m R} \tag{2.9}$$

Combining equations 2.6, 2.7, 2.8 and 2.9 yields the fraction Q of unrepressed genes (X_O / $X_O(t)$) which are transcribed:

$$Q = \frac{1 + K_1 \cdot (C_s)^m}{1 + K_1 \cdot K_2' \cdot (C_s)^m} \tag{2.10}$$

with $K_2' = K_2 \cdot (X_R)_t + 1$

It is known that excess glucose leads to full repression of the penicillin promotor, hence Q = 0 for large C_s. This requires that $K_2' >> 1$ and $K_1(C_s)^m << 1$ (small K_1) so that the numerator of Q can be simplified to 1. A new result for Q can then be written as:

$$Q = \frac{1}{1 + \left(\frac{C_s}{K_p} \right)^m} \tag{2.11}$$

with $K_1 K_2' = \frac{1}{\left(K_p \right)^m}$

For intracellular compounds (i) which are not secreted nor taken up (like proteins and mRNA) in bioreactors Stephanopoulos et al. showed that the mass balance can be written as follows (Stephanopoulos et al., 1998):

$$\frac{dX_i}{dt} = q_i - \left(\mu + k_{di} \right) X_i \tag{2.12}$$

In which q_i is the biomass specific production rate of compound i, μ is the specific growth rate and k_{di} the first order decay rate of compound i. The mass balance for mRNA, which codes for the rate limiting enzyme E, follows as:

$$\frac{dX_{mRNA}}{dt} = q_{mRNA} - (k_{dmRNA} + \mu) X_{mRNA} \tag{2.13}$$

Because mRNA is very unstable $k_{dmRNA} >> \mu$ and mRNA reaches its steady state in a time frame of $1/k_{dmRNA}$, which is minutes. Therefore at a time scale beyond hours (relevant for chemostat and fed batch cultivations) mRNA can be assumed to be in pseudo steady state ($dX_{mRNA}/dt \approx 0$) and we can write:

$$q_{mRNA} = k_{dmRNA} X_{mRNA} \tag{2.14}$$

In this model the synthesis rate of mRNA (q_{mRNA}) for enzyme E is repressed by glucose, since penicillin production is known to be repressed by glucose (Brakhage et al., 1992;

Feng et al., 1994; Gutierrez et al., 1999; Litzka et al., 1999; Martín et al., 1999; Revilla et al., 1986). It is assumed that q_{mRNA} is proportional to the fraction of repressor free operators, Q:

$$q_{mRNA} = k_3 Q \tag{2.15}$$

For the rate limiting enzyme E, of which the intracellular concentration is denoted by X_E (U/Cmol biomass), the mass balance will be as follows:

$$\frac{dX_E}{dt} = q_{sE} - (k_{dE} + \mu) X_E \tag{2.16}$$

If we assume that q_p is proportional to X_E ($q_p = k_5 X_E$) we can write:

$$\frac{dq_p}{dt} = q_{sE} k_5 - (k_{dE} + \mu) q_p \tag{2.17}$$

The specific synthesis rate of the enzyme, q_{sE}, is a function of the enzyme production capacity of a cell which is determined by the amount of mRNA present in the cell and the amount of ribosomes in the cell. The amount of ribosomal RNA present in cells is known to be a function of the growth rate, see review of Condon et al. for the case of *Escherichia coli* (Condon et al., 1995). For reasons of simplicity a simple rate function is assumed, which is linear in mRNA content and ribosome amount.

$$q_{sE} = k_4 X_{mRNA} (a + b\mu) \tag{2.18}$$

Combination of equations 2.11, 2.14, 2.15 and 2.18 gives q_{sE} as function of C_s (because μ is also a function of C_s):

$$q_{sE} = \frac{k_3 k_4}{k_{dmRNA}} (a + b\mu) \frac{1}{1 + \left(\frac{C_s}{K_p} \right)^m} \tag{2.19}$$

We can substitute q_{sE} into the enzyme mass balance to obtain the differential equation which gives q_p as function of time.

$$\frac{dq_p}{dt} = \frac{\alpha + \beta\mu}{1 + \left(\frac{C_s}{K_p}\right)^m} - \left(k_{dE} + \mu\right) q_p \qquad (2.20)$$

In this equation $\alpha = \frac{a \cdot k_3 \cdot k_4 \cdot k_5}{k_{dmRNA}}$ and $\beta = \frac{b \cdot k_3 \cdot k_4 \cdot k_5}{k_{dmRNA}}$

For steady state conditions (chemostat) the steady state relation for q_p is obtained.

$$q_p^{ss} = \frac{\alpha + \beta\mu}{k_{dE} + \mu} \cdot \frac{1}{1 + \left(\frac{C_s}{K_p}\right)^m} \qquad (2.21)$$

Materials and methods

Strain

A high penicillin producing strain of *Penicillium chrysogenum* (codename DS12975) was kindly donated by DSM Anti-Infectives (Delft, The Netherlands). This strain was used for all experiments.

Chemostat experiments

The experimental data of the chemostat experiments are the ones from a series of 14 chemostat experiments with glucose as the sole carbon-source performed by Van Gulik et al (van Gulik et al., 2000).

Fed-batch system

Fed-batch cultivations were carried out in a 20-L turbine-stirred bioreactor (Applikon, Schiedam, The Netherlands), equipped with two Rushton turbines with a diameter of 110 mm operated at a stirrer speed of 350 rpm. The culture was aerated at a rate of 9.5 L/min through a standard sparger located below the stirrer with predried air which was sterilized through a cotton-wool filter and then through a hydrophobic membrane filter with a pore size of 0.2 μm (Millipore). The air flow was kept constant by means of a mass-flow-controller system (Brooks Instruments BV, Veenendaal, The Netherlands). Water was removed from the exhaust gas and brought back into the reactor by passing it through a glass condenser kept at a temperature of 2 °C by means of a cryostat. The temperature of the culture in the reactor was kept at 25.0°C using a flow-through finger, which was

heated/cooled by means of a thermocirculator. The pH of the culture was maintained at 6.5 with 5.8M NH_3 and 2N H_2SO_4 with an automatic pH-control system (Applikon, Schiedam, The Netherlands) using a sterilizable pH probe mounted in the reactor. The dissolved oxygen tension was measured but not controlled. During the experiments the dissolved oxygen tension never dropped below 50% of air saturation. To be able to control the residual concentration of Phenylacetic acid (PAA) two different media were supplied to the culture, one with and one without PAA, which were otherwise identical. By changing the ratio between the feed rates of the two media, which were controlled by means of two peristaltic pumps (Masterflex, Cole Parmer, Vernon Hills, IL, USA), the supply rate of PAA could be adapted, without changing the total medium feed rate.

Medium compositions

The medium for the batch phase contained per kg of medium: 4.4 g glucose·$1H_2O$, 0.8 g KH_2PO_4, 2 g $(NH_4)2SO_4$, 0.5 g $MgSO_4·7H_2O$, 0.55 g PAA, 0.2 g KOH and 10 mL trace element solution. The composition of the trace element solution was (per L): 15 g Na2-EDTA·$2H_2O$, 0.5 g $CuSO_4·5H_2O$, 2 g $ZnSO_4·7H_2O$, 2 g $MnSO_4·1H_2O$, 4 g $FeSO_4·7H_2O$, and 0.5 g $CaCl_2·2H_2O$.

The medium for the fed-batch phase contained per kg of medium: 330 g glucose·$1H_2O$, 2.73 g KH_2PO_4, 2 g $(NH_4)2SO_4$, 23 g $MgSO_4·7H_2O$, 15.1 g $Na_2SO_4·10H_2O$, 0.41 mL silicone antifoam agent (BDH, Poole, UK) and 30 mL trace element solution.

The fed-batch medium with PAA was supplemented with 30 g PAA and 13.8 g KOH per kg of medium.

Medium preparation

The batch medium was autoclaved with the reactor. The feed medium without PAA (4 L) was filter sterilized. For the feed medium with PAA the appropriate amount of PAA was dissolved in 1 L of a KOH solution, with a PAA:KOH molar ratio of 1:1.2. After neutralizing the pH with 2N H_2SO_4, the medium vessel containing the PAA solution was autoclaved for 40 min at 121°C. The other medium components were dissolved in 3 L of demineralized water. This solution was filter-sterilized using a Millidisk filtration system (Millipore, Bedford, MA) and added to the PAA solution in the medium vessel. Both medium vessels were placed on a magnetic stirrer and were allowed to mix for at least 12 h before they were connected to the reactor. Also, during the experiments, the medium vessels were mixed continuously.

Fed-batch experiments

Prior to sterilization the fermentor vessel was filled with 7.5 L of batch medium without the carbon source. Subsequently, the reactor was autoclaved for 40 min at a temperature of 121°C. After cooling down to 25°C, the carbon source glucose was added and the reactor was inoculated with spores from cultures grown on rice grains. Spores from 30 g of rice were suspended in 500 mL of sterile demineralized water. The batch carbon source glucose was dissolved in 500 mL of demineralized water and autoclaved separately (15 min at 110°C). Shortly before the end of the batch culture (i.e., shortly before exhaustion of the carbon source), the feed was started. The time between inoculation and the end of the batch phase was approximately 50 hours. The applied total feed mass profile for the fed-batch cultivation was:

$\Phi_V = 0.00286 \cdot M$ (kg/h)

wherein M is the weight of the culture broth (kg). Two media were used, one with and one without PAA, which were otherwise identical. Initially the feed rates of both media were identical, i.e. equal to 0.5 Φ_V. By controlling both feed streams, such that $\Phi_{V\text{-}PAA} + \Phi_{V+PAA} = \Phi_V$ the residual PAA concentration was kept between 3 and 6 mM. Within this range the residual PAA was neither limiting the production of penicillin-G nor toxic (van Gulik et al., 2000). Approximately every 8 hours samples were taken to measure the residual PAA concentration and both feed streams were adjusted if necessary. The total duration of the fed-batch phase was 180 h.

Enzyme activity analysis

Biomass was collected by filtering over glass fiber filters and washed with deionized water. The metabolism was stopped by wrapping the filter in aluminum foil and submerging it into liquid nitrogen. The cells were freeze dried and stored at -80°C until further analysis. The enzyme activity assays were performed as described previously (Theilgaard et al., 2001; Nielsen and Jørgensen, 1995). The overall relative standard deviation for the measurement was about 10%.

Analytical procedures

Biomass concentration measurement, off-gas analysis, total organic carbon (TOC) determination and Pen-G and PAA concentration measurements were performed as described by van Gulik et al. (van Gulik et al., 2000).

Simulations

All simulations were performed using MATLAB 2008b.

Results and discussion

Steady state relation between growth rate and rate of penicillin-G production

The steady state relation between the specific growth rate μ and the biomass specific rate of β-lactam production q_p (i.e. sum of penicillin-G and penicilloic acid) of the *P. chrysogenum* strain used in this study has been determined in glucose limited steady state chemostat cultures (van Gulik et al., 2000). The relation shows (figure 2.2) that q_p has a clear optimum at a growth rate around 0.03 h^{-1}, whereas the production steeply decreases to nearly zero at higher and lower growth rates.

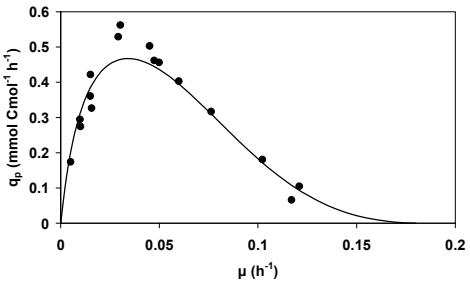

Figure 2.2 Steady state $q_p(\mu)$ relation. Experimental data (●) and steady state prediction by the dynamic gene regulation model (—).

Enzyme activity measurements

In-vitro activity measurements were carried out of two enzymes of the penicillin biosynthesis pathway, namely IPNS and AT. The relation between q_p and the in-vitro activities of IPNS and AT measured in glucose limited chemostat cultures are shown in figure 2.3. From this figure it can be seen that there seems to be no relation between q_p and the AT activity. However, in case of IPNS q_p correlates very well with enzyme activity in a nearly proportional fashion. This indicates that IPNS has the major control on the flux towards penicillin.

The existence of this linear relation was also investigated under dynamic conditions, i.e. during the initial, non-steady state, start-up period in a glucose limited chemostat cultivation at D = 0.01 h^{-1}. During the batch phase and the first 4.5 residence times of

glucose limited growth the activities of IPNS and AT were measured. The results are shown in figure 2.4. From these figures a near linear correlation of the IPNS activity with q_p can be observed, while there seems to be no correlation between the AT activity and q_p. This is an indication that IPNS exerts near total control in the pathway towards penicillin. This is in correspondance with the observations of Theilgaard and Nielsen (1999) who found the flux control to totally reside at IPNS in the penicillin biosynthesis pathway in a different *P. chrysogenum* strain. It also implies that AT and ACVS have very low control in the pathway towards penicillin. Finally it appears that during the batch phase IPNS is absent, supporting the notion of glucose repression of IPNS. These results clearly support two key assumptions of the dynamic gene regulation model for q_p, namely the existence of glucose repression and the control of penicillin biosynthesis by a single rate-limiting enzyme.

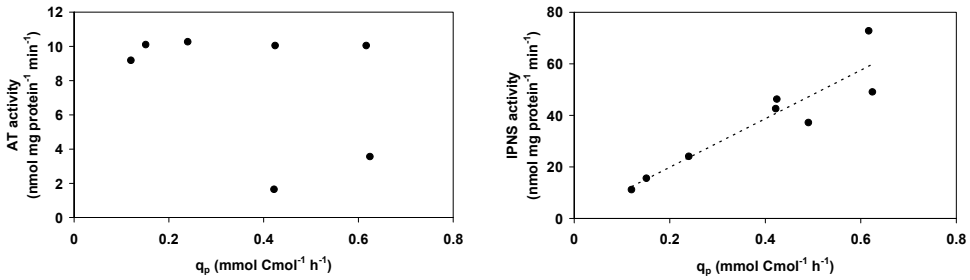

Figure 2.3 Measured AT activity (left) and IPNS activity (right) as function of q_p in glucose limited chemostat cultures of P. chrysogenum.

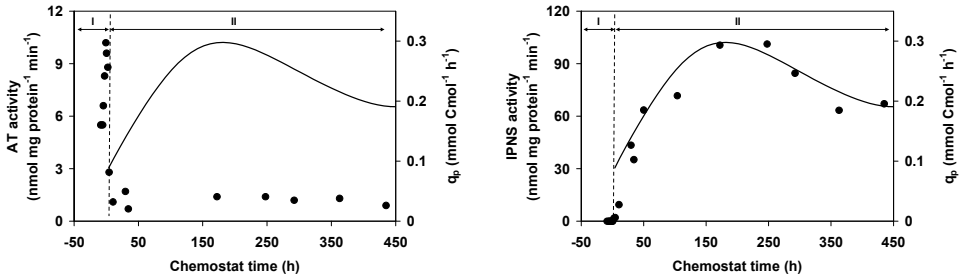

Figure 2.4 AT (●) activity (left), IPNS (●) activity (right) and q_p (—) during the batch phase (I) and the start-up period (II, first 4.5 residence times) in glucose limited chemostat growth at D = 0.01 h^{-1}.

Steady state and dynamic gene regulation model for q_p

The steady state $q_p(\mu)$ relation follows from model equation 2.21. It is compared with the $q_p(\mu)$ relation as obtained by van Gulik et al. from chemostat experiment in figure 2.2 (van Gulik et al., 2000). At low growth rates ($\mu \rightarrow 0$), $q_p \rightarrow 0$ which shows that $\alpha = 0$ in equation 2.21. The steady state $q_p(\mu)$ relation with 4 remaining parameters, equation 2.21, then still has to be fitted to the $q_p(\mu)$ curve in figure 2.2. Values for C_s were calculated for each data point in the $q_p(\mu)$ relation by combining equation 2.2 with 2.3. The quality of the fit for the decreasing part ($\mu > 0.03$ h^{-1}) appeared to be mainly dependent on the value of K_p. Therefore the curve for $0 < \mu < 0.03$ h^{-1} was used to estimate k_{dE} and β with a fixed value for K_p. The curve for $\mu > 0.03$ h^{-1} was used to estimate K_p with fixed values for k_{dE} and β.

Model equation 2.21 also shows that at low μ the relation between q_p and μ becomes proportional, $q_p^{ss} = (\beta / k_{dE})\mu$, meaning that estimated parameters β and k_{dE} are correlated and cannot be identified seperately. Therefore only the ratio between β and k_{dE} can be determined from figure 2.2 and not the individual values of k_{dE} and β. To determine these individual values a dynamic experiment is required. Such dynamic information is available during the start-up period of a chemostat culture. Two chemostat experiments at low growth rates such as shown in figure 2.5 ($D = 0.005$ h^{-1} and $D = 0.01$ h^{-1}) were performed to analyse this dynamic response of the model. These experiments, together with the steady state $q_p(\mu)$ function from the dynamic gene regulation model, equation 2.21, were used to obtain the 4 parameters in the q_p model leading to $\beta = 0.8$ mol penicillin Cmol^{-1} hour^{-1}, $m = 2$, $K_p = 0.00412 \pm 0.00017$ Cmol glucose L^{-1} and $k_{dE} = 0.0147 \pm 0.0012$ h^{-1}.

The obtained dynamic gene regulation model for q_p was combined with a hyperbolic substrate uptake relation (equation 2.3, $K_s = 0.005$ Cmol glucose / kg broth and $q_s^{max} = 0.286$ Cmol glucose / Cmol biomass / h) and the Herbert-Pirt relation according to van Gulik et al., 2001 for identical conditions (equation 2.2, $Y_{sx}^{max} = 0.663$ Cmol biomass / Cmol glucose, $Y_{sp}^{max} = 0.029$ mol penicillin / Cmol glucose and $m_s = 0.0088$ Cmol glucose / h / Cmol biomass).

Figure 2.2 shows the obtained steady state $q_p(\mu)$ relation and figure 2.5 shows the dynamics of penicillin and biomass production during the start-up of the 2 chemostats. It appears that the model describes the mycelium and penicillin concentration in the broth during the fermentation very well for the beginning of the chemostat experiments up to about 350 hours. However, after 350 hours the penicillin concentration was observed to decrease, while the mycelium concentration increased. The phenomenon that penicillin producing

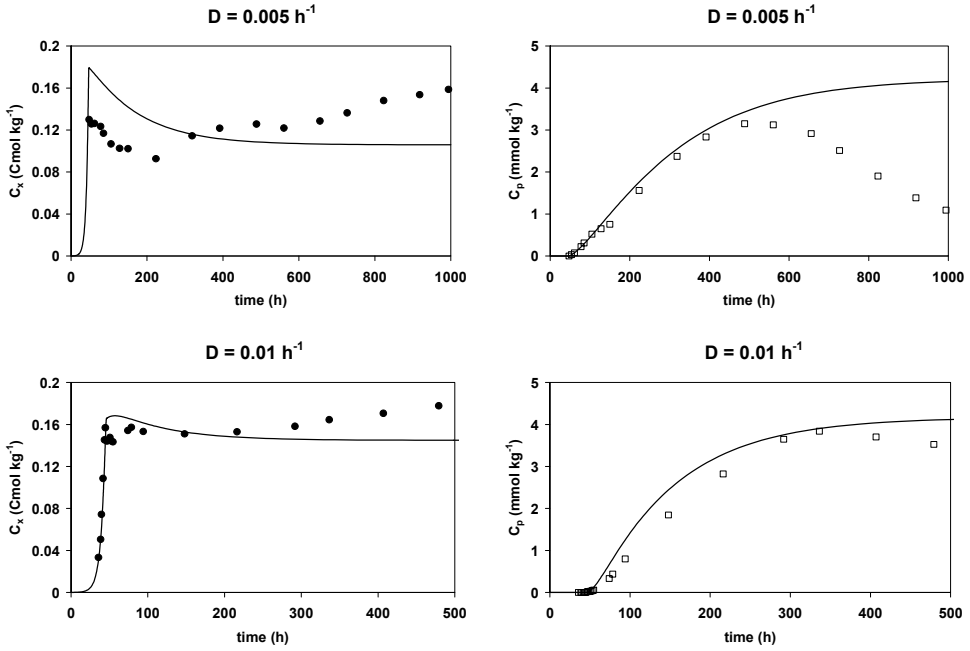

Figure 2.5 Biomass concentration (●), penicillin concentration (□) and prediction by dynamic gene regulation model (—) during two chemostat experiments. The two upper graphs show the results from a chemostat experiment performed at D = 0.005 h^{-1} and the two lower graphs show the results from a chemostat experiment performed at D = 0.01 h^{-1}.

cultures slowly loose their ability to produce penicillin was already observed as early as in 1932 by Clutterbuck et al. as well as by other groups and this phenomenon is usually referred to as degeneration (Clutterbuck et al., 1932; Foster et al., 1943; Righelato, 1976; van Gulik et al., 2001; Christensen et al., 1995). Nielsen and Jørgensen also found decreased penicillin-V (PenV) production rates towards the end of a fed-batch fermentation. The decreased production rate was found to be caused by feedback inhibition by ACV (Nielsen and Jørgensen, 1995). However, the strain used in that study was a PenV producing strain in contrast with the PenG producing strain used for this study. A comparison is therefore difficult. Although feedback inhibition might explain discrepancies between the model and experimental data, it cannot explain the discrepancies observed at the end of this fed-batch fermentation. If stronger feedback inhibition would occur, the model would overestimate the penicillin production, while figure 2.6 shows an underestimation.

The model allows some reflection on how to improve q_p. A higher β leads to a higher q_p which can be achieved by promoting higher levels of enzyme ('b k_3 k_4 / k_{dmRNA}' higher) or by more active enzyme (k_5 higher). A lower k_{dE}, meaning a more stable enzyme also increases q_p. Finally less glucose repression (lower K_p) increases q_p. The model allows to quantitatively evaluate the effect of different enzyme properties on the penicillin production rate.

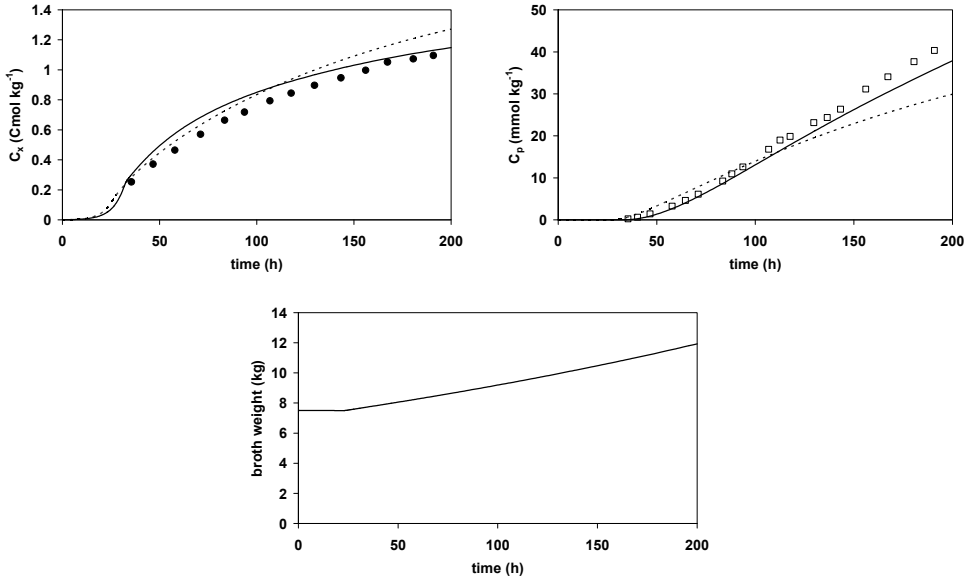

Figure 2.6 Biomass concentration (●), penicillin concentration (□), broth weight, dynamic gene regulation model prediction (—) and prediction using the steady state $q_p(\mu)$ function (---) during a fed-batch cultivation.

Validation of dynamic gene regulation model

Fermentations are operated fed-batch wise in industrial production of penicillin. Therefore a fed-batch fermentation was performed to validate the model. The dynamic gene regulation model was used to predict the mycelium and penicillin concentration during the fed-batch cultivation. In the fed-batch experiment μ decreases continuously and q_p has to follow. According to the steady state $q_p(\mu)$ relation q_p is directly related to μ. According to the dynamic gene regulation model q_p changes with a time delay due to changing enzyme levels.

Figure 2.6 shows that the prediction by the dynamic gene regulation model for the penicillin concentration is much better than the prediction based on the instantaneous $q_p(\mu)$ relation. The steady state $q_p(\mu)$ relation overestimates the penicillin production at the beginning, because in reality the enzymes necessary to produce penicillin still have to be synthesized. In the later phase the prediction by the steady state $q_p(\mu)$ function underestimates the penicillin production. This is caused by the fact that the enzyme levels, which were present in higher amounts in the beginning of the experiment, are changing slower than anticipated by the steady state $q_p(\mu)$ relation.

The biomass prediction is also better with the dynamic gene regulation model, because deviations in penicillin production influence biomass production as there is competition for precursors, cofactor and metabolic energy between growth and penicillin production. The more penicillin is produced, the less biomass is produced and vice-versa. From the mycelium and penicillin concentration in time the specific penicillin production rate and the growth rate can be calculated for the fed-batch experiment. These q_p and μ values are plotted in figure 2.7 together with the $q_p(\mu)$ relation as predicted by the dynamic gene regulation model and the steady state $q_p(\mu)$ relation from the chemostat cultivation.

As can be seen in figure 2.7 the dynamic gene regulation model closely reproduces the experimentally found $q_p(\mu)$ relation from the fed-batch cultivation, which is completely different from the steady state $q_p(\mu)$ relation as found in chemostat experiments.

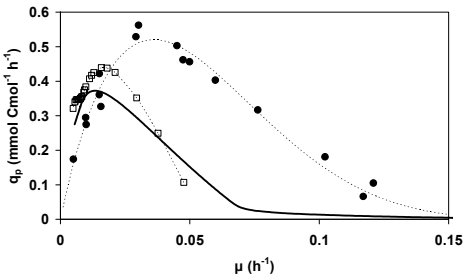

Figure 2.7 $q_p(\mu)$ relation in fed batch (-□-), simulated by the dynamic gene regulation model during the fed-batch cultivation (—) and comparison to the steady-state $q_p(\mu)$ relation obtained from chemostat experiments (-●-).

Conclusions

A simple dynamic gene regulation model for penicillin production was constructed, based on the observation that the penicillin production in an industrial strain of *P. chrysogenum* is

proportional to the concentration of one rate-limiting enzyme in the penicillin biosynthesis pathway. Enzyme activity measurements under dynamic and steady state conditions showed that the specific penicillin production is proportional to the activity of IPNS.

It was shown that the dynamic gene regulation model provided a good description of growth and penicillin production under steady state, i.e. during chemostat cultivation, and dynamic conditions, i.e. during the start-up of chemostat cultivations and fed-batch fermentations with changing q_p. The description of the model of a fed-batch experiment with the dynamic gene regulation model for q_p proved to be significantly better than the description based on a the steady-state $q_p(\mu)$ relation.

Acknowledgements

This project is financially supported by the Netherlands Ministry of Economic Affairs and the B-Basic partner organizations (www.b-basic.nl) through B-Basic, a public private NWO-ACTS programme (ACTS: Advanced Chemical Technologies for Sustainability).
This project was carried out within the research programme of the Kluyver Centre for Genomics of Industrial Fermentation which is part of the Netherlands Genomics Initiative / Netherlands Organization for Scientific Research.

Chapter specific Nomenclature

E	rate-limiting enzyme for penicillin production	
G_mR	effector repressor complex	
mG	m molecules of glucose	
O	free operator	
p	penicillin	
OG_mR	repressed gene	
R	repressor protein	
s	glucose	
x	biomass	
C_i	extracellular concentration (except penicillin) of compound i	Cmol kg^{-1}
$C_{i,in}$	concentration of compound i in ingoing feed	Cmol kg^{-1}
C_p	extracellular penicillin concentration	mol kg^{-1}
k_{di}	first order decay rate of compound i	h^{-1}

K_s	Michaelis Menten constant	Cmol kg^{-1}
K_p	glucose repression constant	Cmol kg^{-1}
M	total broth mass	kg
m	number of glucose molecules binding to the operator	-
m_s	maintenance coefficient	Cmol $Cmol^{-1}$ h^{-1}
Q	fraction of repressor free operators	-
q_i	biomass specific conversion rate of compound i (except penicillin)	Cmol $Cmol^{-1}$ h^{-1}
q_i^{ss}	steady state biomass specific conversion rate of compound i (except penicillin)	Cmol $Cmol^{-1}$ h^{-1}
q_p	biomass specific penicillin production rate	mol $Cmol^{-1}$ h^{-1}
q_s^{max}	maximal biomass specific substrate conversion rate	Cmol $Cmol^{-1}$ h^{-1}
X_i	intracellular concentration of compound i	Cmol $Cmol^{-1}$
X_i^{ss}	steady state intracellular concentration of compound i	Cmol $Cmol^{-1}$
Y_{sx}^{max}	maximum yield of biomass on glucose	Cmol $Cmol^{-1}$
Y_{sp}^{max}	maximum yield of penicillin on glucose	mol $Cmol^{-1}$
β	constant	mol $Cmol^{-1}$ h^{-1}
μ	growth rate	h^{-1}
Φ_{in}	ingoing feed rate	kg h^{-1}
Φ_{out}	outgoing flow rate	kg h^{-1}

Appendix Dynamic fed-batch model

The fed-batch was simulated using:

- The obtained dynamic gene regulation model for q_p (equation 2.20, 2A.5)
- The hyperbolic substrate uptake kinetics (equation 2.3, 2A.6)
- The Herbet-Pirt relation for substrate (equation 2.2, 2A.7)
- A total mass balance (equation 2A.1)
- Mass balances for substrate, biomass and penicillin (equation 2A.2, 2A.3, 2A.4)
- Carbon and degree of reduction balance (equation 2A.8, 2A.5) to obtain q_o and q_c needed for the mass balance

The dynamic fed-batch model contains the following mass balances:

$$\frac{dM}{dt} = \Phi_{in} + MW_o q_o MC_x - MW_c q_c MC_x \qquad (2A.1)$$

$$\frac{dC_s M}{dt} = \Phi_{in} C_{s,in} - q_s MC_x \qquad (2A.2)$$

$$\frac{dC_x M}{dt} = \mu MC_x \qquad (2A.3)$$

$$\frac{dC_p M}{dt} = q_p MC_x \qquad (2A.4)$$

$$\frac{dq_p}{dt} = \beta\mu \frac{1}{1+\left(\frac{C_s}{K_p}\right)^m} - \left(k_{dE} + \mu\right) q_p \qquad (2A.5)$$

And the kinetics are as follows:

$$q_s = q_s^{\max} \frac{C_s}{K_s + C_s} \qquad \text{Hyperbolic} \qquad (2A.6)$$

$$\mu = Y_{sx}^{\max}\left(q_s - \frac{q_p}{Y_{sp}^{\max}} - m_s\right) \qquad \text{Herbert-Pirt} \qquad (2A.7)$$

$$q_o = 0.25\left(4 \cdot q_s + 36 \cdot q_p - 4.154 \cdot \mu - 74 \cdot q_p\right) \quad \gamma \text{ balance} \qquad (2A.8)$$

$$q_c = q_s - \mu - 16 q_p + 8 q_{PAA} \qquad \text{C balance} \qquad (2A.9)$$

$$q_{PAA} = q_p \qquad \text{stoichiometric} \qquad (2A.10)$$

The flow rate:

$0 < t < 23$: $\Phi_{in} = 0$
$t > 23$: $\Phi_{in} = DM$

Energetic parameters from Van Gulik et al. 2000:

$Y_{sx}^{\max} = 0.663$	(Cmol biomass / Cmol glucose)
$Y_{sp}^{\max} = 0.029$	(mol penicillin / Cmol glucose)
$m_s = 0.0088$	(Cmol glucose / Cmol biomass / h)
$q_s^{\max} = 0.286$	(Cmol glucose / Cmol / h)

Other parameter values:

$C_{s,in} = 9.91$	(Cmol glucose / kg broth)
$D = 0.00286$	(1 / h)
$K_s = 0.005$	(Cmol glucose / kg broth)
$\beta = 0.8$	(mol penicillin / Cmol biomass / h)
$K_p = 0.00412$	(Cmol glucose / kg broth)
$m = 2$	(-)
$k_{dE} = 0.0147$	(1 / h)
$MW_o = 0.032$	(kg / mol O_2)
$MW_c = 0.044$	(kg / mol CO_2)

Initial conditions:

$M = 7.5$	(kg broth)
$C_s = 0.133$	(Cmol glucose / kg broth)
$C_x = 0.0009$	(Cmol biomass / kg broth)
$C_p = 0$	(mol penicillin / kg broth)
$q_p = 0$	(mol penicillin / Cmol biomass / h)

CHAPTER 3

Intracellular metabolite determination in the presence of extracellular abundance: application to the penicillin biosynthesis pathway in *Penicillium chrysogenum*

Abstract - Important steps in metabolic pathways are formed by the transport of substrates and products over the cell membrane. The study of *in vivo* transport kinetics requires accurate quantification of intra- and extracellular levels of the transported compounds. Especially in case of extracellular abundance, the proper determination of intracellular metabolite levels poses challenges. Efficient removal of extracellular substrates and products is therefore important not to overestimate the intracellular amounts. In this study we evaluated two different rapid sampling methods, one combined with cold filtration and the other with centrifugation, for their applicability to determine intracellular amounts of metabolites which are present in high concentrations in the extracellular medium. The filtration based method combines fast sampling and immediate quenching of cellular metabolism in cold methanol, with rapid and effective removal of all compounds present outside the cells by means of direct filtration and subsequent filtration based washing. In the centrifugation based method removal of the extracellular metabolites from the cells was achieved by means of multiple centrifugation and resuspension steps with the cold quenching solution. The cold filtration method was found to be highly superior to the centrifugation method to determine intracellular amounts of metabolites related to penicillin-G biosynthesis and allowed the quantification of compounds of which the extracellular amounts were 3 to 4 orders of magnitude higher than the intracellular amounts. Using this method for the first time allowed to measure the intracellular levels of the side chain precursor PAA and the product penicillin-G of the penicillin biosynthesis pathway, compounds of which the transport mechanism in *Penicillium chrysogenum* is still far from being sufficiently understood.

Douma RD*, de Jonge LP*, Jonker CTH, Seifar RM, Heijnen JJ, van Gulik WM. 2010. Intracellular metabolite determination in the presence of extracellular abundance: application to the penicillin biosynthesis pathway in Penicillium chrysogenum. Biotechnology and Bioengineering 107 (1): 105-115
* These authors contributed equally to this work.

Introduction

Important and often rate limiting steps in metabolic pathways are formed by membrane transport of substrates, precursors and end products. The study of *in vivo* transport kinetics requires quantification of intra- and extracellular levels of the transported compounds. Especially in case of extracellular abundance, the proper determination of the intracellular concentration poses challenges.

Many procedures have been described in literature to obtain intracellular metabolite concentrations, which generally consist of a number of steps: i.e. sampling, sample processing, including extraction, and analysis (Mashego et al., 2007). The focus of this paper will be exclusively on sampling and sample processing, i.e. removal of extracellular metabolites. Metabolite extraction (Villas-Bôas et al., 2005a; Winder et al., 2008; Canelas et al., 2009) and subsequent analysis (Buscher et al., 2009; Dunn and Ellis, 2005) have been well addressed in other papers.

The turnover time of many intracellular metabolites is in the order of seconds. To obtain a true 'snapshot' of the metabolome of a microbial culture at a certain time point, sampling should be rapid and metabolic reactions should be stopped immediately. A simple approach is to sample total broth into a solution with an extreme pH or a high temperature, to instantly stop all enzymatic activity (Weibel et al., 1974; Theobald et al., 1993; Weuster-Botz, 1997). These procedures combine quenching of metabolic activity with extraction of metabolites from the cells. Although simple and efficient, a serious disadvantage of such methods is that they do not allow separation of cells and supernatant. Therefore they are only suitable to measure intracellular compounds of which the amounts present in the supernatant are negligible compared to the intracellular amounts, which is often not the case. A well known quenching method which allows separation of cells and supernatant is the cold methanol quenching method (De Koning and Van Dam, 1992; Nasution et al., 2006a), which has the important advantage that the cells remain intact after quenching, allowing washing of the cells to remove extracellular metabolites.

Until now, quantitative metabolomics has focused mainly on intermediates of central metabolic pathways. Less attention has been paid to the intracellular levels of metabolites at the beginning and the end of metabolic processes, i.e. substrates and (excreted) products. In many situations the extracellular amounts of substrates and products are much higher than the intracellular amounts and the extracellular fraction can be expected to be in the order of

99% or even higher. Extremely efficient removal of the extracellular fraction is therefore essential for proper determination of the intracellular amount of a substrate or product.

In many of the recent rapid sampling protocols the samples are quenched in cold aqueous methanol followed by separation of the cells and the quenching liquid by cold centrifugation (Nasution et al., 2006a; Ruijter and Visser, 1996). After centrifugation a large part of the supernatant, and therewith the extracellular metabolites, is removed by decantation. Sometimes this is repeated once or twice. The efficiency of removal of extracellular compounds in this method is limited. Washing of the cells can also be carried out using filtration (Ruijter and Visser, 1996; Sáez and Lagunas, 1976; Wittmann et al., 2004). However, for determination of metabolites with rapid turnover, filtration should be performed at sufficiently low temperatures to keep the metabolism quenched.

The aim of this study was to compare the efficiency of the cold centrifugation and the cold filtration method, for removal of compounds which are abundantly present in the extracellular medium, after rapid sampling and subsequent cold methanol quenching of *P. chrysogenum* cells. To this end we focused on a set of nine metabolites related to the penicillin-G biosynthesis pathway, including one precursor, two intermediates, one product and five byproducts. The reaction network connecting these metabolites is depicted in figure 1.2. In the penicillin-G production process the side-chain precursor phenylacetic acid (PAA) is supplied in the feed and taken up by the mycelium. The product penicillin-G (PenG) is efficiently excreted. Five main byproducts are formed, three by spontaneous chemical reactions (benzylpenicillic acid (PIO), 8-hydroxypenicillic acid (8-HPA) and 6-oxopiperidine-2-carboxylic acid (OPC)) and two by enzyme catalyzed reactions (*ortho*-hydroxyphenyl acetic acid (*o*-OH-PAA) and 6-aminopenicillanic acid (6-APA)). Except for the two intermediates of the pathway, L-α-(δ-aminoadipyl)-L-α-cystenyl-D-α-valine (ACV) and isopenicillin-N (IPN), it can be expected that the extracellular amounts of these metabolites are much larger than the intracellular amounts.

Materials and methods

Strain

A high-yielding production strain of *Penicillium chrysogenum* (code name DS17690) was kindly donated by DSM Anti-Infectives (Delft, the Netherlands) as spores from a culture grown on rice grains. The characteristics of this strain, in terms of productivity and biomass

yield during chemostat cultivation, have been described earlier (van Gulik et al., 2000; Nasution et al., 2006a).

Media

Batch phase medium contained 16.5 g/L glucose-monohydrate, 5.0 g/L $(NH_4)_2SO_4$, 1.0 g/L KH_2PO_4, 0.5 g/L $MgSO_4 \cdot 7H_2O$, 0.41 g/L PAA and 2 mL/L of a trace elements solution. The trace elements solution contained 75.0 g/L $Na_2EDTA \cdot 2H_2O$, 10.0 g/L $ZnSO_4 \cdot 7H_2O$, 10.0 g/L $MnSO_4 \cdot H_2O$, 20.0g /L $FeSO_4 \cdot 7H_2O$, 2.5 g/L $CaCl_2 \cdot 2H_2O$, 2.5 g/L $CuSO_4 \cdot 5H_2O$. The trace element solution was set to pH 6.0 with NaOH pellets. All the medium components except the glucose-monohydrate were dissolved in 3.7 L of demineralised water. The pH of the batch medium was set to 5.5 and the solution was sterilized for 40 minutes at 121°C. The glucose-monohydrate was dissolved in 200 mL of demineralised water and sterilized for 40 minutes at 110°C. The inoculum for the batch phase was prepared by suspending spores from 10 g of rice grains in 100 mL of demineralised water. The glucose solution and spore suspension were transferred to the reactor aseptically.

The composition of the chemostat feed medium was the same as the batch phase medium, except that the PAA concentration was changed as indicated in table 3.1. The PAA was dissolved in 4 L of demineralised water by continuous stirring while adding KOH pellets until a pH of 5.5 was reached. The PAA solution was autoclaved for 40 minutes at 121°C. All other components were dissolved in 46 L of demineralised water, pH set to 5.5 with KOH pellets, and filter sterilized into the vessel containing the PAA solution using Supor DCF 0.2 μm filters (Pall Gelman Sciences, East Hills, NY).

Chemostat cultivation

The strain was grown in a 7 L turbine-stirred bioreactor (Applikon, Schiedam, The Netherlands) with a working volume of 4 L under an aerobic glucose-limited regime at 25°C and a pH of 6.5 as described by Nasution et al. (2006).

Centrifugation based washing method

Cold methanol quenching combined with cold centrifugation for extracellular metabolite removal was performed according to Nasution et al. (2006). A schematic overview of the centrifugation method can be found in figure 3.1. This method consists of rapid sampling of 1 mL of culture broth into 5 mL of a -40°C 60% (v/v) aqueous methanol solution. The quenched sample was centrifuged for 5 minutes at -20°C using a swing-out rotor, precooled at -40°C, at 4800 g. After centrifugation the supernatant was removed by decantation.

Subsequently the cell pellet was washed by resuspension in 5 mL of -40°C 60% (v/v) aqueous methanol solution followed by a second cold centrifugation step and decantation of the supernatant to improve the efficiency of extracellular metabolite removal. To investigate the effect of additional washing steps on the measured intracellular amounts of metabolites related to penicillin biosynthesis, duplicate samples were subjected to one up to four additional washing steps (i.e. a maximum of five washing steps). In case of five washing steps the complete washing procedure took approximately one hour.

Further processing of the cell pellet, metabolite extraction in boiling ethanol and sample concentration and storage, was performed as described in Nasution et al. (2006).

Cold filtration based washing method

A filtration setup was designed for the rapid sampling, and cold methanol quenching, of *P. chrysogenum* broth from a bench scale fermentor, with the aim to quantify intracellular metabolites of which the extracellular amounts are high. A schematic overview of the filtration setup can be found in figure 3.1. A sampling port in the wall of the reactor was connected to a 50 cm long silicone tubing (Masterflex, L/S16, 3.1mm inner diameter). Sample was withdrawn from the port with a Masterflex peristaltic pump at a flow rate of 300 mL/min, which corresponded with a residence time of the broth in the tubing of 0.8 seconds. In order to remove stagnant biomass from the tubing, the first 5 mL of broth was discarded before pumping approximately 10 g of sample in about two seconds into 50 mL of a -40°C 60% (v/v) aqueous methanol solution, present in a vacuum filtration unit placed on a balance. The balance was used to determine the exact weight of the sample. The filtration unit contained a glass fibre filter (type A/E, Pall Corporation, East Hills, NY, USA, 47mm diameter, 1µm pore size). Filtration was started about three seconds after sampling by applying vacuum to the filtration unit. Washing of the cell cake on the filter was accomplished by pouring 50 mL of fresh -40°C 60% aqueous methanol on the cake as soon as the biomass fell dry. Up to 3 washings of the biomass on the filter could be performed within 1.5 minutes.

Once the final washing step was completed, 100 µL of a ^{13}C internal standard solution (0°C) was pipetted on top of the dry filter cake for accurate quantification purposes by IDMS (Wu et al., 2005). The ^{13}C internal standard solution contained all relevant metabolites as U-^{13}C-labeled isotopomers and was obtained from a *P. chrysogenum* fed-batch culture grown on 100 % U-^{13}C-labeled glucose and PAA. Immediately after the addition of internal standard solution the filter with washed biomass cake was transferred,

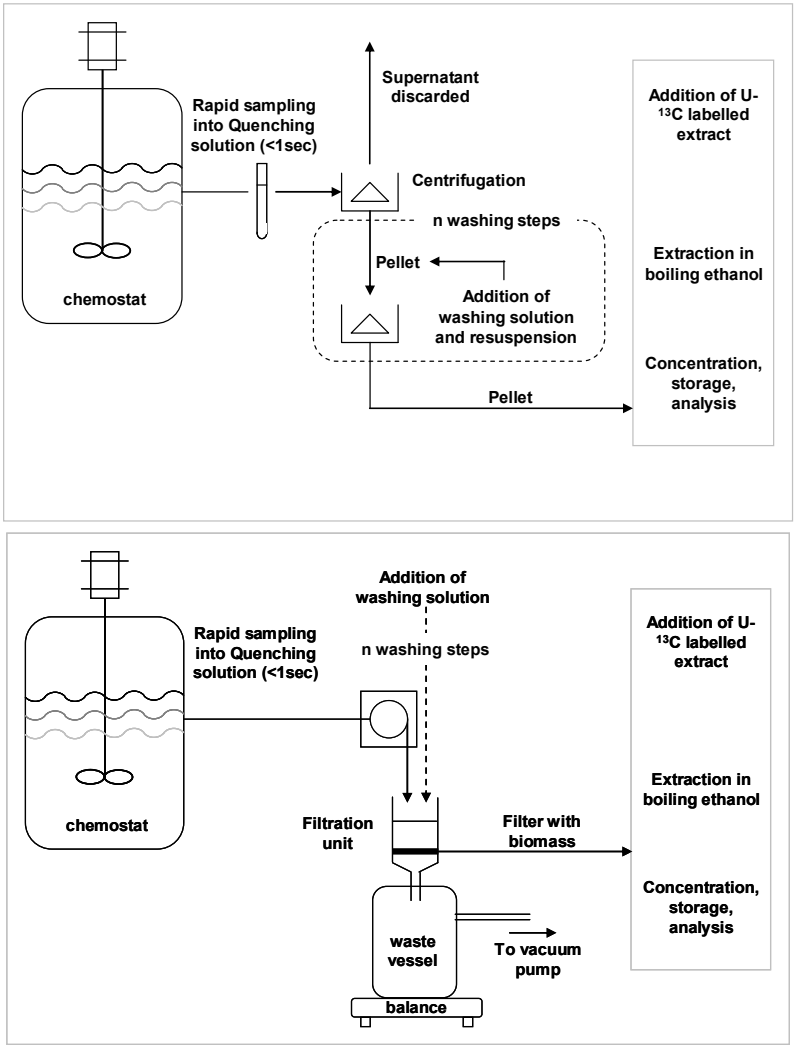

Figure 3.1 A schematic overview of the conventional cold methanol sampling procedure with cold centrifugation (top) and the cold filtration based sampling and processing procedure (bottom).

using tweezers, to a 50 mL tube containing 30 mL of a 73°C (just below boiling point) 75% (v/v) aqueous ethanol solution and completely submerged. The time to transfer the filter from the -40°C washing solution to the boiling ethanol never exceeded 5 seconds, making it unlikely for the temperature of the filter cake to rise much above -40°C. The whole procedure from sampling to submersion into ethanol took maximally 1.5 minutes for three washing steps. The tube was vigorously shaken by hand for approximately five seconds to

disintegrate the filter and to maximize contact of the biomass with the ethanol solution. The tube was then placed for 3 minutes in a water bath at 95°C for extraction of the metabolites and inactivation of the enzymes. Subsequently the tube was cooled on ice and centrifuged for 8 minutes at 4°C and 4400g. After decantation the solution was filtered using a 0.2 µm filter (FP30/0,2 CA-S, Whatman, Maidstone, England) to remove the glass fibres from the solution. The filtered solution was then concentrated under vacuum using a rapidVAP (Labconco Corparation, Kansas City, Missouri, USA) to a final volume of 500-1000 µl. Subsequently, the sample was diluted to a final volume of 1000 µl with demineralised water after which it was centrifuged for 5 minutes at 13,000g and the supernatant was stored at -80°C until analysis.

Determination of leakage

The extent of metabolite leakage induced by cold methanol quenching and washing with the cold filtration based method was examined by carrying out metabolite measurements in the different sample fractions (total broth, mycelium, culture filtrate and quenching/washing liquid) and subsequent mass balancing, according to Canelas et al. (2008). For this evaluation all samples were taken in duplicate. Extracellular metabolite concentrations were determined in culture filtrates that were collected as described below under "Rapid sampling for determination of extracellular metabolites". Sampling and sample processing for determination of intracellular metabolite amounts was carried out as described in "Cold filtration based washing method", except that approximately 3 g of broth was sampled in 15 mL cold aqueous methanol and the cell cake was washed two times with 15 mL of washing solution. After collecting the filtrate a fraction of 300 µL was transferred to an empty tube to which 100 µL of the ^{13}C internal standard solution was added. This fraction was subjected to the ethanol boiling procedure and sample concentration in the RapidVap to ensure that the final sample matrix would resemble the one of the samples for intracellular metabolite determination as close as possible. Finally, a total broth sample was obtained by sampling approximately 1 g of broth in 5 mL cold aqueous methanol using a rapid sampling device (Lange et al., 2001). After thorough mixing (vortex), a fraction of 300 µL was transferred to an empty tube to which the ^{13}C internal standard solution was added. This fraction was subjected to the ethanol boiling procedure and sample concentration in the RapidVap. The reason for processing only a small part of the culture filtrate and total broth samples was that too high concentrations of sulfate and phosphate originating from the culture medium would interfere with our LC-MS/MS based analysis method.

Rapid sampling for determination of extracellular metabolites

Rapid sampling for measurement of the extracellular metabolite concentrations was performed with the cold steel beads method as described earlier (Mashego et al., 2003). Approximately 2mL of broth was rapidly (in less than 2 seconds) transferred from the reactor, through a sampling port in the reactor wall, into a syringe containing 32 g stainless steel beads (4 mm diameter) pre-cooled at -20°C. This resulted in rapid cooling of the sample close to 0 ^{o}C, without freezing. Thereafter the sample was immediately filtered through a Millex HV 0.45 μm filter (Millipore, Bilberica, MA, USA). After addition of the ^{13}C internal standard solution, the obtained filtrate was stored in 2ml cryovials at -80ºC until analysis.

Metabolite quantification

Quantification of amino acids was carried out using GC-MS (Canelas et al., 2009). Quantification of intermediates of glycolysis and the TCA-cycle (van Dam et al., 2002) and the metabolites related to the penicillin pathway (Seifar et al., 2008) was carried out using LC-MS/MS.

Results and discussion

Chemostat cultivations

Three chemostat cultivations were carried out at a dilution rate of 0.05 h^{-1} under aerobic glucose limited conditions. After three residence times a steady-state was reached with respect to the rates of oxygen consumption, carbon dioxide production and biomass concentration. The specific penicillin-G production rate however typically increased to a maximal value during the first 100 h of C-limited growth, corresponding to a period of five residence times, and then slowly decreased. This phenomenon is usually referred to as degeneration of product formation and was observed previously for penicillin production (Righelato, 1976; van Gulik et al., 2001; Douma et al., 2010b). Table 3.1 shows the specific growth rate and specific glucose consumption rate and some relevant quantities at the moment of sampling for intracellular metabolites for the three chemostat cultivations. The carbon and degree of reduction balances closed within 5% for each of the three cultivations, using the assumption that the extracellular protein concentration is proportional to the biomass concentration.

Centrifugation based washing method

A chemostat culture of *P. chrysogenum* was run as described and used to determine the intracellular amounts of metabolites related to the penicillin biosynthesis pathway (chemostat 1). The extracellular concentrations of PenG and PAA at the time of sampling were determined to be 1.08 mM and 3.30 mM, respectively. Expressed per gram dry weight of biomass present in the chemostat, the extracellular amounts were 180 μmol/gDW of PenG and 550 μmol/gDW of PAA. Seifar et al. (2008) reported intracellular amounts of PenG and PAA of 9.6 and 12.2 μmol/gDW respectively for similar chemostat cultivations of *P. chrysogenum*. Clearly the amounts of these compounds in the extracellular medium are one order of magnitude higher than the intracellular amounts, assuming that the values reported by Seifar et al. (2008), are realistic and not affected by carry over from the medium.

However, when using the conventional centrifugation method, as was done by Seifar et al. (2008), it is unavoidable that about 0.1 to 0.3 mL of the 5 mL of the quenching or washing solution remains with the cell pellet (which originates from 1 mL of broth sample containing about 6 gDW/L of biomass) in the test tube after decantation. Assuming a specific cell volume of 2.5 mL/gDW (Jaklitsch et al., 1986; Packer et al., 1992b), only 0.015 mL of the sample consists of mycelium. This implies that, after decantation, the test tube contains only a small volume (0.015 mL) of cell pellet and a much larger volume (0.1 – 0.3 mL) of non-decanted broth/quenching fluid, resulting in a significant carry over of metabolites from the extracellular pool. Assuming that the intracellular amounts reported by Seifar et al. (2008) represent the true amounts, it can be calculated for the above case of PAA and PenG that, after decantation of the quenching solution, at least two washings with 5 mL of quenching/washing solution are required to reduce the carry over to an amount which is insignificant compared to the intracellular amount (e.g. 2% or less). To verify this we took multiple samples from a steady state chemostat of *P. chrysogenum* and subjected each sample to a different number of washing steps. After extraction of the obtained cell pellets, the amounts of eight different metabolites associated with the penicillin biosynthesis pathway were determined.

The results are shown in figure 3.2. The expectation was that the measured amounts would initially decrease with an increasing number of washing steps, whereafter they would stabilize to values representing the true intracellular amounts. However, the results do not show this expected behaviour. Every additional washing step resulted in a further decrease in the amount of each measured metabolite. It is very unlikely that the extracellular

Table 3.1 Results of the chemostat experiments. Specific rates and concentrations are shown with 1 standard error.

Chemostat	General			At time of sampling				
	μ (h^{-1})	$-q_s$ (mmol $Cmol^{-1}$ h^{-1})	$C_{PAA,in}$ (mM)	Chemostat time (h)	C_x (g L^{-1})	C_{PenG} (mM)	C_{PAA} (mM)	q_p (mmol $Cmol^{-1}$ h^{-1})
1	0.0495 ± 0.0002	19.9 ± 0.6	5.6	60	6.00 ± 0.10	1.08 ± 0.01	3.30 ± 0.01	0.25
2	0.0494 ± 0.0006	20.5 ± 0.6	4.5	90	5.79 ± 0.10	1.34 ± 0.02	2.75 ± 0.02	0.32
3	0.0518 ± 0.0003	19.7 ± 0.6	4.5	236	5.72 ± 0.02	1.04 ± 0.01	3.05 ± 0.24	0.23

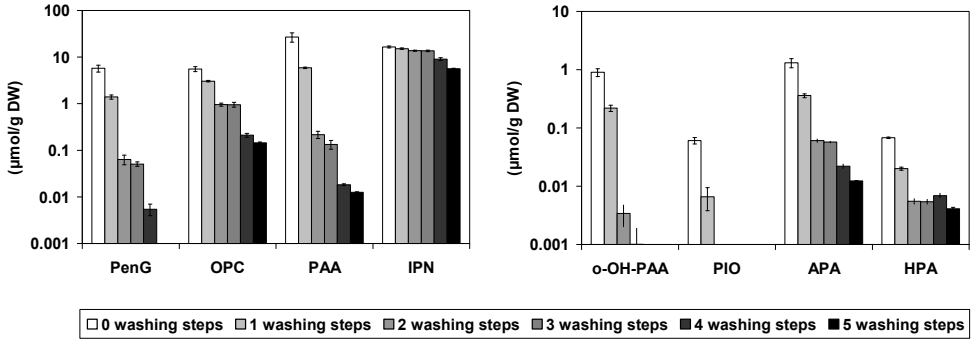

Figure 3.2 Intracellular amounts of metabolites related to penicillin biosynthesis obtained with the centrifugation method after a different number of washing steps with a -40°C 60% (v/v) aqueous methanol solution. Data are averages ± standard deviation of duplicate samples, each analyzed in duplicate.

amounts of the penicillin pathway related metabolites is so large compared to the intracellular amounts that more than 5 washing steps (i.e. a dilution of ten million times) are needed to sufficiently reduce the extracellular pool. As the contact time of the cells with the cold methanol washing solution is increased with each additional washing step (up to one hour for the maximum of five washing steps), the observed continuous decrease has been most probably caused by leakage from the cells into the washing solution. Metabolite leakage into cold methanol has been observed for several micro organisms, including eukaryotes as *Saccharomyces cerevisisae*, and the extent was found to be dependent on the time of exposure to cold methanol (Bolten et al., 2007; Canelas et al., 2008a). The above findings indicate that, unless these losses can be prevented by either modifying the composition of the washing liquid or drastically shortening the processing time, the centrifugation based washing method appears impracticable.

Cold filtration based washing method

Because centrifugation based washing for removal of extracellular metabolites appeared impracticable for our purpose, a rapid sampling procedure was developed, combining cold methanol quenching with a filtration based washing method. With this procedure, which is described in detail in the materials and methods section, the broth was sampled into an amount of cold methanol on top of a glass fiber filter. By immediate filtration after quenching of the sample, the contact time of the cells with the cold methanol could be significantly reduced. Because filtration allows a much more efficient removal of the surrounding liquid from the mycelium compared with centrifugation and subsequent

decantation, it also allows a much more efficient removal of extracellular metabolites. To evaluate the performance of the cold filtration based sampling method a similar experiment was carried out as for the evaluation of the centrifugation based sampling method. Using the cold filtration method, multiple samples were taken within a short period of time (one hour), from a similar steady state chemostat of *P. chrysogenum* (chemostat 2), whereby either zero, one, two or three washing steps with 50 mL cold methanol solution were applied. The same set of metabolites was measured as described above. Although multiple washing steps result in increased exposure to the cold methanol solution, the maximum exposure time to cold methanol, i.e. in case of three washing steps, was only 1.5 minutes and thus significantly lower than for the conventional centrifugation based quenching and washing procedure.

The results are shown in figure 3.3. It can be seen from this figure that for IPN and ACV the measured amounts were the same for the four washing conditions, showing that they represent the true intracellular amounts of these compounds. For the other metabolites the measured amounts were significantly higher when the filter cake was not washed, compared to the results after a single washing with 50 mL of cold methanol solution. These amounts did not decrease further after applying additional washing steps. The intracellular amounts of PIO and 8-HPA could not be quantified because the levels were below the detection limits (which were respectively 1.76 and 1.88 nmol/gDW, for PIO and 8-HPA) in the samples which were washed at least once. Washing of the biomass cake by filtration removes the extracellular metabolites in a plug flow manner. This is orders of magnitude more effective than the centrifugation method where the cell pellet is each time resuspended and centrifuged. Furthermore, the stabilization of the measured metabolite levels after a single washing step strongly indicates that application of the cold filtration method does not lead to significant metabolite leakage from the cells.

The need for thorough washing of the cell cake for proper measurement of the intracellular amounts of most of the metabolites associated with penicillin biosynthesis can be clearly illustrated by comparing the intracellular and extracellular amounts of these metabolites. These were measured in a separate steady state chemostat (chemostat 3) carried out under identical conditions as the previous two. To facilitate comparison, the metabolite amounts measured in the culture filtrate as well as in the cell extracts were expressed in μmol per gram biomass dry weight present in the chemostat. Mycelium samples were obtained using the cold filtration method with two washings with 50 mL cold methanol solution. The results are presented in table 3.2. The differences in intracellular metabolite amounts with

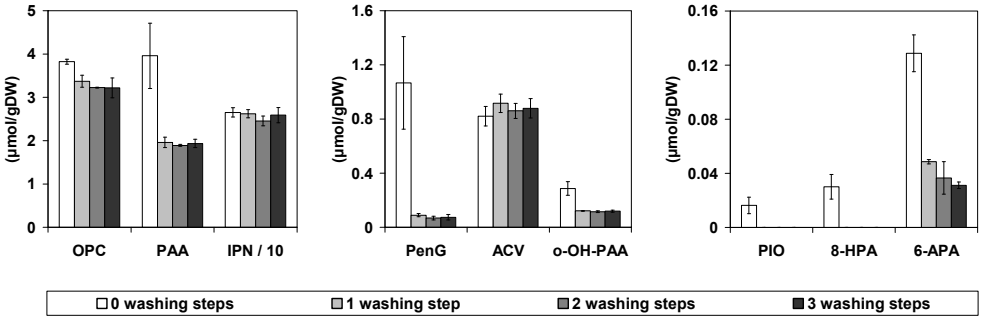

Figure 3.3 Intracellular amounts of metabolites related to penicillin biosynthesis obtained with the cold filtration method after a different number of washing steps with a -40°C 60% (v/v) aqueous methanol solution. As indicated the IPN amount is 10 times higher than depicted in the graph. Data are averages ± standard deviation of triplicate samples, each analyzed in duplicate.

the ones in figure 3.3 can be explained by the difference in culture age. Although the fermentations are very reproducible, the penicillin productivity changes with culture age as described before by Van Gulik et al. (2001). Table 3.2 clearly shows that the extracellular amounts of all metabolites, except for IPN and ACV, are 1 to nearly 4 orders of magnitude larger. Clearly, with the proposed cold filtration method such a good washing efficiency can be obtained that it can easily remove such large extracellular amounts.

Validation of the cold filtration based method with respect to metabolite leakage

To confirm whether metabolite leakage was indeed insignificant during cold filtration based sampling, an additional experiment was performed to quantify whether metabolite leakage into the cold methanol occurred during cold filtration of *P. chrysogenum* cells. Unfortunately, most of the metabolites associated with penicillin biosynthesis, are present metabolites of which the extracellular amounts were known to be low compared to the intracellular amounts. This set contained metabolites with highly different properties and consisted of large and small phosphorylated compounds, organic acids and amino acids (polar, nonpolar, aromatic and charged). The amounts of these metabolites were measured in samples of total broth, extracellular medium, cell extract, and quenching/washing filtrate. This allowed to accurately quantify leakage by comparison of metabolite amounts measured in the cell extract with amounts measured in total broth minus the amounts measured in the extracellular medium. Significantly lower amounts in the cell extract,

Table 3.2 Intracellular amounts using the cold filtration method and extracellular concentrations of metabolites in steady-state

Metabolite	Intracellular amount (µmol/gDW)	Extracellular concentration (mM)	Extracellular amount (µmol/gDW)	Ratio of amounts (Ex/In) (-) a)	Ratio of concentrations (Ex/In) (-) b)
PenG	0.037 ± 0.006	1.038 ± 0.003	181.5 ± 0.8	4905 ± 796	71 ± 11
6-APA	0.017 ± 0.006	0.45 ± 0.06	79 ± 10	4628 ± 1746	67 ± 27
PIO	0.003 ± 0.001	0.015 ± 0.001	2.6 ± 0.2	874 ± 297	15 ± 4
o-OH-PAA	0.17 ± 0.01	0.33 ± 0.02	58 ± 4	339 ± 29	4.9 ± 0.3
OPC	1.13 ± 0.04	0.24 ± 0.01	42 ± 2	37 ± 2	0.53 ± 0.04
PAA	2.97 ± 0.18	3.05 ± 0.24	533 ± 42	180 ± 18	2.6 ± 0.3
HPA	0.0029 ± 0.0002	0.023 ± 0.003	4.0 ± 0.5	1387 ± 205	20.5 ± 3.2
ACV	0.39 ± 0.02	0.0001 ± 0.0001	0.02 ± 0.02	0.045 ± 0.045	0.001 ± 0.001
IPN	1.08 ± 0.03	0.008 ± 0.001	1.4 ± 0.2	1.3 ± 0.2	0.019 ± 0.002

Samples were taken in triplicate and each was analyzed in duplicate. The numbers show the average of the three samples ±1 standard deviation.

a) The amount ratio is calculated as extracellular amount (µmol extracellular/gDW) divided by intracellular amount (µmol intracellular/gDW).

b) The ratio is calculated as extracellular concentration (mM) divided by intracellular concentration (mM). For the intracellular concentration a homogeneous distribution of metabolites within the cells and a cell specific volume of 2.5 mL/gDW (Jaklitsch et al., 1986; Packer et al., 1992b) was assumed.

corresponding with increased amounts in the filtrate after quenching, would be a proof for leakage. The results are shown in figure 3.4. It can be seen from this figure that there is no difference between the metabolite amounts measured in total broth (left bars) and the amounts measured in the cell extract plus the quenching liquid (right bars). Furthermore in such high amounts in the extracellular medium that quantification of leakage from the cells is infeasible. Therefore the occurrence of leakage was checked for a set of primary there is no significant difference between the dark grey and the black areas, which respectively represent the calculated intracellular amounts (total broth minus filtrate) and the amounts measured in the cell extract. Unfortunately the presence of salts and the large dilution factors of the total broth and filtrate samples resulted in relatively large standard errors for these measurements. Nevertheless the results show clearly that metabolite leakage is not significant in *P. chrysogenum* for this set of metabolites with very diverse properties, using the cold filtration based washing procedure.

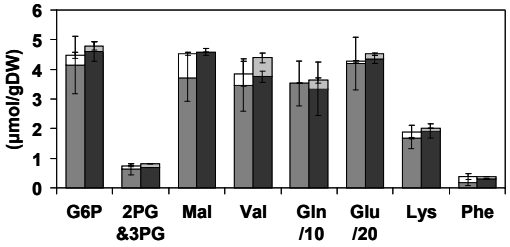

Figure 3.4 Mass balances for glucose-6-phosphate (G6P), 2-phosphoglycerate and 3-phosphoglycerate (2PG&3PG), malate (Mal), valine (Val), glutamine (Gln), glutamate (Glu), lysine (Lys) and phenylalanine (Phe). The left bars represent the measured amounts of metabolites in total broth, whereby the white part represents the measured amounts in the culture filtrate and the dark grey part the calculated intracellular amount (total broth – extracellular). The right bars show the measured intracellular amounts (black part) and the amounts measured in the quenching/washing solutions (light grey). As indicated the Gln amount is 10 times higher than depicted and the Glu amount is 20 times higher than depicted. Error bars indicate standard deviations for duplicate samples.

Intracellular amounts of metabolites related to penicillin biosynthesis

The concentration ratio (table 3.2) shows that the intracellular concentration of PenG was about two orders of magnitude lower than its extracellular concentration. This is in agreement with the conclusion of others that PenG is actively transported out of the cell (van den Berg et al., 2001b; Martin et al., 2005). Uptake of PAA is nowadays believed to occur through passive diffusion of the undissociated acid over the cell membrane (Hillenga et al., 1995), although earlier studies concluded there is a specific uptake mechanism for undissociated PAA (Fernández-Cañón et al., 1989b). It can be calculated that in case of

passive diffusion of the undissociated acid, for a culture pH of 6.5 and assuming a for filamentous fungi typical cytosolic pH of 7.2 (Legerton et al., 1983b; Legisa and Kidric, 1989; Pilatus and Techel, 1991; Sanders and Slayman, 1982), the ratio of the extracellular to the intracellular concentration of PAA at thermodynamic equilibrium is equal to 0.20. The observed ratio of 2.6 ± 0.3 implies that the free energy for import is negative which agrees with the direction of PAA transport. Furthermore the system is relatively far from thermodynamic equilibrium, which indicates that PAA transport might be limiting. This could e.g. be caused by a low membrane permeability coefficient in case of passive diffusion or the existence of a specific facilitated transport system for phenylacetic acid.

Table 3.3 Turnover times of metabolites related to penicillin biosynthesis.

Metabolite	Turnover time (s)
IPN	3×10^2
PAA	9×10^2
ACV (total)	1×10^2
6-APA	3×10^1
Pen-G	2×10^1

The turnover times for the metabolites in the penicillin biosynthesis pathway can be calculated from the measured intracellular amounts and the specific rates of PenG production, 6-APA production and PAA uptake. These turnover times are presented in table 3.3. For a number of the metabolites, like 6-APA and PenG, the turnover time appears to be only a few tens of seconds. This is surprising because it shows that not only primary but also secondary metabolites can have short turnover times. This shows that realistic values of their intracellular amounts can only be obtained when proper rapid sampling and quenching procedures are applied. With the proposed cold filtration based sampling method the time until quenching is approximately 0.8 seconds, which is sufficiently lower than the turnover time of all metabolites involved in the penicillin biosynthesis pathway.

Different conditions require different protocols

Many sampling protocols exist that aim at the quantification of intracellular metabolite amounts. A proper sampling protocol should be sufficiently effective in preventing changes in the amounts of the intracellular metabolites of interest after sampling, i.e. by immediate quenching of all enzymatic activity, and removal of extracellular amounts of these metabolites, if present. Figure 3.5 shows which characteristics of a sampling protocol are

important for different combinations of the intra- and extracellular abundance and turnover time of the metabolites to be quantified. The way different metabolites are distributed among the scenarios in figure 3.5 is highly organism and cultivation condition dependent. The examples given in the figure are specific for the *P. chrysogenum* strain cultivated in this study. Preventing changes in the amounts of the intracellular metabolites of interest (i.e. quenching) is of absolute importance in case of rapid turnover of metabolites, i.e. in scenarios I, II and V. Efficient removal of extracellular metabolites is of high importance in case of high extracellular amounts, i.e. for scenarios IV and V. To our best knowledge none of the existing methods is suitable for proper quantification of intracellular metabolites in case of scenario V (very high extracellular amounts compared to the size of the intracellular pool). The cold filtration method described in this paper complies with the prerequisites of scenario V, namely immediate quenching and highly effective washing.

Although a few sampling protocols have been described in literature that somewhat resemble the cold filtration protocol described here, they would, to our opinion, be ineffective for quantification of the set of metabolites investigated in this study. Wittman et al. (2004) applied rapid filtration and subsequent washing with a 0.9% NaCl washing solution at room temperature for *Corynebacterium glutamicum*. Because their procedure did not include a quenching step it was only possible to quantify metabolites with large turnover times. For our set of metabolites, the rapid turnover of some of them necessitates quenching. Sáez and Lagunas (1976) used filtration and washing of the cell cake of *Saccharomyces cerevisiae* with -40°C 50% (v/v) aqueous methanol to remove extracellular metabolites. However, instead of immediately quenching metabolism by directly sampling into cold aqueous methanol, they only minimized the sample processing time by dividing their samples in ten portions which are processed separately. Ruijter and Visser (1996) developed a procedure in which *Aspergillus niger* cells are rapidly sampled in cold methanol and extracellular metabolites were separated by vacuum filtration. However, vacuum filtration was not carried out immediately, but 5 to 10 minutes after sampling. The authors presented results to show the absence of leakage within 30 minutes after sampling for the 14 metabolites they analyzed. This is, however, not surprising as 11 of the 14 metabolites analyzed were phosphorylated compounds, and relatively large compounds like NAD^+ and NADH. It was demonstrated for *Saccharomyces cerevisiae* that phosphorylated, charged and bulky metabolites leak insignificantly into cold methanol (Canelas et al., 2008a). In contrast to these 13 metabolites, the intracellular amount of pyruvate, which is small and not phosphorylated and therefore more likely to leak, was reported to drop from 0.2 to 0.1 nmol/mL (Ruijter and Visser, 1996). As shown in figure 3.4, no metabolite

leakage could be detected for our cold filtration method for a set of metabolites with highly different properties.

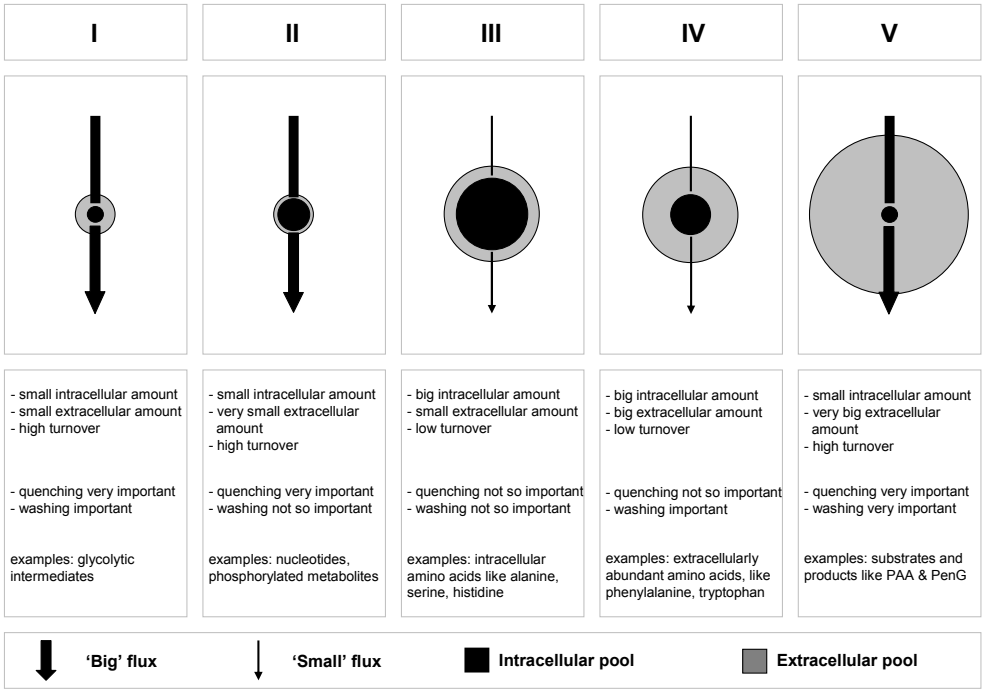

Figure 3.5 Different scenarios for intracellular metabolite sampling. The width of the arrows indicates the magnitude of the flux. The area of the black part of the circle indicates the size of the intracellular pool and the area of the grey part of the circle the size of the extracellular pool. The mentioned examples are specific for P. chrysogenum as cultivated in this study.

Our cold filtration based washing protocol can in principle be applied to measure all metabolites in organisms which do not show cold-shock behavior or significant metabolite leakage during short term exposure to cold solvent/water mixtures. The protocol especially enables to measure intracellular substrate levels, when the amounts of substrates in the extracellular medium are relatively high. This is of particular interest in strains, which are metabolically engineered to grow on non-natural substrates and for which the capacity of transport systems might still be a bottleneck (e.g. yeast strains able to grow on C5 sugars like xylose and arabinose). Such limitations would be revealed by a very low intracellular substrate concentration. Also intracellular amounts of other medium components like ammonium or phosphate can be determined, allowing the study of their transport kinetics. Furthermore, our sampling method allows the study of transport energetics and kinetics of

secreted products (e.g. penicillin-G) under in-vivo conditions. Another advantage of the cold filtration method is that extracellular salts from the medium are more thoroughly removed from the sample, which reduces problems with interference of these compounds with LC-MS/MS based analysis methods. Drawback of the current method is that, due to the many manual handlings, the number of samples that can be withdrawn in certain timeframe is limited. This is a problem for stimulus response experiments when rapid changes in metabolite amounts need to be observed. However, if the procedure would be (partly) automated this problem could be solved.

Conclusions

A method combining rapid sampling with cold methanol quenching and cold filtration based washing was developed and found to be especially suitable for the determination of intracellular amounts of metabolites which abundantly appear in the extracellular environment of the cells. The washing efficiency of the method appeared much higher than washing by repeated resuspension, cold centrifugation and decantation as applied in the conventional cold methanol quenching procedure. Our method allows immediate cold filtration and washing after quenching of the sample, and thus assures a short contact time (maximum 1.5 minutes in case of three washings) of the cells with the washing liquid, thereby minimizing metabolite leakage. The results obtained with this method proved to be reproducible. A surprising result was that the turnover time of several metabolites in a secondary metabolic pathway, i.e. penicillin biosynthesis, was only a few tens of seconds. Because of its high washing efficiency, this method is very well suited for the study of *in vivo* kinetics of transport of substrates and products.

Acknowledgements

This project is financially supported by the Netherlands Ministry of Economic Affairs and the B-Basic partner organizations (www.b-basic.nl) through B-Basic, a public private NWO-ACTS programme (ACTS: Advanced Chemical Technologies for Sustainability). This project was carried out within the research programme of the Kluyver Centre for Genomics of Industrial Fermentation which is part of the Netherlands Genomics Initiative / Netherlands Organization for Scientific Research. The authors would like to thank Zheng Zhao for providing *P. chrysogenum* U-13C-labeled cell extract.

CHAPTER 4

Novel insights in transport mechanisms and kinetics of phenylacetic acid and penicillin-G in *Penicillium chrysogenum*

Abstract - Although penicillin-G (PenG) production by the fungus *Penicillium chrysogenum* is a well-studied process, little is known about the mechanisms of transport of the precursor phenylacetic acid (PAA) and the product PenG over the cell membrane. To obtain more insight in the nature of these mechanisms, in vivo stimulus response experiments were performed with PAA and PenG in chemostat cultures of *P. chrysogenum* cultures at time scales of seconds to minutes. The results indicated that PAA enters the cell by passive diffusion of the undissociated acid at a high rate, but is at the same time actively excreted, possibly by an ABC transporter. To validate this assumption, a mathematical model was constructed, including passive diffusion of the undissociated acid over the membrane and active export. With this model a good description of the dynamic data could be obtained. It was found that PenG was rapidly taken up by the cells upon extracellular addition, indicating that PenG transport is reversible. The measured concentration gradient of PenG over the cell membrane corresponds well with transport in the absence of ATP hydrolysis. Also for PenG a simple kinetic model was constructed and validated with experimental data. The model confirmed the presence of a facilitated transport system for PenG.

Douma RD, Deshmukh AT, De Jonge LP, De Jong BW, Seifar RM, Heijnen JJ, Van Gulik WM. Novel insights in transport mechanisms and kinetics of phenylacetic acid and penicillin-G in *Penicillium chrysogenum* (submitted for publication).

Introduction

Fermentation processes are increasingly used to produce fine and bulk chemicals. Improvement of these processes is often approached by genetically increasing the flux capacity from substrates to product within the micro organism. An important aspect for increasing production rates is the presence of suitable transport proteins, for importing the substrate(s) and exporting the product with sufficient affinity and capacity. Relatively little has been published about transport of substrate into the cell and of product out of the cell even though inefficient transport can dramatically limit the substrate and product fluxes. Transport mechanisms have been reviewed for filamentous fungi (Burgstaller, 1997) and *Saccharomyces cerevisiae* (van der Rest et al., 1995) amongst others.

Penicillin has been produced for more than 50 years via industrial fermentation and is a good example of a well-established fermentation process with an annual market of $5 billion in 1999 (Demain and Elander, 1999). If the side-chain precursor phenylacetic acid (PAA) is supplied to the medium of *Penicillium chrysogenum,* it produces penicillin-G (PenG), which is excreted into the medium. Although penicillin production in *P. chrysogenum* is a well-studied process, there is still debate about the mechanisms behind the transport of PAA and PenG across the plasma membrane.

Hillenga et al. (Hillenga et al., 1995) concluded that the uptake of PAA occurs through passive diffusion of the undissociated acid over the cell membrane, which was supported by Eriksen et al. (Eriksen et al., 1998). However, in an earlier study a specific protein mediated uptake mechanism for undissociated PAA was identified (Fernández-Cañón et al., 1989b). The latter claim was supported by a functional category analysis on the effect of PAA on genome wide expression levels in *P. chrysogenum* (Harris et al., 2009), which revealed that several transport-related genes were up regulated in the presence of PAA. In this study no distinction could be made, however, between uptake or secretion mechanisms. It was found that *S. cerevisiae* is able to actively excrete the anion form of PAA, using an ATP-binding cassette (ABC) transporter Pdr12, as a detoxification mechanism(Hazelwood et al., 2006). The authors showed that, although also in the wild type strain the presence of PAA resulted in a decrease of the growth rate in batch culture, the growth rate of Pdr12Δ strains was significantly lower under these conditions.

Measurement of the intracellular concentration of PAA of *P.* chrysogenum cells cultivated in the presence of the acid, revealed that the concentration was significantly lower than the

calculation based on thermodynamic equilibrium (Douma et al., 2010a). This could be caused by a low membrane permeability coefficient in case of passive diffusion or the presence of a specific facilitated uptake system for PAA with a low capacity. Alternatively there could be active export and simultaneous passive import (as shown in *S. cerevisiae*). This would result in an energy consuming futile cycle.

Although many groups have been studying the transport of antibiotics over the cell membrane, very little is known about the mechanism of penicillin export in *P. chrysogenum.* Nijland et al. (Nijland et al., 2008) found that the expression of the *cefT* gene of *Acremonium chrysogenum* results in an increased cephalosporin secretion rate in *P. chrysogenum,* showing the implications of transport over the cell membrane for the productivity. Although no irrefutable evidence has been provided, secretion of PenG from the cell was linked to the presence of the ABC transporter (van den Berg et al., 2001a; Martin et al., 2005; Andrade et al., 2000).

To obtain more insights in the mechanisms, thermodynamics and kinetics of transport of PAA and PenG in whole cells of *P. chrysogenum*, different stimulus response experiments with glucose limited *P. chrysogenum* chemostat cultures were performed on different time scales using a recently developed rapid sampling and washing method (Douma et al., 2010a). A short (seconds) time frame pulse experiment was performed in which PAA and PenG were pulsed into a chemostat where PAA and PenG were absent due to cultivation in absence of PAA. During these experiments the intracellular levels of PAA and PenG and the oxygen consumption and carbon dioxide production were measured. To get more insights in the mechanisms of transport, a mathematical model for PAA and PenG transport was constructed. The model parameters were derived using the experimental results from these pulse experiments.

The model structure was validated on a long (minutes) time frame ramp experiments. In these ramp experiments the intracellular concentration of PAA and PenG was monitored in a PenG producing culture in which extracellular PAA and PenG concentrations were increased linear over a large concentration range in time over a period of tens of minutes. The oxygen consumption was monitored to reveal the presence of a possible futile cycle in PAA transport.

Theoretical aspects

Kinetics of PAA transport

In solution PAA attains a pH dependent equilibrium between the undissociated (HPAA) and dissociated (PAA^-) forms:

$$HPAA \rightleftharpoons PAA^- + H^+ \qquad (4.1)$$

With the dissociation equilibrium constant $K = \frac{C_{H^+} \cdot C_{PAA^-}}{C_{HPAA}}$ and the total phenylacetic acid concentration $C_{PAA} = C_{HPAA} + C_{PAA^-}$. The pH dependent concentration of undissociated HPAA is formulated as a function of the total acid (C_{PAA}):

$$C_{HPAA} = \frac{C_{PAA}}{1+10^{pH-pK}} \qquad (4.2)$$

The undissociated form of apolar weak acids, such as phenylacetic acid, can easily permeate through cell membranes (Burgstaller, 1997; van der Rest et al., 1995), whereby the concentration gradient of the undissociated acid over the cell membrane is the driving force for passive import of PAA.

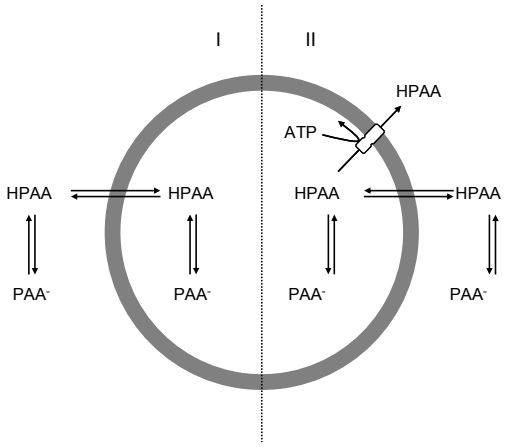

Figure 4.1 Different hypotheses for transport of PAA in P. chrysogenum over the plasma membrane: (I) passive diffusion alone and (II) passive diffusion in combination by active export by an ABC transporter.

Figure 4.1 shows two possible hypotheses for PAA transport. In hypothesis I there is only uptake by passive diffusion of the undissociated form of PAA (Hillenga et al., 1995). Hypothesis II combines uptake by passive diffusion of the undissociated form of PAA with active export with ATP dissipation as is the case in *S. cerevisiae* (Hazelwood et al., 2006), leading to an energy consuming futile cycle.

In hypothesis I with passive diffusion only, the net influx of PAA can be written as:

$$q_{diff,HPAA} = k_{diff,HPAA} \cdot A \cdot \left(\frac{C_{PAA,ex}}{1+10^{pH_{ex}-pK}} - \frac{C_{PAA,in}}{1+10^{pH_{in}-pK}} \right) \quad (4.3)$$

In which $k_{diff,HPAA}$ ($m \cdot h^{-1}$) is the membrane permeability constant for PAA, A ($m^2 \cdot CmolDW^{-1}$) is the biomass specific membrane surface area and $C_{PAA,ex}$ and $C_{PAA,in}$ are the total phenylacetic acid concentrations outside and inside the cell. The specific area A can be calculated, assuming that the *P. chrysogenum* cell has a cylindrical shape and the top and bottom ends are not taken into account (Packer et al., 1992a), as:

$$A = \frac{4}{d_{cell}} \cdot V_x \quad (4.4)$$

Herein V_x is the specific cell volume, $7.0 \cdot 10^{-5}$ $m^3 \cdot CmolDW^{-1}$ (Packer et al., 1992a; Jaklitsch et al., 1986), and d_{cell} is $5 \cdot 10^{-6}$ m (Packer et al., 1992a). The total acid concentration ratio (in / ex) in thermodynamic equilibrium is given by the following equation:

$$\left(\frac{C_{PAA,in}}{C_{PAA,ex}} \right)^{eq} = \frac{1+10^{pH_{in}-pK}}{1+10^{pH_{ex}-pK}} \quad (4.5)$$

As shown by Douma et al. (Douma et al., 2010a) the (in / ex) equilibrium ratio can be calculated to equal 5.0 assuming an extracellular pH of 6.5 and an intracellular pH of 7.2, which is typical for filamentous fungi (Pilatus and Techel, 1991; Legerton et al., 1983a; Legisa and Kidric, 1989; Sanders and Slayman, 1982).

Active export of PAA in hypothesis II (figure 4.1) is assumed to occur by an irreversible ABC exporter which exports PAA^- + H^+. This exporter can be modeled by Michaelis-Menten kinetics with respect to the total intracellular PAA concentration as:

$$q_{\sec,PAA} = \frac{k_{\exp ort,PAA}}{1 + K_{m,PAA\exp ort} \cdot C_{PAA}^{-1}} \tag{4.6}$$

In which $k_{export,PAA}$ (mmol·CmolDW^{-1}·h^{-1}) is the rate constant, while $K_{m,PAAexport}$ (mmol·CmolDW^{-1}) is the affinity constant of the exporter expressed in total acid.
HPAA export occurs against the concentration gradient and herewith requires energy. The additional oxygen consumption rate can be modeled by considering that the ABC transporter requires 1 mol of ATP to excrete 1 mol of undissociated PAA and that respiratory ATP generation yields P/O mol ATP per ½ mol O_2 consumed. Using the relation for $q_{sec,PAA}$ (equation 4.6) this leads to the following oxygen consumption rate due to PAA export:

$$q_{O_2,PAA} = \frac{q_{\sec,PAA}}{2 \cdot (P/O)} \tag{4.7}$$

The P/O ratio used for our calculations was the experimentally determined maximal value of 1.84 by van Gulik et al. (van Gulik et al., 2001).

Kinetics of PenG transport

For a charged solute A^Z the Gibbs energy associated with facilitated export is:

$$\Delta G = RT \ln\left(\frac{C_{ex,A^Z}}{C_{in,A^Z}}\right) - Z \cdot F \cdot \Psi_{in} \tag{4.8}$$

with Z the charge of the transported species, F the Faraday constant of 96.5 kJ·V^{-1}·mol^{-1}, Ψ (V) the intracellular electrical potential (note that $\Psi < 0$) and C the concentration.

Figure 4.2 shows three possible mechanisms for the export of PenG (which is a negatively charged molecule, Z = 1) namely facilitated export, export by proton antiport and export with ATP hydrolysis using an ABC transporter. The equilibrium constants for these three different mechanisms are respectively:

$$\left(K_{eq,penG}\right)_{fac} = \frac{C_{ex}}{C_{in}} = e^{\frac{-1 \cdot F \cdot \Psi_{in}}{R \cdot T}} \tag{4.9}$$

$$\left(K_{eq,penG}\right)_{antip} = \frac{C_{ex}}{C_{in}} = \frac{C_{H^+,ex}}{C_{H^+,in}} e^{\frac{-2 \cdot F \cdot \Psi_{in}}{R \cdot T}} = 10^{pH_{in} - pH_{ex}} \cdot e^{\frac{-2 \cdot F \cdot \Psi_{in}}{R \cdot T}} \tag{4.10}$$

$$\left(K_{eq,penG}\right)_{ABC} = \frac{C_{ex}}{C_{in}} = e^{\frac{-1\cdot F\cdot\Psi_{in}-\Delta G_p}{R\cdot T}} \qquad (4.11)$$

Under physiological conditions the energy gained from ATP hydrolysis (ΔG_p) is approximately -50 kJ·mol^{-1} (Nelson and Cox, 2000).

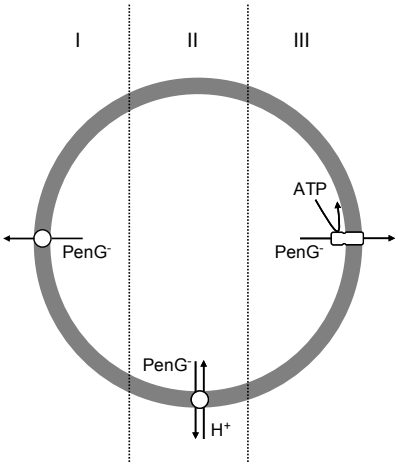

Figure 4.2 Different hypotheses for transport of PenG in P. chrysogenum over the plasma membrane: (I) facilitated diffusion of the anion of PenG driven by the membrane potential, (II) proton antiport of the anion of PenG and (III) active export by an ABC transporter.

As shown in Appendix I the kinetics of facilitated secretion of PenG can be described as:

$$q_{\mathrm{sec},PenG} = q_{\mathrm{sec},PenG}^{\max}\cdot\left(1-\frac{C_{PenG,ex}}{C_{PenG,in}\cdot\left(K_{eq,penG}\right)_{fac}}\right) \qquad (4.12)$$

Materials and methods

Strain

A high penicillin producing strain of *P. chrysogenum* (DS17690) was kindly donated by DSM Biotechnology Center (Delft, The Netherlands). This strain was used for all experiments.

Media

All cultivation medium was prepared according to Douma et al. (Douma et al., 2010a), except that the PAA and PenG concentrations in the medium were adapted as indicated in table 4.1. PenG was added aseptically to the PenG ramp medium using a 0.2 µm filter (FP30/0.2 CA-S, Whatman, Maidstone, England).

Table 4.1 Cultivation medium composition was according to Douma et al. (Douma et al., 2010a), with the exception of PAA and PenG concentration in the medium.

Medium	PAA concentration (mM)	PenG concentration (mM)
-PAA medium	0	0
+PAA medium	5	0
PAA-ramp medium	80	0
PenG-ramp medium	0	80

Chemostat cultivation

Aerobic, glucose limited chemostat cultivations were performed in 7 L turbine stirred bioreactors with a working volume of 4 L. All cultivations were performed at a dilution rate of 0.05 h^{-1}, a cultivation temperature of 25°C, a pH of 6.50 ± 0.05 and 0.3 bar overpressure. Further details can be found in Nasution et al. (Nasution et al., 2006a). The aeration rate in the PAA and PenG pulse experiments was 1 $L \cdot min^{-1}$ instead of 2 $L \cdot min^{-1}$ to obtain better resolution in the offgas data.

Perturbation experiments

A schematic representation of the perturbation experiments can be found in figure 4.3. The pulse experiments were performed using chemostat cultivations without PAA in the feed medium (–PAA medium). After 5 residence times of chemostat cultivation the pulse experiments of PAA and PenG were initiated by rapidly injecting the described pulse solution. Ramp experiments were performed in chemostats cultivated with PAA in the medium (+PAA medium) leading to the presence of about 2 mM of PAA and 2 mM of PenG in the culture broth during steady-state. After 5 residence times the medium supply was switched from chemostat feed medium to ramp medium (with the same feed rate of carbon source). During all perturbation experiments samples for intra- and extracellular PAA and PenG were taken. There was no DO control active during the pulse experiments.

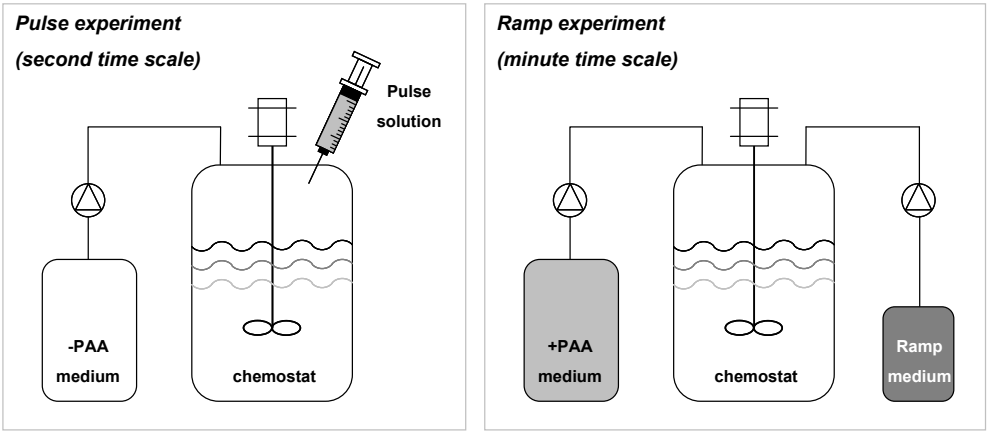

Figure 4.3 Schematic representations of the perturbation experiments. On the left a pulse experiment (seconds time scale) which is started by adding a pulse solution to a chemostat. On the right a ramp experiment (minutes time scale) which is started by switching from chemostat medium to ramp medium.

Pulse solutions

The solutions for the pulse experiments were prepared by dissolving 40 mmol of undissociated PAA (M_w = 136.15 g·mol^{-1}) in 20 mL of H_2O and dissolving 40 mmol of KPenG (M_w = 372.48 g·mol^{-1}) in 30 mL of H_2O. The pH in the PAA solution was set to 6.5 with KOH.

Rapid sampling for intracellular metabolites

Samples for intracellular metabolite determination were taken by rapid sampling. For the ramp experiments 10 mL broth samples were taken into a rapid, cold filtration unit containing 50 mL of quenching and washing solution (in all cases -40°C 60% v/v aqueous methanol) (Douma et al., 2010a). After filtration the filter cake was immediately washed 2 times with 50 mL of washing solution. To facilitate sampling at second time scale during pulse experiments the rapid sampling method of Lange et al. (Lange et al., 2001) was combined with the sample processing method of Douma et al. (Douma et al., 2010a). Broth samples of 1 mL were quenched within one second in a tube containing 5 mL of cold aqueous quenching and washing solution using the rapid sampling device as described by Lange et al. (Lange et al., 2001) to ensure rapid sampling and allow to take multiple samples in a short time frame. Immediately after sampling the content of the tube was transferred to a filtration unit containing 50 mL of washing solution. The tube was rinsed twice with the washing solution to ensure quantitative transfer of the cells to the filtration

unit. After filtration the filter cake was immediately washed with 2 x 50 mL of washing solution.

For accurate quantification with IDMS (Wu et al., 2005), 100 µL of U-^{13}C labeled *P. chrysogenum* cell extract was added as internal standard to all filters containing the cold quenched biomass. Subsequently the filters containing the cell cakes were extracted using the boiling ethanol method and further processed towards MS-MS based quantification as described previously (Douma et al., 2010a). The complete procedure of sampling and subsequent sample processing until the boiling ethanol extraction took maximally one minute.

Samples of culture filtrate were taken using the cold steel beads method (Mashego et al., 2003) as described earlier (Douma et al., 2010a) for extracellular PAA and PenG analysis.

Validation experiment of the washing procedure intracellular metabolite amounts

To investigate whether the applied filtration based washing method completely removed all extracellular metabolites, a validation experiment was performed. Therefore a 1 mL sample from a chemostat culture grown in the absence of PAA was rapidly withdrawn and immediately quenched in 5 mL -40°C 60% v/v aqueous methanol solution containing ^{13}C labeled PAA and PenG (> 2mM each). This sample was further processed using the cold filtration method according to Douma et al. (Douma et al., 2010a) and analyzed for its contents of ^{13}C labeled PAA and PenG.

Analytical procedures

Quantification of intracellular PAA and PenG was performed according to Seifar et al. using IDMS (Seifar et al., 2008). Extracellular PAA and PenG were obtained with HPLC-UV according to Christensen et al. (Christensen et al., 1994). Biomass concentration and offgas analysis were performed as described previously (van Gulik et al., 2000).

Parameter estimation

In order to determine the kinetic parameters for the model, parameter estimation was performed by minimizing the sum of squares using the following equation (Moles et al., 2003).

$$\min \frac{\left\| x_{data} - x_{sim} \right\|^2}{\sigma^2} \qquad (4.13)$$

In which $x_{sim} = \int_{t_i}^{t_f} \frac{dx}{dt} dt$

Simulations

All simulations of intracellular and extracellular PAA and PenG concentrations during perturbation experiments were performed using the mass balances described in appendix II using MATLAB 7.9.0.

Results and discussion

Chemostat cultivations

The chemostat cultivations used for the perturbation experiments in this study were replicates of the ones carried out by Douma et al. (Douma et al., 2010a). The cultivations were very reproducible and the carbon and degree of reduction balances closed within 5% for each of the six cultivations.

Validation experiment of the washing procedure

Culture broth from chemostat cultivations was sampled into a tube containing ^{13}C labeled PAA and PenG in concentrations higher than 2 mM in a -40°C 60% v/v aqueous methanol solution. Samples were processed and analyzed as described in the section materials and methods to analyze whether extracellular ^{13}C labeled PAA and PenG would be found in the washed biomass. No labeled PAA and PenG could be found in the cell extract, while the limits of detection were 0.0090 μmol·gDW^{-1} for PAA and 0.0016 μmol·gDW^{-1} for PenG. This proves the efficiency of the filtration method to remove extracellular metabolites. Furthermore, this clearly shows that extracellular PAA and PenG do not enter the cells during cold methanol quenching nor bind to the cell membrane of *P. chrysogenum*.

PAA transport

Two independent chemostat cultures without PAA in the feed medium were subjected to an instantaneous increase in the extracellular concentration of PAA from 0 to 10 mM. The biomass concentration at steady state was about 6 g/L. The results of the PAA pulse for these two independent experiments are shown in figure 4.4. It can be seen from this figure

that the sudden extracellular abundance of PAA resulted in a fast increase in the intracellular PAA level.

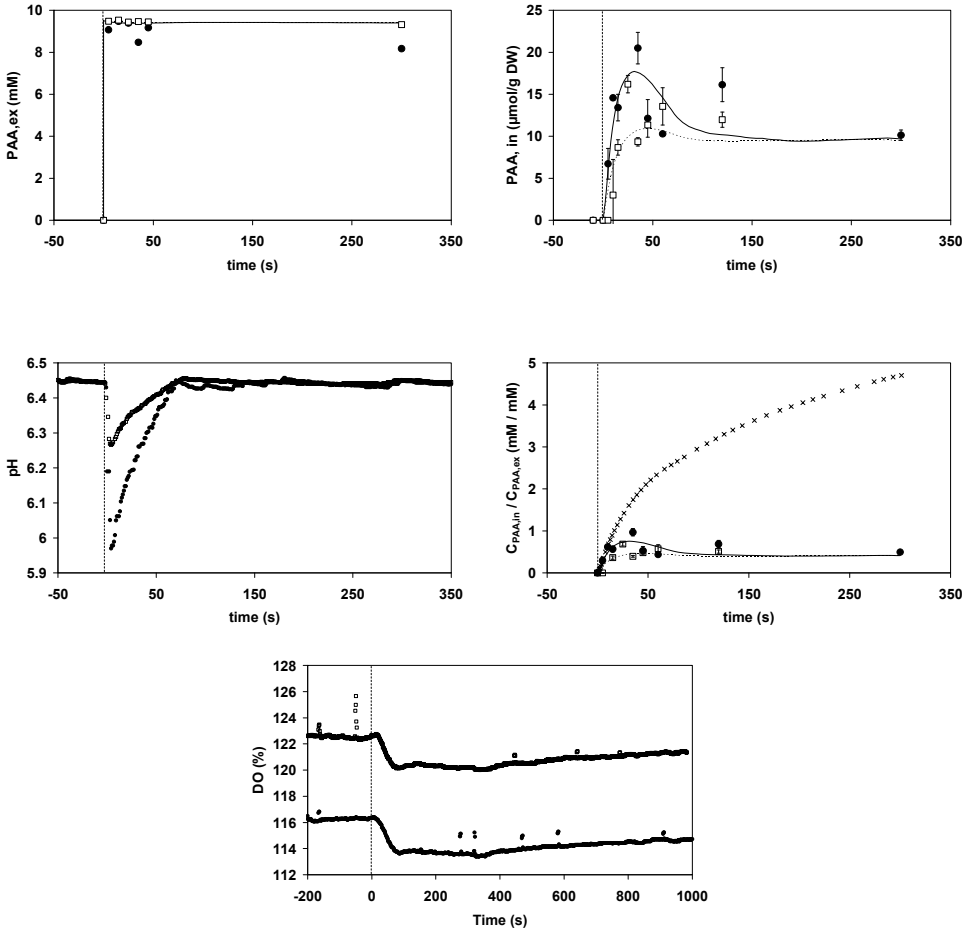

Figure 4.4 PAA pulse 1&2: extracellular PAA concentration, intracellular PAA concentration, pH, ratio of intracellular to extracellular concentration and dissolved oxygen. Experimental data of pulse experiment 1 (●) and pulse experiment 2 (□), model prediction of pulse experiment 1 (—), pulse experiment 2 (--) and model based on passive diffusion alone at pH_{in} = 7.2 and the measured pH_{ex} during PAA pulse 1 (xx). The pulse solution was added to the reactor at t = 0 s.

Interestingly, the PAA pulse resulted in an overshoot of the intracellular PAA level, with a maximum around 30 seconds, corresponding with the sudden decrease of the culture pH after injection of the PAA solution. Furthermore, it can be seen from the results of the two

independent experiments that the more pronounced decrease of the pH in experiment 1 coincides with a more pronounced overshoot of the intracellular PAA level. This observation indicates that PAA enters the cells via passive diffusion of the undissociated acid. If this is the only transport mechanism present and the rate of PAA consumption, e.g. for penicillin synthesis, is negligible compared to the rate of diffusion of PAA into the cells, the intracellular PAA level would reach its thermodynamic equilibrium. For a cultivation pH of 6.5 and assuming a cytosolic pH of 7.2 it can be calculated that the ratio of the intracellular to the extracellular concentration of PAA at thermodynamic equilibrium would be equal to 5.0 (Douma et al., 2010a). However, approximately 50 seconds after the PAA pulse a stable ratio of about 0.5 was reached, far below the expected thermodynamic equilibrium. This would indicate that PAA is catabolized and/or consumed for penicillin-G synthesis and byproduct formation with such a rate that the diffusion into the cells is rate limiting.

The initial slope of the intracellular PAA concentration vs. time was used to obtain a rough estimate of the membrane permeability constant for HPAA, $k_{diff,HPAA}$ (see Equation 4.3) assuming that PAA import occurs via passive diffusion. This gives a $k_{diff,HPAA}$ of $5 \cdot 10^{-6}$ m·s^{-1} and an initial PAA uptake rate of 50 mmol·CmolDW^{-1}·h^{-1}. The maximum biomass specific penicillin production rate of *P. chrysogenum* DS17690 was found to be 0.56 mmol·CmolDW^{-1}·h^{-1} (van Gulik et al., 2000), which is 2 orders of magnitude lower than the found uptake rate, rejecting the hypothesis of limiting PAA import. Our observation that the diffusive PAA import is not limiting for PenG production is in agreement with Hillenga et al. (Hillenga et al., 1995).

After the PAA pulse an immediate decrease in DO was observed (see Figure 4.4). This coincided with a decrease of the oxygen and increase of the carbon dioxide concentration in the offgas after the pulse, indicating increased oxygen consumption and carbon dioxide production (results not shown). This could be caused by catabolism of the imported PAA, but *P. chrysogenum* DS17690 is a strain which does not catabolize PAA due to a point mutation in the *pahA* gene encoding phenylacetate hydroxylase (van den Berg et al., 2008). In addition, the PAA balance can be closed in PenG producing cultures taking PAA, o-OH-PAA and PenG into account (data not shown), proving that PAA catabolism is absent.

In analogy to *P. chrysogenum*, the well-studied yeast *S. cerevisiae* contains a broad substrate ABC transporter which exports PAA and benzoic acid, which molecular structure highly resembles the molecular structure of PAA (Hazelwood et al., 2006). The

undissociated form of benzoic acid passively diffuses into the cells and is not catabolized by *S. cerevisiae*. In cultivations of *S. cerevisiae* in the presence of benzoic acid a higher respiration due to the ATP requirement for benzoic acid export was observed (Kresnowati et al., 2008). Our hypothesis (figure 4.1, hypothesis II) is that in *P. chrysogenum* PAA is imported by passive diffusion and simultaneously exported by an active ABC transporter. This hypothesis is confirmed by both the higher oxygen consumption and carbon dioxide production upon PAA addition and the lack of thermodynamic equilibrium between intra- and extracellular PAA. Most remarkable is that the DO decreased nearly immediately after PAA addition. The immediate higher respiration causing the DO drop indicates that the ABC transporter is already present and is therefore most probably a non-specific transporter. This is in agreement with the broad substrate function of Pdr12p, the ABC transporter responsible for PAA transport in *S. cerevisiae* (Hazelwood et al., 2006).

To test the hypothesis of passive import and active export, a model was constructed and the parameters were fitted using the experimental data of the pulse experiment. The model predictions are shown in figure 4.4. As already mentioned, the sudden addition of the PAA solution caused a drop in the pH in the reactor, which was compensated for by NaOH addition by the pH control system. It took a few tens of seconds to recover the steady-state pH of 6.5 ± 0.05. Since the pH was not constant, it was used as a model input. The model parameters estimated from the two pulse experiments are $k_{diff,HPAA} = 4.8 \cdot 10^{-6}$ m·s^{-1}, $k_{export,PAA}$ = 242 mmol·CmolDW^{-1}·h^{-1} and $K_{m,PAAexport}$ = 0.84 mmol·CmolDW^{-1}. The permeability coefficient is lower than $23 \cdot 10^{-6}$ m·s^{-1} as found by Hillenga et al. in a study using *P. chrysogenum* liposomes (Hillenga et al., 1995). The mathematical model shows a good description of the experimental data as shown in figure 4.4. This quantitatively supports the hypothesis of active export of PAA from the cells.

The predicted change in oxygen consumption rate was calculated by assuming that the ABC transporter requires 1 mol of ATP to excrete 1 mol of undissociated PAA and that respiratory ATP generation yields 1.84 mol ATP per ½ mol O_2 consumed, which is the experimentally determined maximal P/O value by van Gulik et al. (van Gulik et al., 2001), although the operational P/O might be slightly lower. The predicted change in oxygen consumption rate is compared with the experimental change in oxygen consumption rate upon the PAA pulse in table 4.2. The predicted $q_{O2,PAA}$ is larger than the measured increase in oxygen consumption, which indicates that in reality less energy for export is needed than assumed. This might be caused by additional export of protons with the exported HPAA, which results in a lower net energy requirement for PAA export. Furthermore the oxygen

consumption rate indicates that it is the undissociated form of PAA which is actively exported, because export of PAA^- by the ABC transporter would result in double respiration rates, as the H^+ needs to be exported by the H^+/ATP-ase.

Table 4.2 Measured and predicted increase in biomass specific oxygen consumption rate upon 10 mM PAA pulse. $q_{O2}{}^0 = 41.7$ mmol·Cmol^{-1}·h^{-1}.

	Experimental data		Model prediction
	PAA pulse 1 (mmol·Cmol^{-1}·h^{-1})	PAA pulse 2 (mmol·Cmol^{-1}·h^{-1})	(mmol·Cmol^{-1}·h^{-1})
$q_{O2,PAA}$	6.7	6.2	16.0

The obtained model was further challenged by testing its prediction of the intracellular PAA concentration upon a linearly increasing extracellular PAA concentration in the PAA-ramp experiments. Results are depicted in figure 4.5. Also in these experiments the oxygen consumption and carbon dioxide production increased, while the DO level decreased with increasing extracellular PAA concentrations.

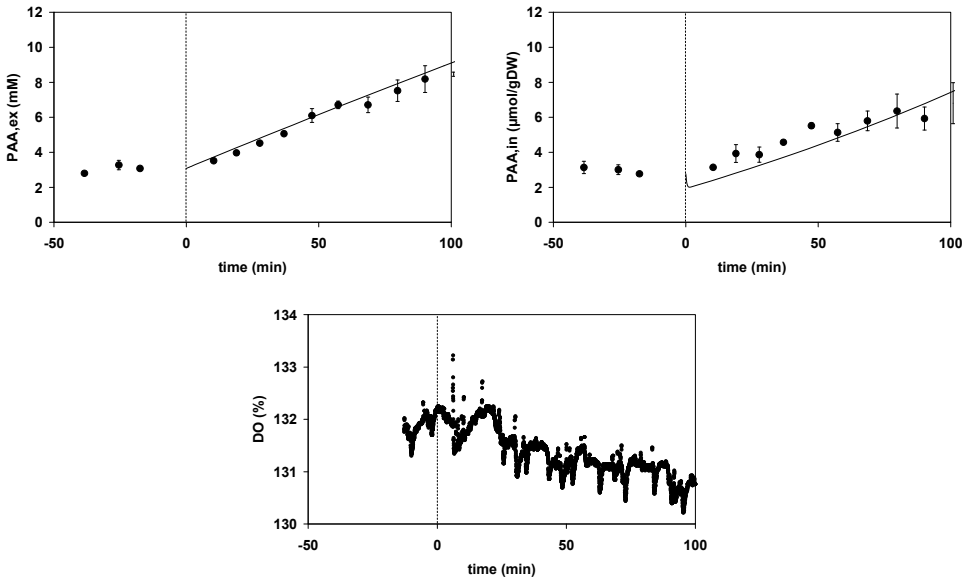

Figure 4.5 PAA-ramp experiment: extracellular PAA concentration, intracellular PAA concentration and dissolved oxygen. Experimental data (●) and model prediction (—). Addition of the ramp medium started at t = 0 min.

Hillenga et al. concluded that PAA was taken up by passive diffusion from transport studies with PAA in liposomes of *P. chrysogenum*. This finding was confirmed by the *in vivo* whole cell experiments performed in this study. However, the coupled active export of PAA out of the cells observed in our *in vivo* study was not observed in the liposome studies. A possible explanation could be that the PAA transporter was inactive or absent under the conditions applied in the liposome studies (Hillenga et al., 1995).

Similar stimulus response experiments were performed with *S. cerevisiae* Pdr12Δ with benzoic acid, which highly resembles the molecular structure of PAA, to examine the intracellular pH. Import and export of benzoic acid happened only by passive diffusion in *S. cerevisiae* Pdr12Δ, creating a thermodynamic equilibrium between the intra- and extracellular benzoic acids concentration. The permeability constant for benzoic acid in *S. cerevisiae* was found to be $(9.2 \pm 7.4)\cdot10^{-6}$ m·s^{-1} (Kresnowati et al., 2007), which is close to our permeability constant for PAA of $4.8\cdot10^{-6}$ m·s^{-1} for PAA in *P. chrysogenum*.

From our study it appears that the transporter of PAA in P. chrysogenum could be responsible for a futile cycle causing additional oxygen consumption. In P. chrysogenum several transport related genes are upregulated in cultures grown in the presence of PAA. Pc22g14600 belongs to the ABC-G transporter cluster and was appointed as primary candidate to be a PAA exporter (8). Although we find that the PAA-ABC transporter might already be present in absence of PAA in the cultivation medium, the strain might adapt to PAA presence by upregulating expression of the transporter gene.

PenG transport

Similar to the PAA pulse experiments PenG pulse experiments were performed. The results of the PenG pulse experiment, in which the extracellular PenG concentration was increased from 0 to 10 mM instantaneously, can be found in figure 4.6. Irrefutably very rapid intracellular accumulation of PenG can be observed. Apparently PenG is not only excreted from the cells, but can also be taken up, making PenG transport not unidirectional. The ratio of the extracellular to the intracellular concentration ratio swiftly moves towards a value in the same order of magnitude as in PenG producing cultures, which was reported to be 71 ± 11 (Douma et al., 2010a), although we experienced that this value might vary depending on conditions (data not shown).

Figure 4.2 shows three hypotheses for PenG transport mechanisms and table 4.3 shows the predicted concentration ratios in thermodynamic equilibrium for these three hypotheses and

for different values of membrane potential ΔΨ. As can be seen only the K_{eq} values for facilitated transport are in the same range of the measured concentration ratios, indicating that this is the most likely transport mechanism.

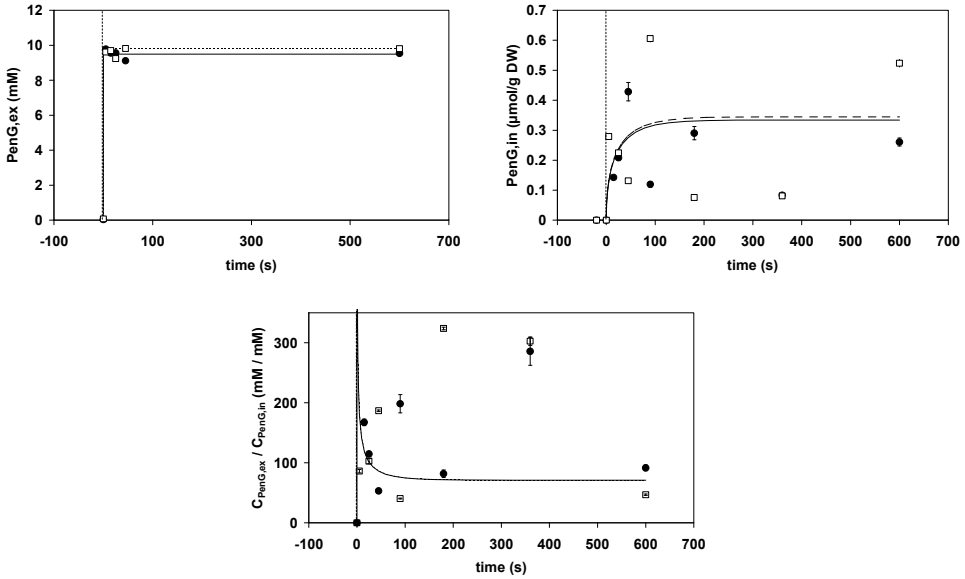

Figure 4.6 PenG pulse 1&2: extracellular PenG concentration, intracellular PenG concentration and ratio of intracellular to extracellular concentration. Experimental data of pulse experiment 1 (●), pulse experiment 2 (□), model prediction of pulse experiment 1 (—) and pulse experiment 2 (--). The pulse solution was added to the reactor at t = 0 s.

Table 4.3 Predicted extracellular to intracellular PenG concentration ratios for different transport modes for different values of ΔΨ.

Transport mode	$C_{p,ex} \cdot C_{p,in}^{-1}$ (mM·mM^{-1})		
	ΔΨ = -80 mV	ΔΨ = -100 mV	ΔΨ = -130 mV
Facilitated transport	23	49	158
With proton antiport	$1.6 \cdot 10^{3}$	$7.6 \cdot 10^{3}$	$79 \cdot 10^{3}$
With ATP hydrolysis	$1.3 \cdot 10^{10}$	$2.8 \cdot 10^{10}$	$9.1 \cdot 10^{10}$

In the PenG ramp experiment an extracellular increasing PenG concentration caused the intracellular PenG concentration to increase proportionally in a PenG producing culture as is shown in figure 4.7. During the time course of this experiment the concentration ratio remained equal.

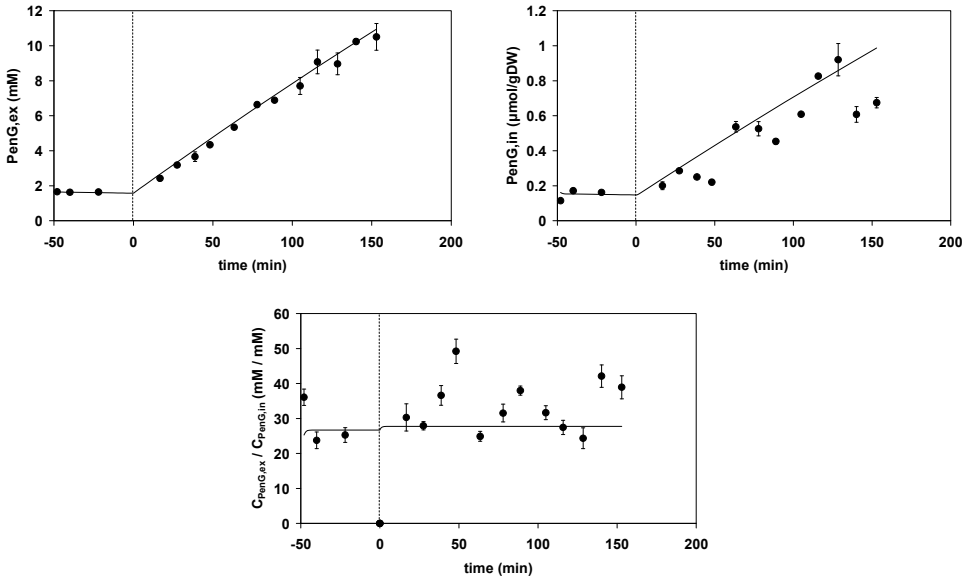

Figure 4.7 PenG-ramp experiment: Experimental data of the extracellular PenG concentration, intracellular PenG concentration and ratio of intracellular to extracellular concentration. Experimental data (●) and model prediction (—). Addition of the ramp medium started at t = 0 min.

There is significant scattering in the data of the PenG-pulse complicating an accurate prediction of the model parameter of a dynamic model based on facilitated PenG transport. Therefore the model parameter was estimated using the experimental data from the PenG-ramp and the model was tested to the PenG-pulse experiment. The model simulations of the perturbation experiments are shown in figure 4.6 and 4.7. The maximum capacity of the transporter proteins, $q_{sec,PenG}^{max}$, was calculated to be 0.68 mmol·CmolDW^{-1}·h^{-1} for $(K_{eq})_{fac}$ = 71 (Douma et al., 2010a), which is only slightly higher than the maximal penicillin production rate of 0.56 mmol·CmolDW^{-1}·h^{-1} as found by Van Gulik et al. (van Gulik et al., 2000). Product export is therefore not expected to be limiting for PenG production in *P. chrysogenum* DS17690. However, the calculated value for $q_{sec,PenG}^{max}$ is dependant on the value for $(K_{eq})_{fac}$, which was found to vary from condition to condition (data not shown). With an industrial production strain limitation of PenG export might well be reached. The model prediction of intracellular PenG in the PenG-pulse and PenG-ramp experiments is satisfactory.

Conclusions

Stimulus response experiments at two time scales with PAA and PenG were performed in cultures of *P. chrysogenum*. The results indicate the undissociated form of PAA to be transported into the cells by passive diffusion. Like in *S. cerevisiae*, *P. chrysogenum* seems to possess an exporter hydrolyzing ATP to transport PAA out of the cell, keeping the intracellular to extracellular concentration ratio at values lower than its thermodynamic equilibrium. A model based on import by passive diffusion and active export shows good description of experimental data and reconfirms the presence of ABC transporters for aromatic acids in *P. chrysogenum*. The capacity of PAA import was found to be 2 orders of magnitude higher than the maximal biomass specific production rate, showing PAA import does not limit PenG production. About 15% of the respiration in presence of PAA is PAA export related.

Export of PenG over the cell membrane is reversible, because PenG was imported into the cell upon extracellular addition. The equilibrium ratio of extracellular to intracellular PenG strongly points at facilitated export where the negatively charged PenG is pushed over the membrane by the negative membrane potential. This hypothesis is further supported by model predictions. Parameter values show that the exporter capacity is higher than the maximal biomass specific PenG production rate, posing no limitation for PenG production in *P. chrysogenum* DS17690.

Acknowledgement

This project is financially supported by the Netherlands Ministry of Economic Affairs and the B-Basic partner organizations (www.b-basic.nl) through B-Basic, a public private NWO-ACTS programme (ACTS: Advanced Chemical Technologies for Sustainability). This project was carried out within the research programme of the Kluyver Centre for Genomics of Industrial Fermentation which is part of the Netherlands Genomics Initiative / Netherlands Organization for Scientific Research.

Appendix I PenG secretion

Facilitated transport as depicted in figure 4.2 of negatively charged $PenG^-$ can be described as follows:

$$T + PenG_{in}^{-} \rightleftarrows (TPenG)_{in} \tag{4AI.1}$$

$$(TPenG)_{in} \rightleftarrows (TPenG)_{ex} \tag{4AI.2}$$

$$(TPenG)_{ex} \underset{k_{up}}{\overset{k_{sec}}{\rightleftarrows}} T + PenG_{ex}^{-} \tag{4AI-3}$$

In which T is a transporter protein and with the following equilibrium constants:

$$K_1 = \frac{C_T \cdot C_{PenG,in}}{C_{TPenG,in}} \tag{4AI.4}$$

$$K_2 = \frac{C_{TPenG,ex}}{C_{TPenG,in}} \tag{4AI.5}$$

The secretion rate of PenG will then be:

$$q_{\sec,PenG} = k_{\sec} \cdot C_{TPenG,ex} - k_{up} \cdot C_T \cdot C_{PenG,ex} \tag{4AI.6}$$

The total permease species can be described as follows:

$$C_{T_O} = C_T + C_{TPenG,in} + C_{TPenG,ex} \tag{4AI.7}$$

Substituting equations 4AI.4, 4AI.5 into 4AI.7:

$$C_T = \frac{C_{T_O}}{1 + \frac{C_{PenG,in}}{K_1} + \frac{K_2}{K_1} \cdot C_{PenG,in}} \tag{4AI.8}$$

Substituting equations 4AI.5 and 4AI.7:

$$C_{TPenG,ex} = \frac{K_2}{K_1} \cdot C_{PenG,in} \cdot \frac{C_{T_O}}{1 + \frac{C_{PenG,in}}{K_1} + \frac{K_2}{K_1} \cdot C_{PenG,in}} \tag{4AI.9}$$

The secretion rate can be rewritten substituting 4AI.8 and 4AI.9 into 4AI.6:

$$q_{\sec,PenG} = \frac{k_{\sec} \cdot C_{T_O} \cdot \frac{K_2}{K_1}}{1 + \frac{C_{PenG,in}}{K_1} + \frac{K_2}{K_1} \cdot C_{PenG,in}} \cdot \left(C_{PenG,in} - \frac{C_{PenG,ex}}{\frac{K_2}{K_1} \cdot \frac{k_{\sec}}{k_{up}}} \right) \quad (4AI.10)$$

When $C_{PenG,in} = 0$:

$$q_{\sec,PenG} = q_{\sec,PenG}^{\max} = -k_{up} \cdot C_{T_O} \cdot C_{PenG,ex} \quad (4AI.11)$$

When $C_{PenG,ex} = 0$:

$$\left(q_{\sec,PenG}\right)_{PenG,ex=0} = \frac{k_{\sec} \cdot C_{T_O} \cdot \frac{K_2}{K_1} \cdot C_{PenG,in}}{1 + \frac{C_{PenG,in}}{K_1} + \frac{K_2}{K_1} \cdot C_{PenG,in}} \quad (4AI.12)$$

At equilibrium, $q_{sec} = q_{up} = 0$ from 4AI.10:

$$\frac{C_{PenG,ex}}{C_{PenG,in}} = \frac{K_2}{K_1} \cdot \frac{k_{\sec}}{k_{up}} = \left(K_{eq,penG}\right)_{fac} \quad (4AI.13)$$

From 4AI.10 we can write:

$$q_{\sec,PenG} = \frac{k_{\sec} \cdot C_{T_O} \cdot \frac{K_2}{K_1} \cdot C_{PenG,in}}{1 + \frac{C_{PenG,in}}{K_1} + \frac{K_2}{K_1} \cdot C_{PenG,in}} \cdot \left(1 - \frac{C_{PenG,ex}}{C_{PenG,in} \cdot \frac{K_2}{K_1} \cdot \frac{k_{\sec}}{k_{up}}} \right) \quad (4AI.14)$$

At maximal secretion rate $K_2 >> K_1$, substituting 4AI.12 and 4AI.13 into 4AI.14:

$$q_{\sec,PenG} = q_{\sec,PenG}^{\max} \cdot \left(1 - \frac{C_{PenG,ex}}{C_{PenG,in} \cdot \left(K_{eq,penG}\right)_{fac}} \right) \quad (4AI.15)$$

This simplified, one parameter version of the secretion rate cannot be simulated at initial $C_{PenG,in}$ equal to zero. For practical purposes this value is taken to be very small (1×10^{-10})

and is valid till (1 x 10^{-150}), which is a negligible concentration (≈ 0) as compared to the intracellular concentrations of PenG.

Appendix II Simulation

To describe the system mass balances for intracellular PAA and PenG were constructed:

$$\frac{dC_{PAA,in}}{dt} = q_{diff,PAA} - q_{sec,PAA} - q_p - \mu \cdot C_{PAA,in} \quad (4AII.1)$$

$$\frac{dC_{PenG,in}}{dt} = -q_{sec,PenG} + q_p - \mu \cdot C_{PenG,in} \quad (4AII.2)$$

Furthermore extracellular PAA and PenG mass balances were constructed:

$$\frac{dC_{PAA,ex}}{dt} = -q_{diff,PAA} \cdot C_x + q_{sec,PAA} \cdot C_x + D \cdot \left(C_{PAA,feedin} - C_{PAA,ex} \right) \quad (4AII.3)$$

$$\frac{dC_{PenG,ex}}{dt} = q_{sec,PenG} \cdot C_x + D \cdot \left(C_{PenG,feedin} - C_{PenG,ex} \right) \quad (4AII.4)$$

The specific growth rate μ (h^{-1}) is included in the model to account for the dilution of the intracellular metabolites caused by growth of the cells, while D (h^{-1}) is included to account for the dilution of extracellular metabolites because of wash out. C_x (CmolDW·m^{-3}) is the measured biomass dry weight.

CHAPTER 5

Degeneration of penicillin production in ethanol limited chemostat cultivation of *Penicillium chrysogenum*: A systems biology approach

Abstract - In microbial production of non-catabolic products a loss of production capacity upon long-term cultivation (for example chemostat), a phenomenon called strain degeneration, is nearly always observed. In this study a systems biology approach (monitoring changes from gene to produced flux) was used to study degeneration of penicillin production by Penicillium chrysogenum in ethanol-limited chemostat fermentations where the biomass specific penicillin production rate decreased 10-fold within 30 generations. Results showed that copy number of penicillin gene clusters and expression levels of central metabolism showed little decrease. With respect to penicillin production major changes were observed; a strong downregulation of the cysteine pathway in agreement with its nearly 10-fold flux reduction. Also levels of ACVS and IPNS, two penicillin pathway enzymes, and the penicillin transport capacity decreased many fold. This indicates that degeneration is caused by changed regulation of post-translational modification or an increased protein degradation rate of these proteins. Continued subcultivation of a degenerated culture resulted in partial recovery of the biomass specific penicillin production rate, however, still 5-fold lower than the peak biomass specific penicillin production rate.

Douma RD, Batista JIM, Touw KM, Kiel JAKW, Krikken AM, Zhao Z, Veiga Dos Inocentes T, Klaassen P, Bovenberg RA, Daran J, Heijnen JJ, Van Gulik WM. Degeneration of penicillin production in ethanol limited chemostat cultivation of *Penicillium chrysogenum*: A systems biology approach (manuscript in preparation).

Introduction

The rate and yield of penicillin production by the fungus *Penicillium chrysogenum* have been increased many-fold after its discovery by Alexander Fleming in 1928 (Fleming, 1928). Initially this was performed by successive rounds of mutagenesis and selection (Newbert et al., 1997; Peñalva et al., 1998; Thykaer and Nielsen, 2003). Recently, the genome sequence was elucidated (van den Berg et al., 2008) facilitating transcriptome (Harris et al., 2009) and proteome studies (Kiel et al., 2009; Jami et al., 2010). In combination with fluxome and metabolome studies (van Gulik et al., 2000; Nasution et al., 2008; Douma et al., 2010a) this enables a systems biology analysis to find metabolic engineering targets to enhance penicillin production.

Although in current industrial production strain the biomass specific penicillin production rate (q_p) has increased many fold, *P. chrysogenum* does not maintain its high production capacity in extended continuous fermentations. As early as 1932 the loss of production capacity was reported upon continued subcultivation of penicillin producing cultures of *P. chrysogenum* (Clutterbuck et al., 1932) and also strains further on in the lineage were reported to loose penicillin productivity in extended chemostat fermentations (Righelato, 1976; Künkel et al., 1992; Christensen et al., 1995; van Gulik et al., 2001; Douma et al., 2010b). Degeneration of product formation was not only observed for PenG production in *Penicillium chrysogenum*, but also for adipoyl-7-aminodeacetoxycephalosporanic (ad-7-ADCA) acid production in *Penicillium chrysogenum* (Robin et al., 2003), oxytetracycline production in *Streptomyces rimosus* (Gravius et al., 1993) and tylosin production in *Streptomyces fradiae* (Baltz and Seno, 1981) among others. This generally observed (partial) loss of production capacity during extended cultivation is usually referred to as degeneration. This phenomenon is of major relevance because it unables a continuous production processes. Therefore current production processes are fed-batch fermentations which, for bulk production such as penicillin, are less economical than chemostat fermentations, because of extra start-up time and costs.

It is easily understood that if a micro-organism (partially) looses its production capacity, more substrate and energy can be used for growth, leading to a competitive advantage. Penicillin production requires a significant amount of metabolic energy (van Gulik et al., 2001) giving non-producing cells a competitive advantage. A strain which can keep its high productivity for a longer time (absence of degeneration) would result in more productive,

perhaps even allowing penicillin fermentation to run in continuous mode instead of the now applied fed-batch mode.

In this paper for the first time different -omics techniques were simultaneously applied in an attempt to obtain a systems understanding of degeneration of production of PenG in *P. chrysogenum* in chemostat

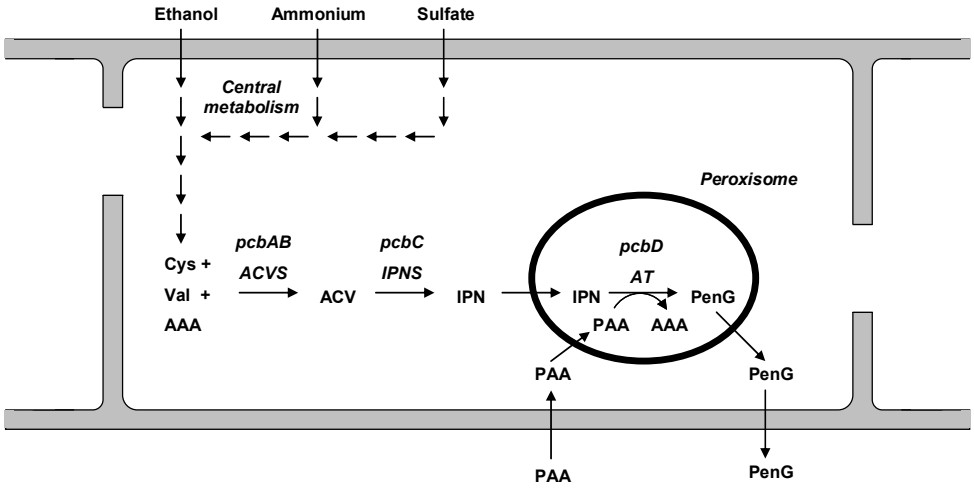

Figure 5.1 Penicillin pathway in P. chrysogenum. L-cysteine (Cys), L-valine (Val) and α-amino adipic acid (AAA) are produced from ethanol in central metabolism. These three precursor amino acids are converted into L-α-(δ-aminoadipyl)-L-α-cystenyl-D-α-valine (ACV) by the enzyme L-α-(δ-aminoadipyl)-L-α-cystenyl-D-α-valine synthetase (ACVS, which is coded for by the gene pcbAB). ACV is subsequently converted to isopenicillin-N (IPN) by the enzyme isopenicillin-N synthase (IPNS, which is coded for by the gene pcbC). IPN is then transported into the peroxisome where it is converted into PenG with the precursor PAA, which is added to the medium and imported in the cell and then activated by ligase to PAA-CoA which is used by the enzyme acyl coenzyme A: Isopenicillin N acyltransferase (AT, which is coded for by the gene pcbD). The product PenG is then transported out of the peroxisome and out of the cell into the cultivation medium.

cultivation. This system study focuses mainly on the penicillin pathway (figure 5.1), in an industrial high penicillin producing strain, *P. chrysogenum* DS17690. Prolonged chemostat cultivations up to 600 hours (30 generations) with ethanol as the sole limiting carbon source were performed, because degeneration is found to be more pronounced with ethanol as limiting sole carbon source compared to glucose (van Gulik et al., 2000). Measurements included genome level (number of penicillin gene clusters), genome-wide transcriptome, protein levels of penicillin pathway enzymes, number of peroxisomes (microbodies where part of the penicillin pathway occurs), metabolome (of central metabolism, nucleotides, penicillin pathway intermediates including intracellular PAA and PenG) and fluxome.

Materials and methods

Strain

Chemostat experiments were performed with the industrial high penicillin production strain *Penicillium chrysogenum* DS17690, kindly donated by DSM Biotechnology Center (Delft, The Netherlands). Microbody quantification chemostat experiments were performed with *Penicillium chrysogenum* DS58274, which contained green fluorescent protein containing the carboxyterminal tripeptide serine lysine leucine that functions as a peroxisomal targeting signal (GFP•SKL) and was developed from *P. chrysogenum* DS17690. This strain was described as DS54465 GFP•SKL before (Meijer et al., 2010) and was kindly donated by W.H. Meijer (University of Groningen, The Netherlands).

Media and chemostat cultivation

Cultivation medium was prepared as described earlier (van Gulik et al., 2000) and contained 0.25 Cmol/L ethanol and 4 mM PAA and was used for the batch and chemostat phase of fermentations, allowing a biomass concentration of about 3 gDW/L.

Ethanol-limited chemostat cultivations were performed according to Nasution et al. (2006) in a 7 L turbine stirred reactor with a working volume of 4 L under aerobic conditions (DO > 70%) and a dilution rate of 0.03 h^{-1} at 25°C and pH 6.5.

Sampling for transcriptome measurements, Western blotting and metabolome measurements was performed after about 75, 200, 350 and 500 h.

Continued subcultivation of degenerated culture

From a nearly completely degenerated penicillin producing chemostat culture a biomass sample was taken aseptically after about 500 hours of cultivation (15 residence times). Of this sample 4 mL were used to inoculate a fermentor with 4L of fresh cultivation medium using a sterile syringe, which was cultivated (batch start-up followed by chemostat) under the exact same conditions as its parent culture after inoculation.

General fermentation analysis

Concentrations of PAA and PenG in the culture supernatant were obtained with HPLC-UV (Christensen et al., 1994). Biomass concentration and offgas oxygen and carbon dioxide analysis were performed as described earlier (van Gulik et al., 2000).

Penicillin gene cluster copy number quantification

Biomass sampling was performed as described previously (Harris et al., 2009). DNA was isolated using a beat-bead procedure using 2-4 glass beads (2.5 mm) to accomplish cell lysis and subsequent DNA purification using the FastDNA® SPIN Kit (MP Biomedicals, Solon, OH). Real-time quantitative PCR was performed in triplicate in 25 µL reaction volume of IQ SybrGreen Supermix (Bio-Rad, Hercules, CA), 0.5 µM of each primer and 2 ng genomic DNA using iQ5-Multicolor Real-Time PCR (Bio-Rad, Hercules, CA, USA). To quantify the number of penicillin gene clusters, *pcbAB* was amplified (forward primer: GGAGCAGGTCTGACGAAGG, reverse primer: AACGAACGGTGTGATATGAACG) together with *niaD* as internal reference (1 genomic copy, forward primer: TGGAGGAAC TGGCATCACAC, reverse primer: ACATAAGCATCAAGGTCAGAACG). The following PCR settings were used: 1 cycle of 95°C for 3 min and cycles of 95°C for 10 s, 58°C for 45 s, 72°C for 45 s and 95°C for 1 min. As a control we used *P. chrysogenum* Wisconsin 54-1255 as it is known to have 1 penicillin gene cluster (Fierro et al., 1995; Thykaer and Nielsen, 2003).

Transcriptome analysis

Sampling, RNA extraction, microarray analysis, data analysis and clustering were performed as described earlier (Kresnowati et al., 2006; Harris et al., 2009).

Western blotting

Samples for Western blotting were obtained in freeze buffer as described previously (Harris et al., 2006), precipitated with 12.5 % TCA and stored at -20 °C. After thawing on ice, from each sample three independent aliquots were taken and crude protein extracts were prepared as described previously (Kiel et al., 2009). Protein concentrations were determined using the RC/DC Protein Assay system (Bio-Rad, Hercules, CA,) using bovine serum albumin as standard. Subsequently, western blots were prepared in triplicate utilizing the three independently taken aliquots, with equal amounts of protein loaded per lane - for ACVS, IPNS and AT determinations, 60 µg, 3/30 µg and 30 µg of protein, respectively. SDS/PAGE and Western blotting were performed according to established procedures. Western blots were decorated with specific polyclonal antibodies against ACVS, IAT and IPNS. As secondary antibody anti-rabbit IgG-AP (Santa Cruz biotechnology, Santa Cruz, CA) was used with NBT/BCIP (Roche, Penzberg, Germany) as substrate. After detection, Western blots were scanned using a Bio-Rad GS-710 densitometer. ACVS, IAT and IPNS-specific bands were quantified three times each using ImageJ 1.40

(http://rsbweb.nih.gov/ij/index.html). After averaging, values were expressed as percentages of the initial value, which was set to 100 %.

Microbody quantification

For microbody quantification chemostat experiments were performed with *P. chrysogenum* DS58274 which contained a microbody-targeted green fluorescent protein. These chemostats were performed exactly as all other chemostats with *P. chrysogenum* DS17690.

Biomass from 1.5 mL culture broth samples was fixed using 3.7% formaldehyde in a 50 mM pH 7.2 potassium phosphate buffer on ice for 1 h (centrifugation for 5 min. at 6000 rpm) and stored at 4°C until further analysis. From each hyphae the peroxisomes in two subapical cells were counted and averaged using a confocal laser scanning microscopy (CLSM) as described earlier (Krikken et al., 2009; Meijer et al., 2010). The number of peroxisomes per cell was determined by counting up to 200 peroxisomes and dividing by the number of cells.

Metabolome analysis

Sampling and sample processing for intracellular metabolite analysis was performed as described earlier (Nasution et al., 2006a). Quantification was performed as described earlier for metabolites of central metabolism (van Dam et al., 2002), for adenine nucleotides (Seifar et al., 2008) and for free amino acids (Canelas et al., 2009). Sampling and sample processing for intracellular metabolites related with penicillin biosynthesis including intracellular PAA and PenG levels was performed using a new rapid quenching and filtration based washing technique as described before (Douma et al., 2010a) to wash away the very large extracellular amounts of PAA and PenG.

Calculation methods

A steady-state regarding PenG in chemostats with ethanol as sole limiting carbon source is never reached because degeneration is very pronounced. Therefore the biomass specific penicillin production rate q_p as function of time is calculated from the dynamic penicillin mass balance using polynomial fits for the measured biomass and penicillin concentration as a function of time:

$$\frac{dC_p(t)}{dt} = q_p(t) \cdot C_x(t) - D \cdot C_p(t) \qquad (5.1)$$

The other specific rates q_s, q_{O2}, q_{CO2} and μ were calculated using proper mass balances and these rates were used for metabolic flux calculation with the stoichiometric model from Van Gulik et al. (2000).

The reversible reactions from F6P to Mannitol6P and FBP to G3P can be used as a sensor reaction to determine the change in redox status in the cytosol. The relative ratio of NADH to NAD (Canelas et al., 2008b) compared to the first time point (t1, high q_p) can be calculated as follows:

$$\frac{\left(NADH/NAD\right)_t}{\left(NADH/NAD\right)_{t1}} = \frac{\left(Mannitol6P/F6P\right)_t}{\left(Mannitol6P/F6P\right)_{t1}} \tag{5.2}$$

$$\frac{\left(NADH/NAD\right)_t}{\left(NADH/NAD\right)_{t1}} = \frac{\left(G3P/\sqrt{FBP}\right)_t}{\left(G3P/\sqrt{FBP}\right)_{t1}} \tag{5.3}$$

A model for penicillin transport over the plasma membrane was developed in chapter 4. The PenG secretion capacity can be calculated from the measured biomass specific penicillin production q_p, the measured extra- to intracellular concentration ratio of PenG and the equilibrium constant for PenG transport for facilitated transport.

$$q_{\mathrm{sec},PenG}^{\max} = \frac{q_p}{1 - \frac{C_{PenG,ex}}{C_{PenG,in} \cdot \left(K_{eq,penG}\right)_{fac}}} \tag{5.4}$$

For the calculation of the extra- to intracellular concentration ratio of PenG the assumed intracellular volume was 2.5 mL/gDW (Jaklitsch et al., 1986; Packer et al., 1992a). The equilibrium constant for PenG transport for facilitated transport was found to be 71 (Douma et al., 2010a).

Results and discussion

General observations

To study the degeneration of penicillin production, four chemostat fermentations with *P. chrysogenum* DS17690 were performed under identical conditions with ethanol as the sole limiting carbon source and the results for the concentrations of biomass, PenG, PAA and

the biomass specific PenG production rate q_p can be found in figure 5.2. Clearly a high reproducibility was achieved. All chemostat cultivations were preceded by a batch phase during which the culture grew exponentially until all ethanol was depleted. In this batch phase no penicillin was produced. Apparently penicillin is not only not produced at μ_{max} with glucose as carbon source (Feng et al., 1994; Gutiérrez et al., 1999), but also with ethanol as carbon source. Addition of the chemostat cultivation medium was started at a dilution rate of 0.03 h^{-1} just before ethanol depletion. The chemostat cultivation was maintained until maximally 750 h, representing about 30 generations. The carbon and redox balances could be closed and showed negligible (<10%) byproduct formation (results not shown). Taking o-OH-PAA (data not shown) into account the PAA balance could be closed, indicating the absence PAA catabolism, which is in agreement with earlier observations (Rodríguez-Sáiz et al., 2001).

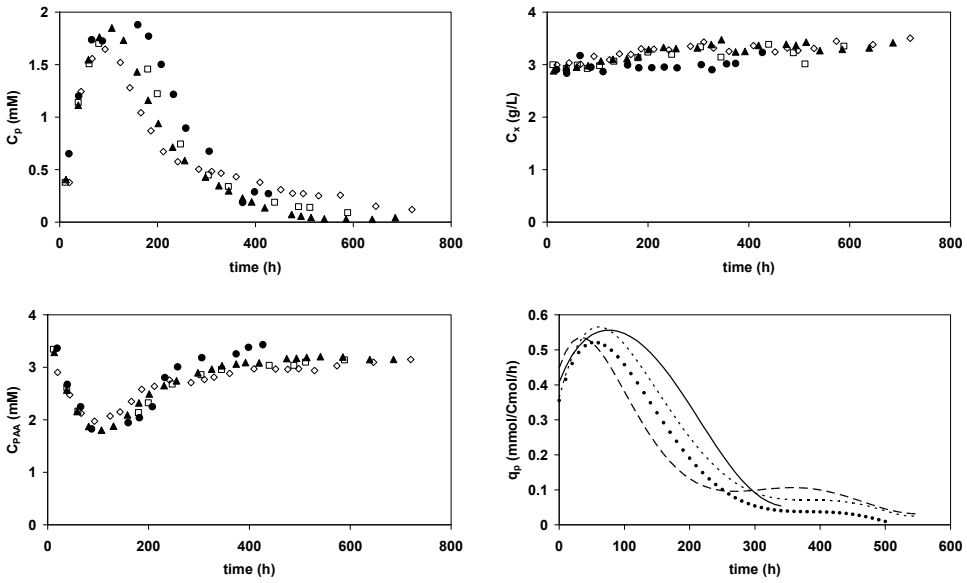

Figure 5.2 PenG, biomass and PAA concentration in chemostat 1 (●), 2 (□), 3 (▲) and 4 (◊) and q_p in chemostat 1 (—), 2 (--), 3 (··) and 4 (——).

The biomass specific penicillin production rate (q_p) reached its peak value after about 50-100 hours, which is caused by the time needed for the penicillin pathway enzyme levels, which are repressed in batch, to reach their maximum (Douma et al., 2010b). However, around 100 -150 h degeneration of q_p set in, as seen by the decreased PenG concentration and a mirror increase in the PAA concentration. The decrease in q_p correlated with a slight

increase of the biomass concentration as expected because ethanol not used for penicillin production can be used for growth (van Gulik et al., 2001). The degeneration profile was reproducible as can be seen in figure 5.2, although the degeneration profile was slightly shifted in time in the replicate cultures. During degeneration q_p decreased about 10-fold.
The stoichiometric model for growth and PenG production of van Gulik et al. (2000) was used to estimate the metabolic flux distribution on the PenG production peak (t = 75 h) and for a degenerated culture (t = 500h). The fluxes at these two time points in central carbon metabolism and penicillin precursor pathways are depicted in figure 5.3. The biggest changes in flux were found in Cys biosynthesis. Because almost all produced cysteine is used for PenG production, the degenerated culture had an 8-fold reduced flux in the pathway towards cysteine. Although less drastic, the biosynthetic flux towards Val decreased 2.5-fold, while the flux towards AAA remained unaltered, because there is no net AAA-consumption in PenG biosynthesis. The production of 6-APA and OPC (which is a byproduct of AAA) decreased (supplementary materials, figure 5.S15). The reduced need for NADPH for penicillin production in the degenerated culture also resulted in a significantly reduced activity of the pentose phosphate pathway and a 30% reduced gluconeogenic flux.

Penicillin gene cluster copy number

The penicillin production pathway genes (figure 5.1) are organized as a cluster in the genome (Fierro et al., 1995). The higher penicillin production by *P. chrysogenum* DS17690 is partly explained by the occurrence of 6-7 copies (van den Berg et al., 2008) of this penicillin gene cluster compared to *P. chrysogenum* NRRL1951 which contains 1 penicillin gene cluster (Thykaer and Nielsen, 2003). A logical hypothesis for the loss of penicillin production is that the loss of production capacity is caused by the loss of penicillin gene clusters due to mutation, like observed by Christensen et al. (1995) for PenV synthesis in a different industrial *P. chrysogenum* strain.

Figure 5.4A shows the result for two time points (t = 75 h high q_p, t = 500 h degenerated low q_p) of the penicillin gene cluster copy number quantification by real-time quantitative PCR in 2 independent chemostat cultures (chemostat 3 and 4). This quantification method gives accurate results up to a number of 6 penicillin gene clusters and shows that both at the penicillin production peak and in the degenerated state of the chemostat culture there are more than 6 penicillin gene clusters present. No indication was found that a large fraction of the penicillin gene clusters were lost, as could be expected to explain the 10-fold loss in biomass specific penicillin production rate q_p. This shows that degeneration is not caused

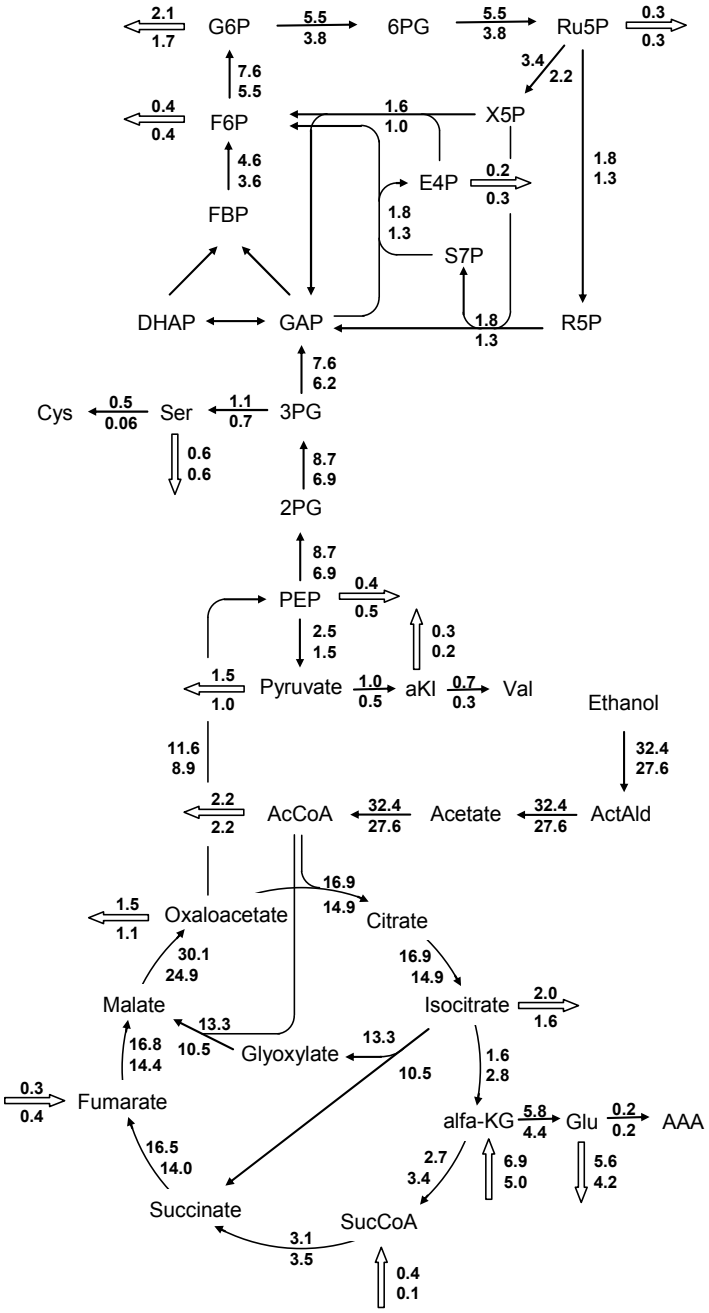

Figure 5.3 Averaged flux distribution for chemostat 3 and 4 in mmol/Cmol/h at the penicillin production peak (t = 75 h, upper number) and the degenerated culture (t = 500 h, lower number). Not all fluxes in the network are shown.

by a loss of penicillin gene clusters. Furthermore, the q_p – time degeneration profile is reproducible, which also does not indicate random mutation events at gene cluster level as the cause of degeneration. Although the final state of adaptation (growth rate) of micro-organisms to a constant environment by mutations is shown to be reproducible in many cases, the path and time required may be different between experiments (Poelwijk et al., 2007).

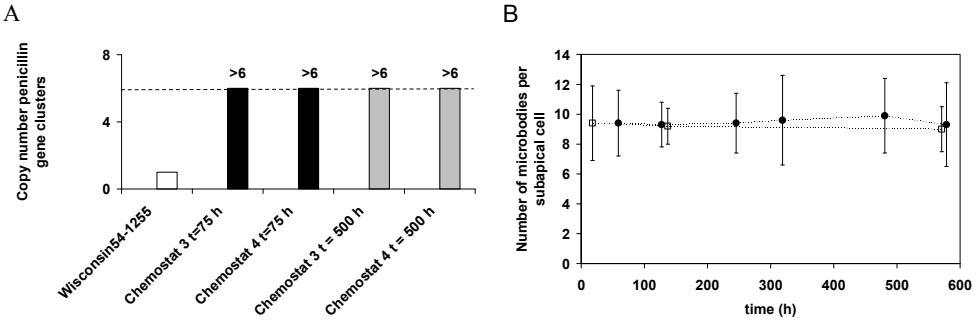

Figure 5.4 A- Penicillin gene cluster copy number quantification in the reference strain (Wisconsin 54-1255, 1 penicillin gene cluster, white) and in two prolonged chemostat runs of P. chrysogenum DS17690 at the penicillin production peak (t = 75 h, black) and the degenerated state (t = 500 h, grey). B- Number of microbodies per subapical cell in chemostat 5 (●) and chemostat 6 (□).

Microbody quantification

P. chrysogenum is a eukaryotic, compartmentalized microorganism in which the last step in the penicillin production pathway is located in the peroxisomes (see figure 5.1). Overproduction of Pc-Pex11p in *P. chrysogenum* Wis54-1255, which has only 1 penicillin gene cluster and therefore a low q_p value, resulted in higher microbody abundance and a 2-fold higher penicillin production (Kiel et al., 2005). Although a different strain with much lower q_p was used in that study, a possible hypothesis for degeneration of q_p in our industrial strain, *P. chrysogenum* DS17690, could be that the number of microbodies decreased in time during the degeneration of this high producing industrial strain.

Penicillium chrysogenum DS58274, a microbody-targeted GFP•SKL producing mutant of *P. chrysogenum* DS17690 (Meijer et al., 2010), showed an identical q_p degeneration profile, gave the same biomass concentration and gave the same penicillin production as *Penicillium chrysogenum* DS17690 in chemostat cultivation (data not shown). As can be seen the number of microbodies per subapical cell (figure 5.4B) did not decrease

throughout chemostat cultivation of *Penicillium chrysogenum* DS58274, while the specific penicillin production rate decreased 10-fold.

Transcriptome analysis

The hypotheses that degeneration was either caused by a loss of copies of the penicillin gene cluster or by a decrease in the number of microbodies were tested and rejected based on the finding that no significant decrease could be found in either of them. Since the genes and the microbodies seem fully present, the phenomenon of degeneration of penicillin production must be in regulation of the penicillin production.

To investigate whether the cause for degeneration of penicillin formation is caused by regulation leading to changed expression levels of genes, a transcriptome analysis was performed on two sets of four samples which were taken throughout a duplicate chemostat run (chemostat 1 and 2). The data were treated as a time series experiments in duplicate. Firstly, the results were tested for the hypothesis that in this time series of samples no changes in the level of the transcript would occur. Of the 14000 transcripts in *P. chrysogenum* about 1000 transcripts were significantly differentially expressed throughout the prolonged chemostat cultures.

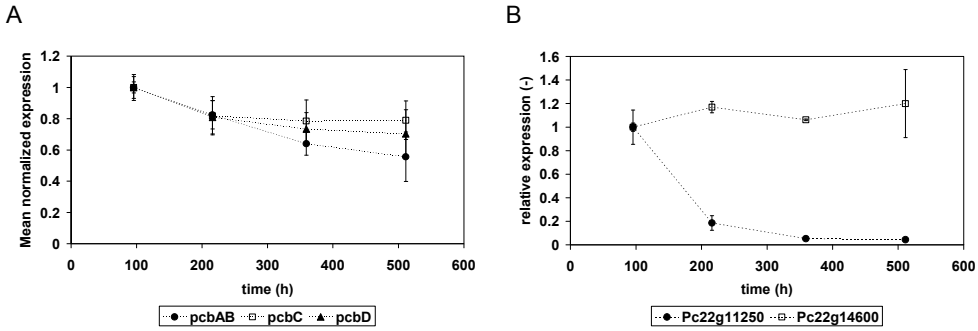

Figure 5.5 Mean normalized expression of genes throughout ethanol limited chemostat cultivation. The number is an average of chemostat 1 and 3. A- The penicillin pathway genes pcbAB (ACVS, ●), pcbC (IPNS, □) and pcbD (AT, ▲). B- The genes Pc22g11250 (●) and Pc22g14600 (□).

Of particular interest are of course the decreases in fold changes in expression of the three penicillin biosynthesis genes. The expression levels of all penicillin gene cluster genes decrease (figure 5.5A), but only the decrease in *pcbAB* (ACVS) is significant, while the decrease in *pcbC* (IPNS) and *pcbD* (AT) is not significant (< 2-fold). However, the less

than 2-fold decrease in these transcript levels is clearly very different from the 10-fold decrease in pathway flux and is in line with the previous result that there is no significant loss of the copy number of penicillin gene clusters.

Another explanation lies in the possible transporters for PenG and PAA. A genome-wide expression study with *P. chrysogenum* in PenG producing and non-producing cultures indicated a possible transporter gene for PenG (Pc22g11250) and PAA (Pc22g14600) transport (Harris et al., 2009). The expression of these genes is depicted in figure 5.5B. The indicated PenG transporter gene, Pc22g11250, showed a very strong correlation with PenG production in the study of Harris et al. (Harris et al., 2009) and is also strongly downregulated during degeneration of penicillin production in the current experiments. The indicated candidate for PAA transport, Pc22g14600 did not change its expression level throughout the prolonged chemostat run.

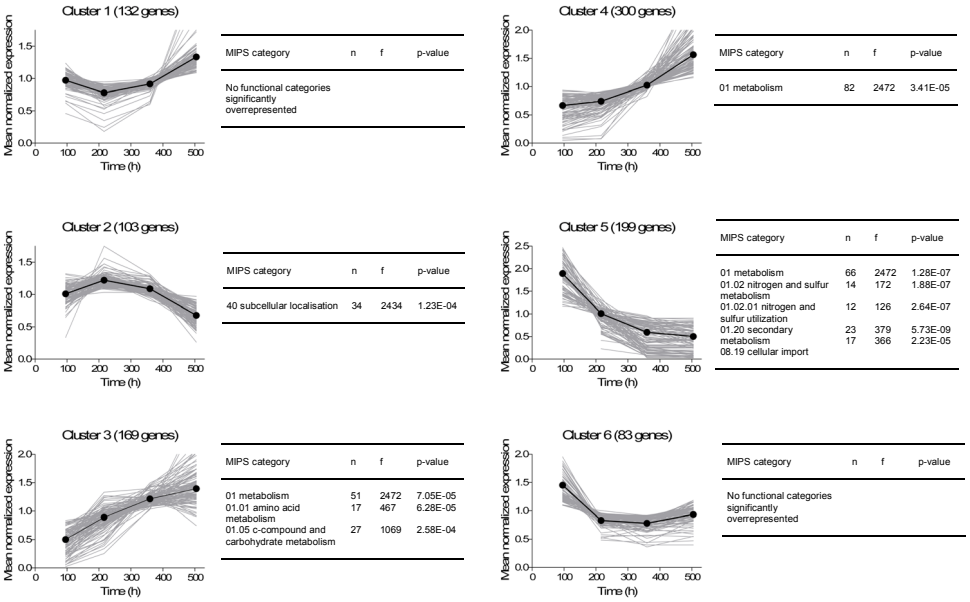

Figure 5.6 The 6 different transcriptome clusters in which the differentially expressed genes were divided and subjected to a functional category analysis.

Changes in expression levels of other genes might give additional indications about the cause of degeneration of penicillin production. Therefore the 1000 differentially expressed genes were grouped into six different clusters based on the trend of their behavior as can be seen in figure 5.6. In three clusters the fold changes of expression were minor (less than 2

fold; cluster 1, 2 and 6). Of the remaining three clusters only cluster 5 showed significant gene downregulation (4-fold), while in clusters 3 and 4 genes were upregulated. Subsequently, a functional category analysis was made within the six clusters. Most interesting observations are made in the functional categories in cluster 5, the one in which the genes are continuously down regulated throughout the experiment. Mainly in sulfur metabolism genes were down regulated throughout the prolonged chemostat cultivations. Most interestingly, many downregulated genes are in the synthesis pathway of cysteine, one of the precursors of the penicillin pathway (supplementary data, figure 5.S4). This should

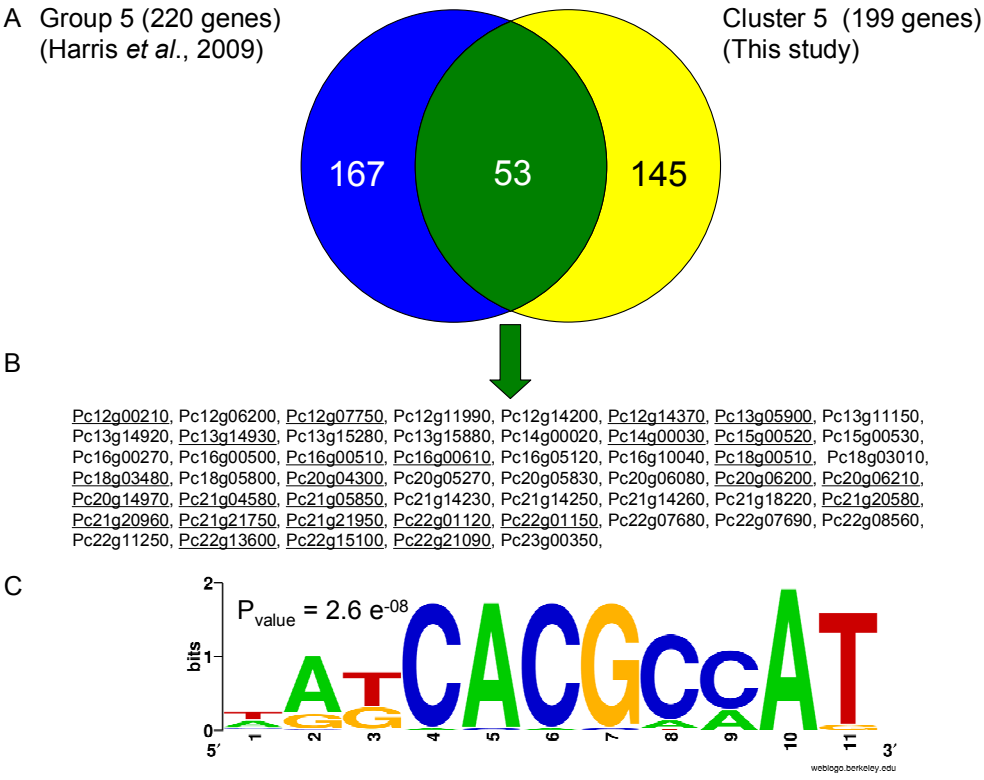

Figure 5.7 A- Venn diagram of the genes comprising the cluster 5 and of the genes that specifically were responding to PenG production (cluster 6) according to Harris et al. (2009). B- 53 genes that are overlapping the two sets. The genes underlined contained at least one cis-regulatory motif as indicated in C in their promoter sequences (promoter sequences includes the region -900, -1). C- overrepresented cis-regulatory motif in the set of the 53 genes. The motif has been identified using the MEME software and the logo has been edited by the weblogo software.

not be surprising because in the high producing strain the majority of all produced cysteine is related to penicillin production as can be seen in figure 5.3 showing that during degeneration the cysteine pathway experienced an 8-fold decrease in flux. In the study of Harris et al. (2009) PenG production was stopped in two ways, namely by using a mutant without the penicillin gene cluster and by cultivating in the absence of PAA. In both cases genes in the cysteine biosynthesis pathway were strongly downregulated, like observed in this study as well. This shows the downregulation of the cysteine pathway is the result, not the cause of degeneration.

An interesting observation was made in the comparison between the downregulated 145 genes in cluster 5 and the 167 genes which were only upregulated under PenG producing conditions, according to Harris et al. (2009). As shown in figure 5.7A and 7B, 53 genes could be found in both of these groups, meaning that these genes are positively associated with the presence of PenG production. Using the MEME software (Bailey and Elkan, 1994; Harris et al., 2009) an overrepresented *cis*-regulatory motif was found in the 900 base pairs upstream of the mentioned 53 genes (figure 5.7C). This implies that this group of genes might be coregulated.

Table 5.1 maximum growth rate and biomass specific penicillin production rate in 4 chemostats and 2 subchemostats inoculated with degenerated culture of chemostat 4.

Chemostat run	μ_{max} in batch phase (h^{-1})	$q_{p,max}$ in chemostat phase (mmol $Cmol^{-1}$ h^{-1})	q_p at time of continued subcultivation (mmol $Cmol^{-1}$ h^{-1})
Chemostat 1	0.088	0.52	-
Chemostat 2	0.086	0.52	-
Chemostat 3	N.D.	0.52	-
Chemostat 4	0.089	0.54	-
Subchemostat 4.1	0.109	0.11	0.04
Subchemostat 4.2	0.112	0.10	0.04

An analysis of the expression levels of gluconeogenesis and TCA cycle genes shows that transcript levels of central metabolism did not significantly change which is not surprising because of the small flux change. An exception is that the possible gene encoding for alcohol dehydrogenase, Pc21g22820, was upregulated throughout the chemostat runs although the biomass specific substrate uptake rate (figure 5.3) decreased. This adaptation is also supported by the 25% higher maximum specific growth rate in the batch phase of the continued subcultivation compared to the maximum specific growth rate in the batch phase of the parent culture (table 5.1). The upregulation of Pc21g22820 and possible higher ADH

activity might have resulted in a decrease in the limiting ethanol concentration in the chemostat in time. Unfortunately, this residual ethanol concentration was too low to measure.

Western blotting

Total protein amounts of ACVS, IPNS and AT were analyzed via Western blotting during degeneration in chemostat 1 and 4. Figure 5.8 (left panel) shows how their change correlates with the decrease in q_p. Note that the low q_p corresponds to the degenerated condition. The total protein amount of ACVS could only be measured throughout chemostat 1 and showed a clear 5-fold decrease after about 400 h. While also the amounts of IPNS decreased up to 20-fold throughout both chemostats, the amount of AT decreased far less. Figure 5.8 (left panel) shows that q_p is proportional to the amount of IPNS and not to the amount of AT is in agreement with earlier findings (Douma et al., 2010b). The total protein amounts of ACVS and IPNS show a much larger decrease than the mean normalized expression of the genes encoding for these proteins, of *pcbAB* and *pcbC* (figure 5.4A). Such a lack of correlation has been found multiple times before (Griffin et al., 2002; Greenbaum et al., 2003). Possible explanations for the lack of correlation between mRNA and total protein amount might be that during degeneration translation efficiency, post-translational modification or protein degradation change or a combination of them. A drawback of the Western blot method used to quantify the total protein amount of ACVS and IPNS is that no distinction is made between active and inactive enzyme.

Metabolome analysis

Intracellular levels of 17 central carbon metabolism intermediates, 16 free amino acids, 9 penicillin biosynthesis related metabolites and the adenine nucleotides were monitored throughout the chemostat cultivations (supplementary material, figure 5.S5-14). Most intracellular metabolites did not show significantly changing levels throughout degeneration. Interestingly, mostly the penicillin pathway related metabolites show large changes (figure 5.8).

As shown in chapter 4 intracellular levels of PAA and PenG can be compared with their extracellular levels to get insights in their transport mechanism. The intracellular PenG levels (figure 5.8, lowest middle panel) decreased many-fold with decreasing q_p during degeneration, while the extracellular to intracellular concentration ratio (figure 5.8, lowest right panel) remained relatively stable at a slightly lower value as observed for glucose-limited chemostat cultures (Douma et al., 2010a). The maximal penicillin export rate

$q_{sec,PenG,max}$ (shown in figure 5.8 lowest left panel) , which corresponds to the amount of transporter protein present, was calculated and shows a clear proportionality with q_p for

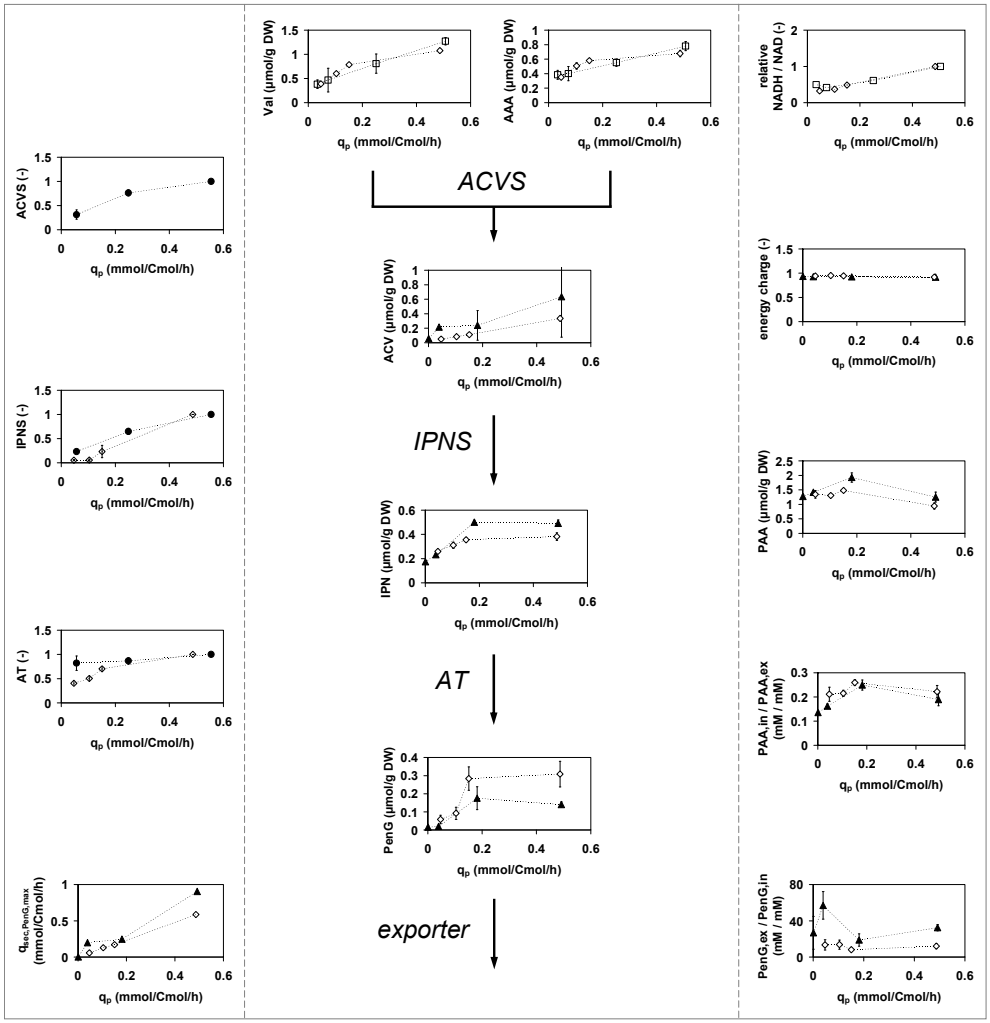

Figure 5.8 Left panel: Relative protein amounts compared to the reference condition at the penicillin production peak (first time point) in chemostat 1 (●) and chemostat 4 (◊) of proteins in the penicillin pathway (see figure 5.1) against q_p. Also shown is the calculated transporter capacity. Middle panel: Intracellular levels of penicillin precursors and intermediates against q_p in chemostat 2 (□), 3 (▲) and 4 (◊). Right panel: Energy charge, calculated ratio of NADH/NAD from the Mannitol6P/F6P sensor reaction, intracellular PAA and the concentration ratios of PAA and PenG against q_p in chemostat 2 (□), 3 (▲) and 4 (◊) on the right.

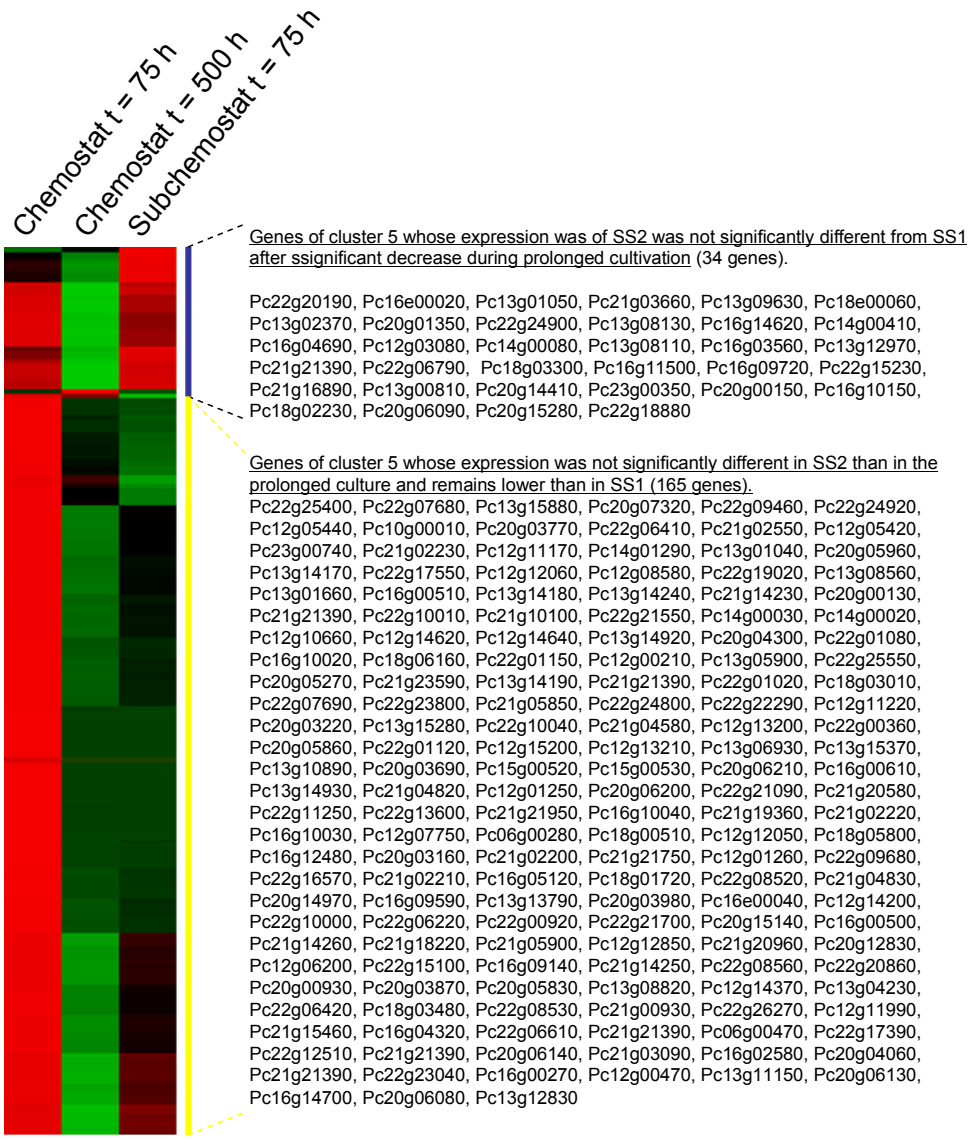

Figure 5.9 Heatmap of the transcript level of the genes comprising cluster 5. The heatmap display the mean normalized data at the penicillin production peak (t = 75 h), of the degenerated culture (t = 500 h) 504h and at the steady state of the continued subcultivation (t = 75h) obtained by inoculation of a new chemostat cultivation with biomass sample of the prolonged culture.

two independent chemostats. This steep decrease also correlates well with the expression of Pc22g11250 (figure 5.5B). This information shows that the transport capacity decreases in time indicating that Pc22g11250 might indeed be the gene coding for this transporter. The

intra- to extracellular PAA concentration ratio (figure 5.8, right panel) remained constant at a lower value as observed for glucose-limited chemostat cultures (Douma et al., 2010a). This coincides with the observation that the PAA exporter candidate gene Pc22g14600 (figure 5.5B) showed no change in expression level.

The production pathway of one of the precursors for penicillin production, Cys, is strongly downregulated throughout the chemostat experiment, which is in line with the decreased flux towards Cys. Unfortunately, the intracellular level of Cys was too low to be quantified accurately. The intracellular levels of the other penicillin pathway precursors, Val and AAA, decreased in time (figure 5.8, middle panel). This decrease in precursor supply is not expected to be the cause of degeneration, because earlier observations comparing penicillin production in non-degenerated glucose and ethanol limited cultures show that highly different metabolite levels of central metabolism and amino acids including Val and AAA still lead to the same high q_p (van Gulik et al., 2000; Nasution et al., 2008). Therefore it appears that the lower concentration of AAA and Val are more the result that the cause of the lower q_p.

The penicillin pathway flux is in principle dependent on the enzyme/transport levels in the pathway and the amino and precursor levels as discussed before, but there is also consumption of energy and redox (van Gulik et al., 2000). The decreased penicillin production could therefore be due to a decreased availability of metabolic energy in the form of ATP, since PenG production has been reported to be associated with a large additional consumption of ATP (van Gulik et al., 2001). However, the intracellular amounts of adenine nucleotides and the energy charge were similar as found previously (Nasution et al., 2006a). The values remained constant while the penicillin production decreases significantly (figure 5.8, upper right panel). Lack of ATP availability can therefore not be a reason for the lowered penicillin production. To study the possible effect of changed redox supply, we need information on the NAD(P)H to NAD(P) ratio. The ratio of Mannitol6P to F6P can be used as a sensor reaction for the cytosolic NADH to NAD ratio (Canelas et al., 2008b). The calculated relative NADH to NAD ratio (figure 5.8, right panel) decreased with decreasing q_p, indicating a more oxidized cytosol in the degenerated culture. In a more oxidized cytosol the availability of NADPH might also decrease, negatively influencing the ratio between ACV and bis-ACV (Theilgaard and Nielsen, 1999), which can decrease the flux through the penicillin pathway. The results from the other redox-couple, FBP and G3P showed similar changes in the NADH to NAD ratio. Finally the degenerated culture showed decreased pathway intermediate concentrations (ACV, IPNS, PenG in) which can

be expected to be a result of the decreased q_p. These metabolite changes can only be interpreted by constructing a complete kinetic model of the penicillin pathway, taking changes in protein, redox and metabolite levels into account.

Continued subcultivation

To verify whether degeneration is reversible, the degenerated culture of chemostat 4 was used to perform a continued subcultivation by inoculating subchemostat 4.1 and 4.2, diluting the culture 1000 times by adding 4 mL of degenerated culture into 4 L of fresh medium. The maximal specific growth rate in the batch phase of this continued subcultivation was higher than the value in the initial culture during its batch phase as is shown in table 5.1. The amounts of penicillin gene clusters, protein amount of enzymes in the penicillin pathway and metabolites showed little difference compared with the parent culture at the time of inoculation of continued subcultivation (supplementary material, figure 5.S2, S3, S5-14). Figure 5.9 shows that most genes downregulated throughout degeneration of penicillin production, remain downregulated upon continued subcultivation. However, the $q_{p,max}$ of the continued subcultivation was 2-fold higher than the q_p of the parent culture at the time of obtaining the inoculum biomass, although it was still 5-fold lower than the parent culture. Apparently the loss of penicillin production of the parent cultures is slightly reversible after a period of cultivation in a carbon abundant environment. The mechanism for this reverse remains unknown.

Conclusions

A systems biology approach was performed to analyze degeneration of product formation in high penicillin producing cultures of *P. chrysogenum*. The genome (copy number of penicillin gene clusters), transcriptome, metabolome, the penicillin pathway enzyme amounts and the fluxome were analyzed during the highly reproducible degeneration process in 4 independent ethanol limited chemostat cultures. The analysis showed that:

- there was a 10-fold decrease in q_p.
- there was no significant change in the copy number of penicillin gene clusters and the number of peroxisomes in subapical cells.
- a diminished supply of energy (constant energy charge), precursor (constant concentration of intracellular PAA and constant AT level) or of the amino acid precursors used in the penicillin pathway could be ruled out as cause for decreased q_p.

- a strong downregulation occurs in the cysteine pathway, in agreement with the 8-fold decreased need for cysteine, which is a result and not the cause of degeneration.
- the 10-fold decrease in q_p is most probably related to decreased levels of IPNS and ACVS (whose mRNA levels did not decrease) and a decreased capacity of the exporter (also seen in the transcript of the candidate transporter gene) and a changed, more oxidized, redox status.
- the explanation for these changes probably lies in changed post translational regulation, in increased protein degradation or a combination of them.

Acknowledgement

This project is financially supported by the Netherlands Ministry of Economic Affairs and the B-Basic partner organizations (www.b-basic.nl) through B-Basic, a public private NWO-ACTS programme (ACTS: Advanced Chemical Technologies for Sustainability). This project was carried out within the research programme of the Kluyver Centre for Genomics of Industrial Fermentation which is part of the Netherlands Genomics Initiative / Netherlands Organization for Scientific Research. J.A.K.W.K. was financially supported by DSM, Delft, The Netherlands. The authors would like to thank Denise van Suylekom, Najat Saddik and Rémon Boer for performing and coordinating the penicillin gene cluster copy number determinations.

Supplementary material

Physiological data continued subcultivation

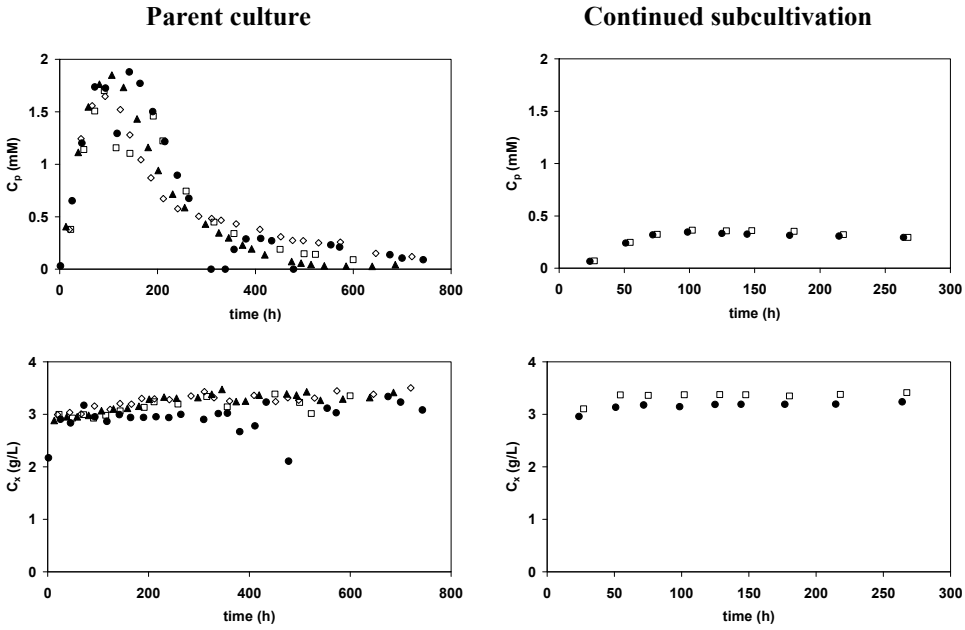

Figure 5.S1 Penicillin concentration in Chemostat 1 (●), 2 (□), 3 (▲) and 4 (◊) (left) and subchemostat 4.1 (●) and 4.2 (□) (right).

Penicillin gene cluster quantification continued subcultivation

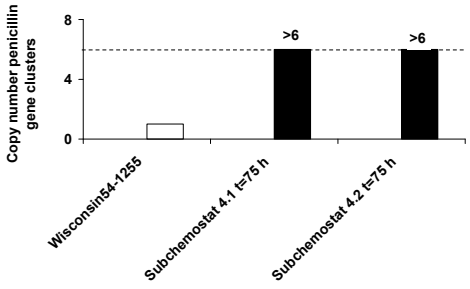

Figure 5.S2 Penicillin gene cluster copy number quantification in the reference strain (Wisconsin 54-1255, 1 penicillin gene cluster, white) and the continued subcultivations 4.1 and 4.2 at the penicillin production peak (t = 75 h, black).

Proteome continued subcultivation

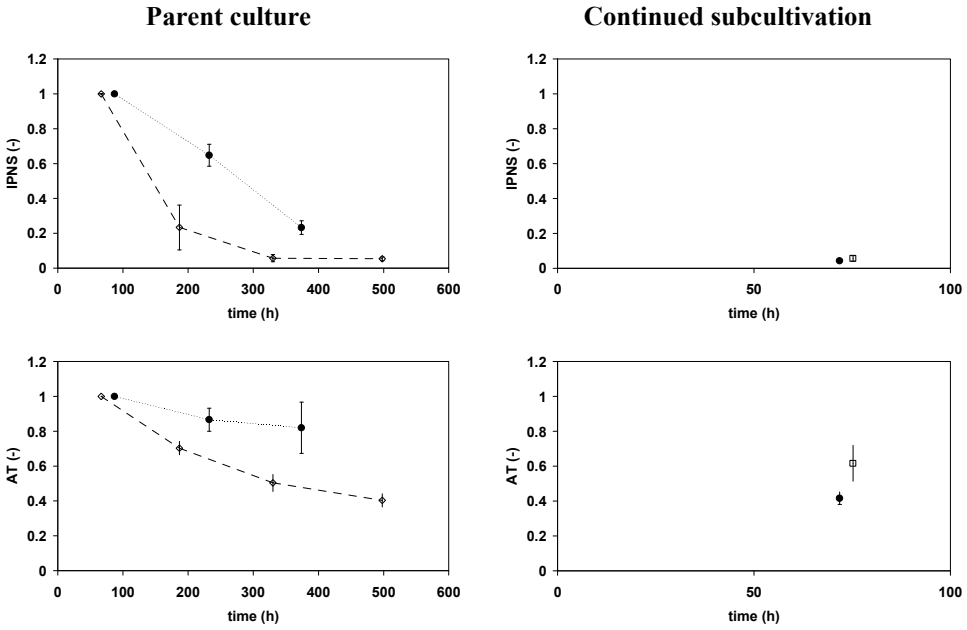

Figure 5.S3 Relative total protein amount of IPNS and AT during chemostat 1 (●) and 4 (◊) (left) and subchemostat 4.1 (●) and 4.2 (□) (right).

Transcriptome

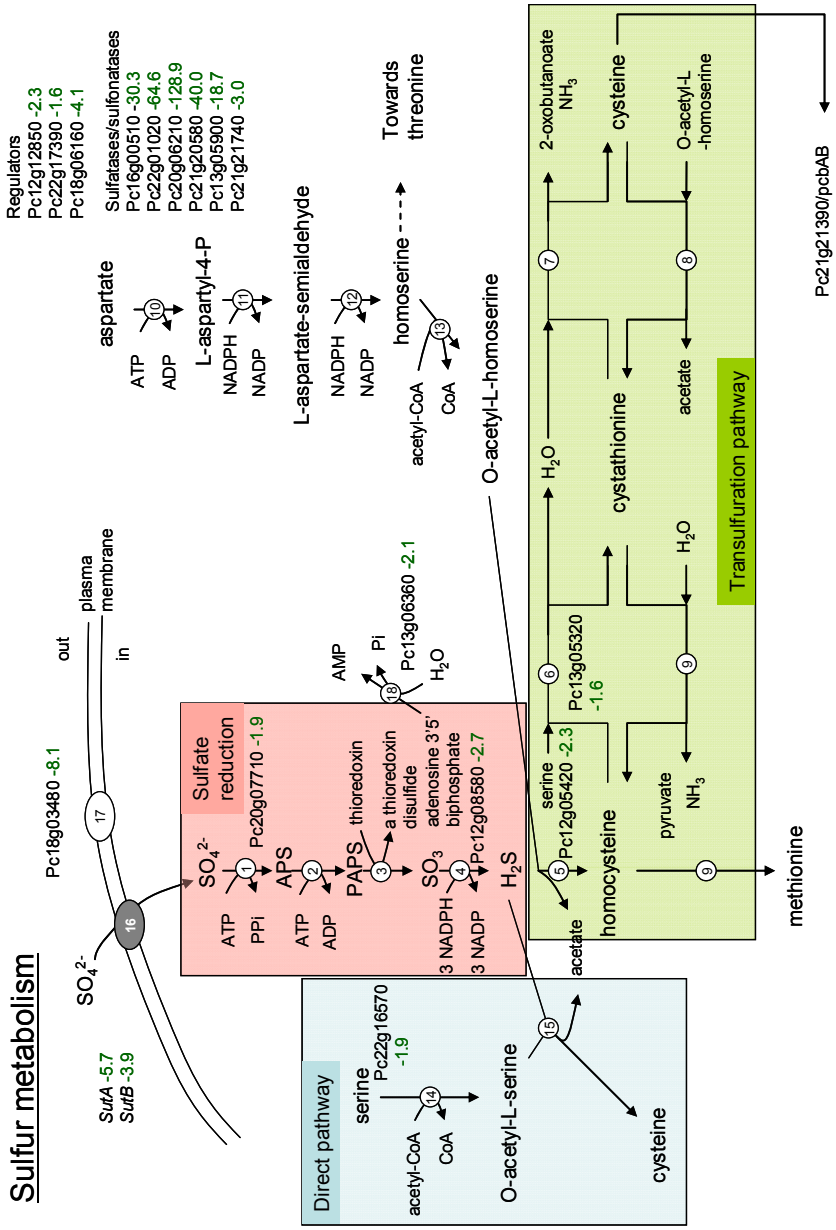

Figure 5.S4 Mean normalized expression of genes in sulfur metabolism in P. chrysogenum throughout ethanol limited chemostat cultivation. The numbers behind the transcripts represent the average fold change of chemostat 1 and 3 of expression in the degenerated culture at t = 500 h versus the penicillin production peak at t = 75 h in the prolonged ethanol-limited chemostat run

Metabolome

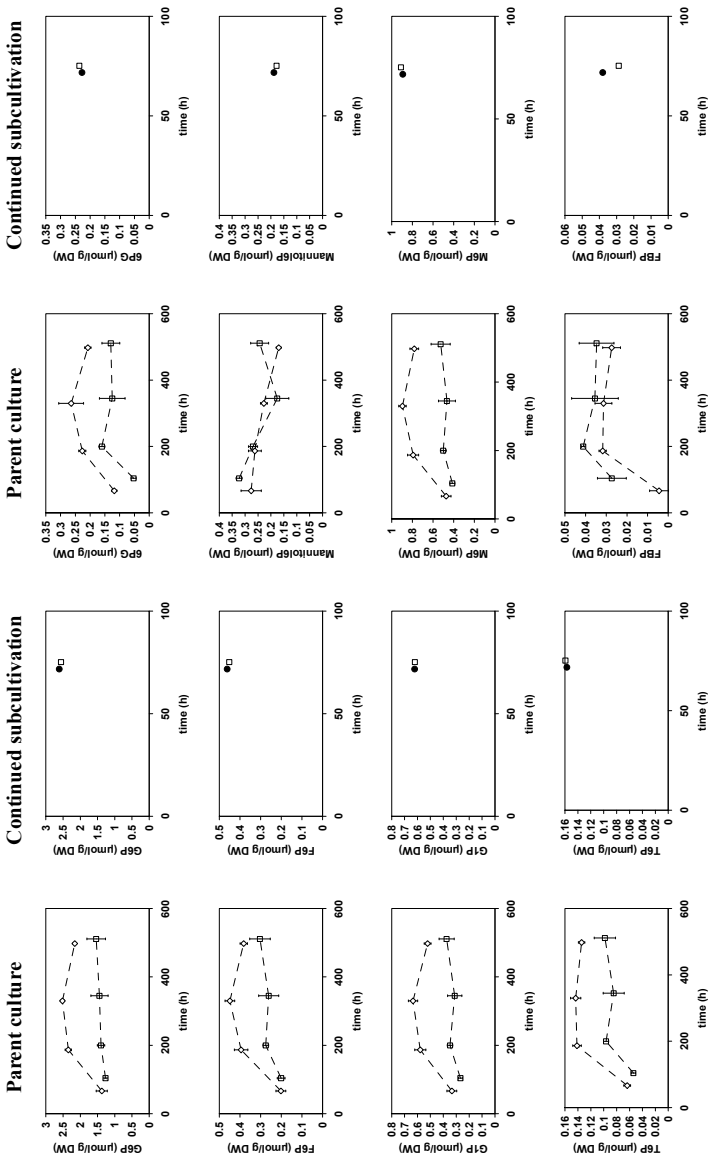

Figure 5.S5 Metabolite amounts of upper gluconeogenesis and related metabolites in chemostat 2 (□) and 4 (◊) (left) and subchemostat 4.1 (●) and 4.2 (□) (right).

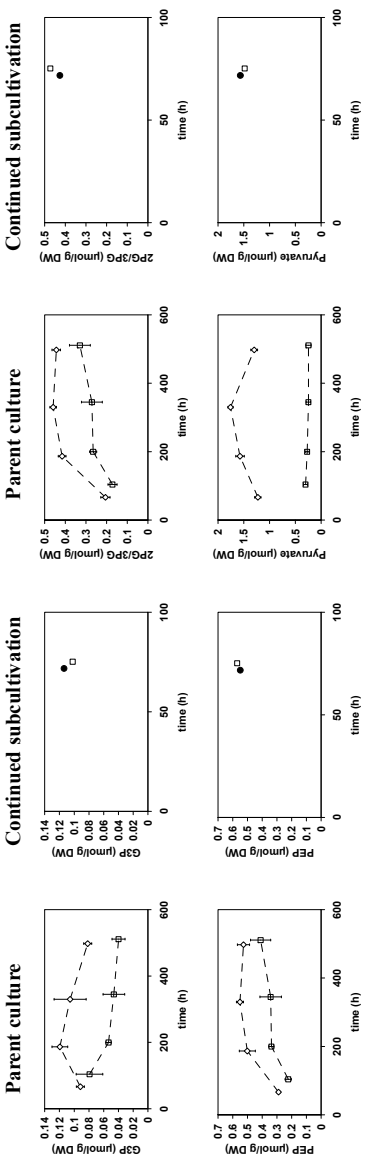

Figure 5.S6

Metabolite amounts of lower gluconeogenesis in chemostat 2 (□) and 4 (◊) (left) and subchemostat 4.1 (●) and 4.2 (□) (right).

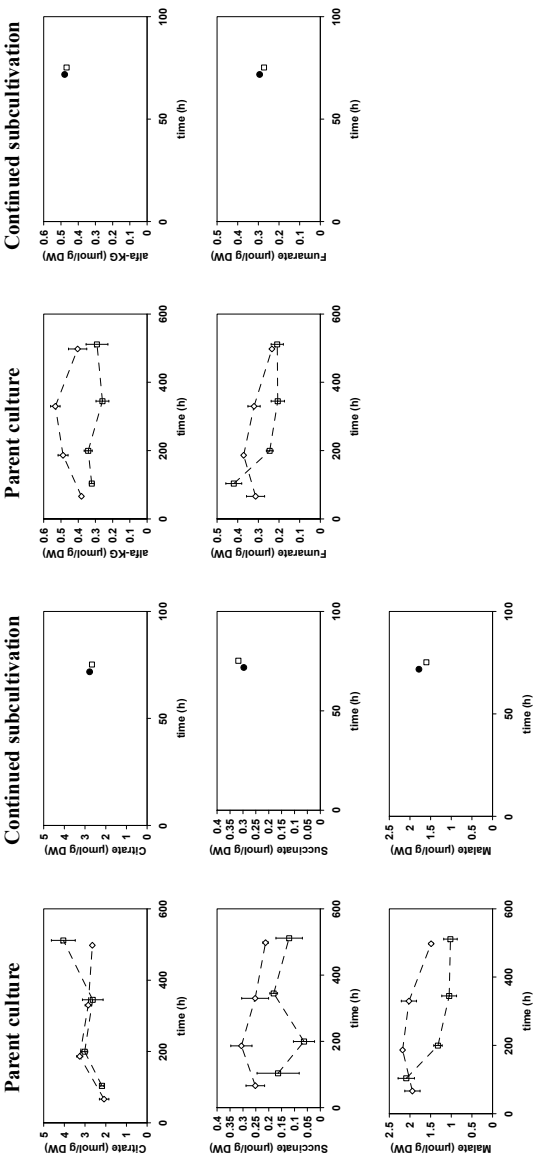

Figure 5.S7

Central metabolite in chemostat 1 (●), 2 (□) and 4 (◊) (left) and subchemostat 4.1 (●) and 4.2 (□) (right).

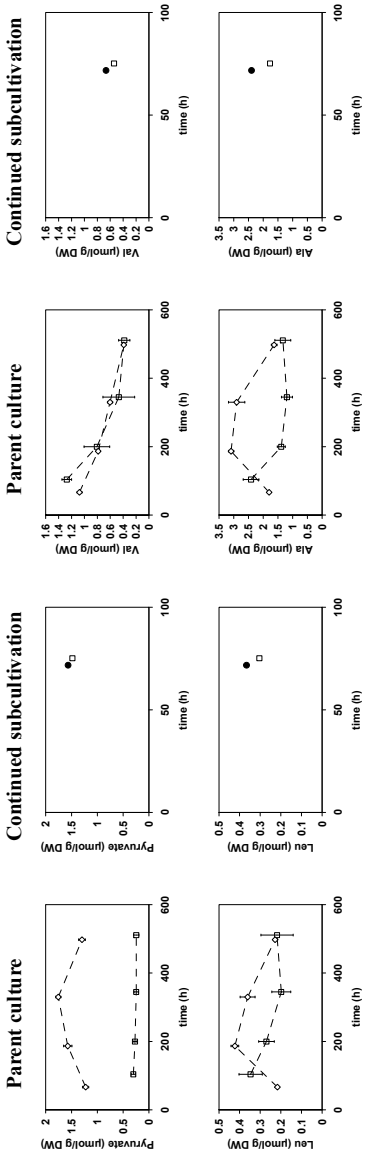

Figure 5.S8

Amino acids from pyruvate in chemostat 2 (□) and 4 (◊) (left) and subchemostat 4.1 (●) and 4.2 (□) (right).

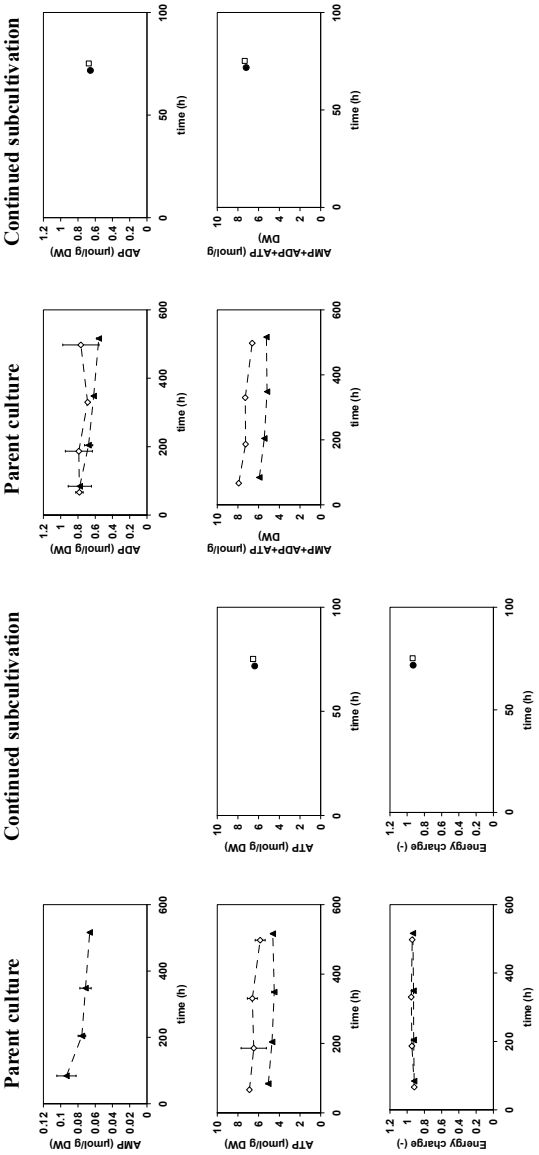

Figure 5.S9

Adenine nucleotides in chemostat 3 (▲) and 4 (◊) (left) and subchemostat 4.1 (●) and 4.2 (□) (right).

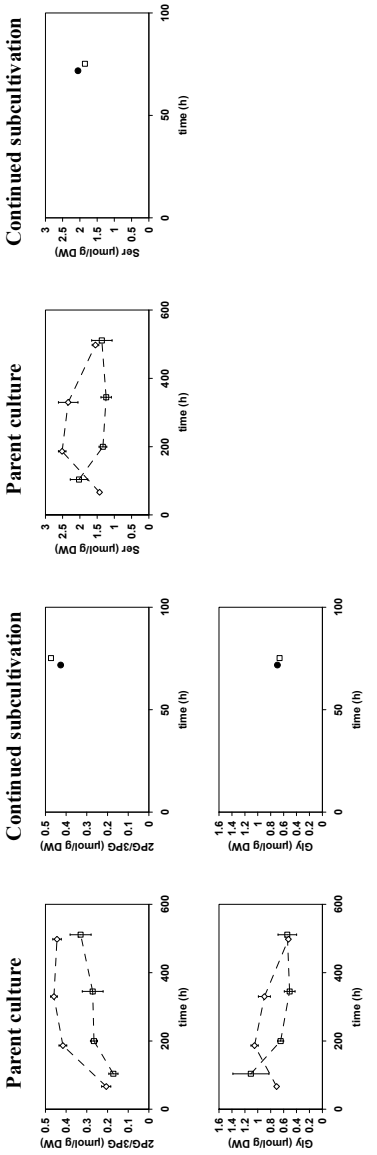

Figure 5.S10

Amino acids from 3PG in chemostat 2 (□) and 4 (◊) (left) and subchemostat 4.1 (●) and 4.2 (□) (right).

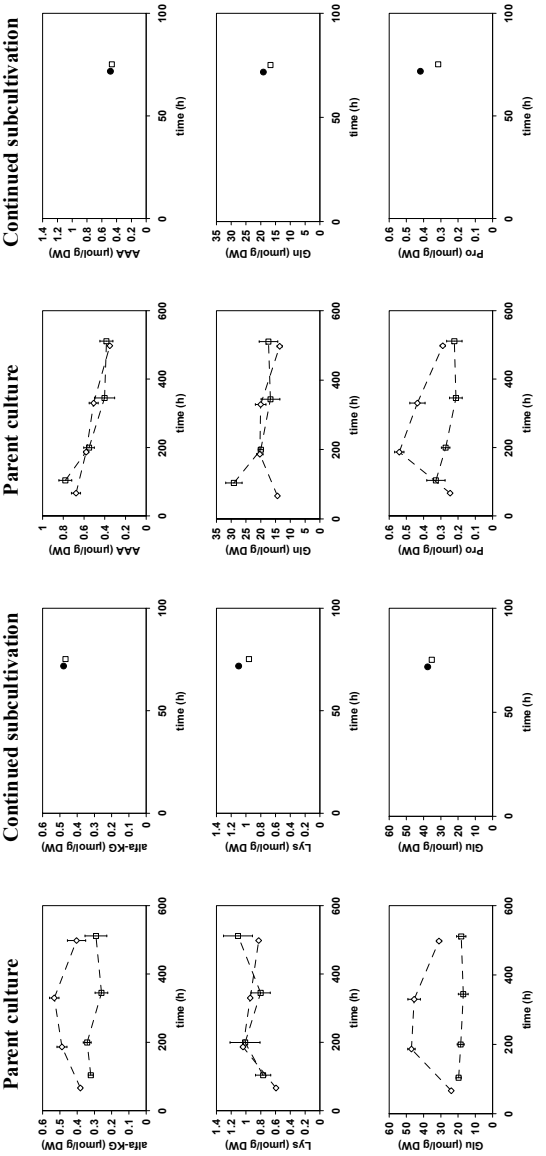

Figure 5.S11

Amino acids from alfa-KG in chemostat 2 (□) and 4 (◊) (left) and subchemostat 4.1 (●) and 4.2 (□) (right).

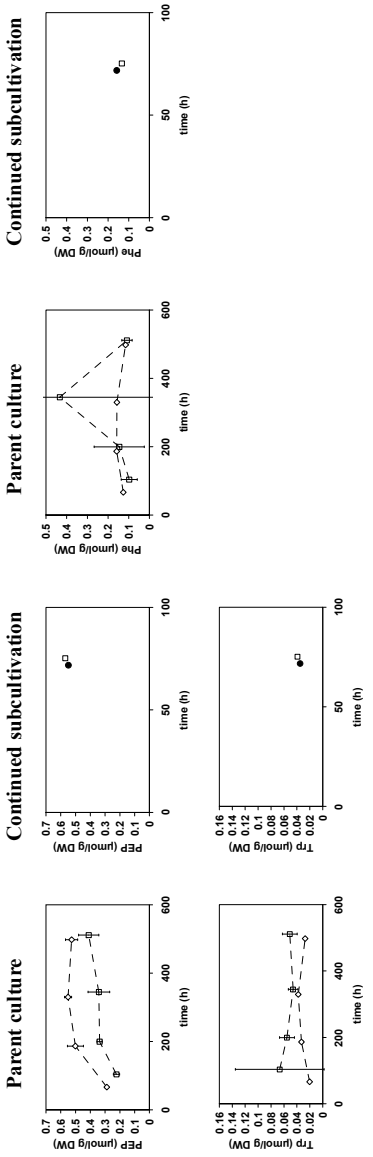

Figure 5.S12

Amino acids from E4P and PEP in chemostat 2 (□) and 4 (◊) (left) and subchemostat 4.1 (●) and 4.2 (□) (right).

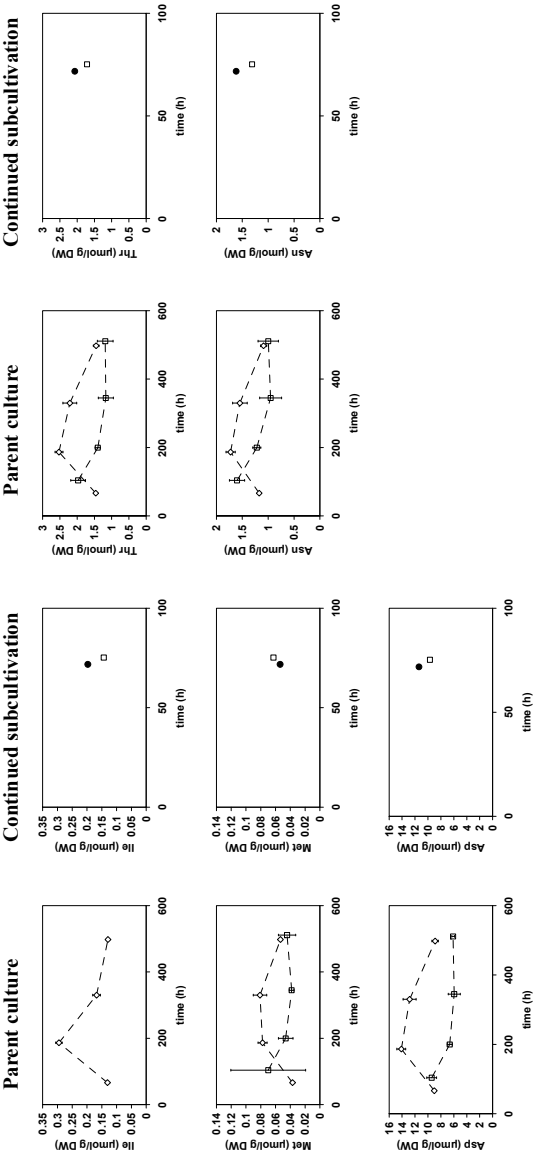

Figure 5.S13

Amino acids from oxaloacetate in chemostat 2 (□) and 4 (◊) (left) and subchemostat 4.1 (●) and 4.2 (□) (right).

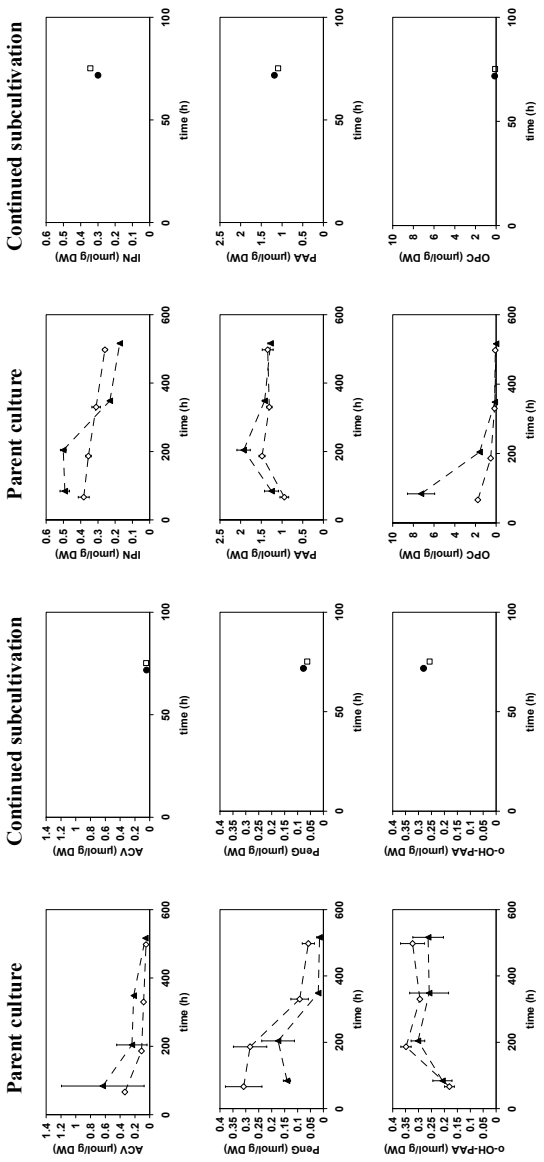

Figure 5.S14 Metabolites related with penicillin biosynthesis during chemostat 3 (▲) and 4 (◊) (left) and subchemostat 4.1 (●) and 4.2 (□) (right).

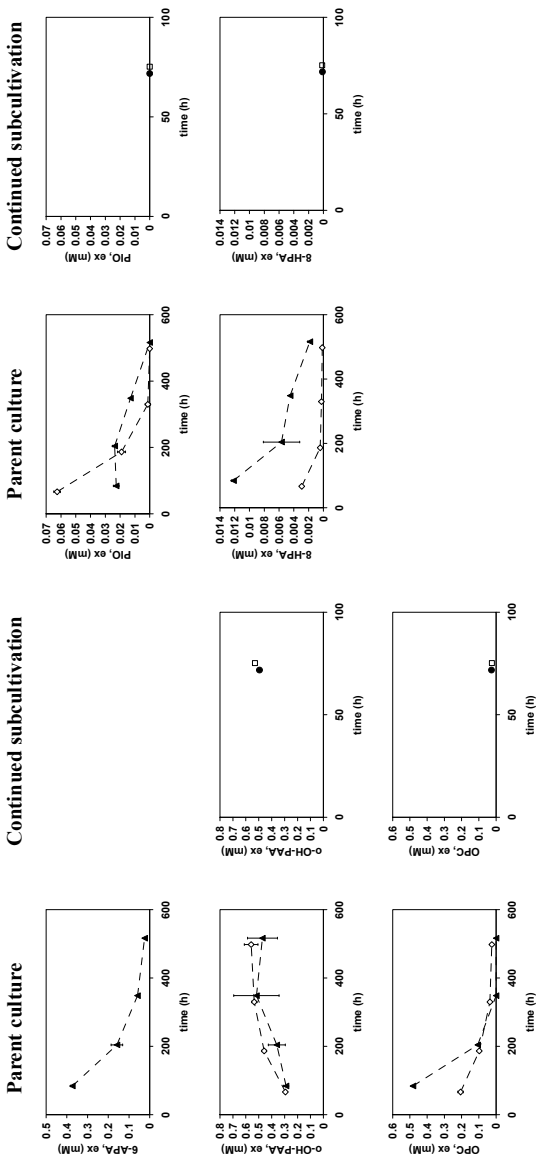

Figure 5.S15 Extracellular levels of metabolites related with penicillin biosynthesis during chemostat 3 (▲) and 4 (◊) (left) and subchemostat 4.1 (●) and 4.2 (□) (right).

CHAPTER 6

Outlook

Penicillin production is performed on an industrial scale for several decades. Throughout the years the overall understanding of cellular functioning increased and this knowledge has been used to enhance product yields and rates in penicillin fermentations. As discussed in the first chapter of this thesis, the development of several –omic techniques opened new possibilities to find metabolic engineering targets to enhance penicillin production by *Penicillium chrysogenum* using a systems approach. This thesis shows the most interesting findings of 4 years of research on *P. chrysogenum.* A simple genetic regulation model for penicillin production (from gene to flux) was developed. Furthermore, the first *in vivo* study of transport mechanism and kinetics of the precursor PAA and the product PenG were conducted, using a newly developed quenching and filtration-based washing method to measure the endometabolome. Lastly, the first study was conducted in which several –omics techniques (from gene to flux) were integrated to perform a systems study on degenerating penicillin producing cultures of *P. chrysogenum*. However, still many uncertainties remain and several issues need to be addressed in the future.

Culture heterogeneity

Throughout this thesis measurements were reported on penicillin cluster copy numbers, transcripts, protein amounts, enzyme activities and metabolite levels. However, all these results represent culture averages. As *Penicillium chrysogenum* is a multicellular organism, it is known that cells in a hypha are in a different developmental phase and have different functions. These differences will certainly be expressed in local different metabolic states, but cannot be distinguished with the techniques used in this thesis. Although overall changes in metabolic states will be represented in changing culture averages, one should remain cautious with data interpretation. Han Wösten and co-workers used a technique to measure different metabolic states in different cells in plate cultured hypha of *Aspergillus niger* (Levin et al., 2007b; Levin et al., 2007a). Such studies can shed light on differentiation in hyphae and its effect on cellular metabolism. Still it will remain difficult to measure differentiation in submerged cultures used in production processes. As an alternative, penicillin biosynthesis can also be studied in a non-hyphal organism such as was recently achieved in *Hansenula polymorpha* (Gidijala et al., 2009).

Not only are fungi multicellular organisms, also the cells are highly compartmentalized and the penicillin pathway is also compartmentalized. Metabolite levels, protein amounts and enzyme activities will have different values in the compartment where the specific reaction takes place than the culture average. Also in this respect caution with data analysis is necessary. So far attempts to measure metabolites in compartments were unsuccessful.

However, Canelas et al. show that metabolite ratios in compartment can be measured with sensor reactions (Canelas et al., 2008b). Further developments in measuring or determining different metabolic states between compartments will be essential to get a full understanding of the complete cellular metabolism.

Transport

Metabolic engineering has focused on increased intracellular fluxes from substrate to product. Two possibly rate-limiting steps are often overlooked, namely the transport of the substrate from the culture medium into the cell and the transport of the product from the cell into the culture medium. So far it proved to be very hard to track whether these steps were rate limiting, because of limitations in our capacity to study their kinetics under *in vivo* conditions. With recent developments in separation between the endo- and exometabolome it becomes possible to track whether transport steps are rate-limiting. This should lead to increased awareness of possibly limiting transport steps.

A key assumption while studying transport reactions is the value for the intracellular volume, because its effect on the determined intracellular concentration is significant. It proved to be very difficult to determine its value and only few reports in literature can be found on this matter. Furthermore we assume that the intracellular volume remains constant upon stimulus response experiments, although it is not known whether this is a legitimate assumption.

Another assumption used is a constant proton motive force, which needs to be supported by independent measurements of $\Delta\Psi$ and ΔpH. Finally it is usually assumed (or used to study PAA and PenG transport) that in stimulus response experiments the intracellular pH remains constant. Orij et al show that it is possible to measure the intracellular pH by inserting the pH-sensitive GFP derivative 'ratiometric pHluorin' in yeast (Orij et al., 2009). Performing a stimulus response experiments with strains containing this pH-sensitive GFP derivative 'ratiometric pHluorin' would allow to verify whether the pH does remain constant in stimulus response experiments.

Stimulus response experiments indicated that PAA is imported by passive diffusion and exported with an ABC transporter, while the PenG anion is exported over the cell membrane with a facilitated transporter using the electrochemical potential. A genome-wide transcript analysis by Harris et al. yielded candidates for transporter genes which were supported by this research. It would be interesting to perform knockout studies with these

candidates and measure intracellular and extracellular levels of PAA and PenG to validate the effect of the absence of the transporter on the intracellular to extracellular concentration ratio.

Systems studies

This thesis shows two results of systems studies from gene to flux. In chapter 2 enzyme activity measurements are used to analyze gene regulation which strongly indicates IPNS to play a rate-limiting role for penicillin production. This knowledge is applied by constructing a dynamic gene regulation model from gene to flux which successfully described penicillin and biomass production in chemostat and dynamic fed-batch experiments.

In chapter 5 a systems study was performed to get insights in the mechanisms which contribute to degeneration of product formation. The copy number of penicillin gene clusters, the number of peroxisomes in subapical cells, genome wide transcripts, most metabolites in central carbon metabolism, most amino acids, the PAA and metabolites related to penicillin biosynthesis, protein amounts of the three enzymes in the penicillin pathway and fluxes were measured. In the system from genome to flux the most direct link with the metabolome/fluxome is the proteome. In this systems study only protein amounts of the three enzymes in the penicillin pathway were measured and in indirect measure of the penicillin transport capacity was obtained. The transcriptome and proteome of these three enzymes is ill correlated. Therefore great caution should be taken when linking the genome wide transcriptome measurements with the metabolome and flux measurement. A future full systems study requires genome wide proteome measurements. With recent developments in mass spectrometry it should become possible to perform such a proteome analysis.

Results of our systems study on degeneration of penicillin production in fermentations indicate that the cause of degeneration must be found in a changed regulation of penicillin pathway enzymes and transporter proteins leading to changed translation efficiency, post-translational modification efficiency or protein degradation rate. To shed light on these changes further proteome based research should be dedicated on the quantification of transporter proteins, the level of all penicillin pathway enzyme including their post translational modification, protein turnover rate and regulation on proteins.

Finally, to fully understand the relationship between changing enzyme amounts and metabolite levels in the penicillin pathway a kinetic model is necessary. Such a kinetic model would allow an analysis of the reasons for metabolite changes in systems studies. Although there are still many hurdles to overcome before such a kinetic model can successfully developed, recent developments in model reduction and parameter approximation look promising (Nikerel, 2009).

The incomplete annotation of the genome which is mainly based on homology with other fungal genomes, with many gaps and unknown genes, proved to be problematic for the analysis of the results of the current systems study with *P. chrysogenum*. For example, little is known about transcription factors, regulatory genes and regulatory motifs in *P. chrysogenum*. A better annotated genome in these areas would lead to more efficient data mining in future systems studies.

Improved analytics enabled researchers to obtain very large datasets from the first years of this new millennium onwards. The general optimistic idea was that once big datasets were available, hypotheses for mechanisms would automatically follow. However, it proved to be quite difficult to analyze these enormous datasets with the human eye. An important and possibly rate-limiting step in systems studies at the moment might well be visualization. Developments in this field are definitely necessary to efficiently mine the increased dataset; towards a science of visualomics. Furthermore the old-fashioned manner of isolating a problem from a network will be necessary again to obtain a full understanding of the functioning of individual pieces of a network.

References

Abraham EP, Chain E, Fletcher CM, Gardner AD, Heatley NG, Jennings MA, Florey HW. 1941. Further observations on penicillin. *The Lancet* **238** (6155): 177-189.

Andrade AC, Van Nistelrooy JGM, Peery RB, Skatrud PL, De Waard MA. 2000. The role of ABC transporters from *Aspergillus nidulans* in protection against cytotoxic agents and in antibiotic production. *Molecular and General Genetics* **263** (6): 966-977.

Bailey TL, Elkan C. 1994. Fitting a mixture model by expectation maximization to discover motifs in biopolymers. *Proc Int Conf Intell Syst Mol Biol* **2**28-36.

Bajpai RK, Reuss M. 1980. A Mechanistic Model for Penicillin Production. *Journal of Chemical Technology and Biotechnology* **30** (6): 332-344.

Bajpai RK, Reuss M. 1981. Evaluation of Feeding Strategies in Carbon-Regulated Secondary Metabolite Production Through Mathematical-Modeling. *Biotechnology and Bioengineering* **23** (4): 717-738.

Baltz RH, Seno ET. 1981. Properties of *Streptomyces fradiae* Mutants Blocked in Biosynthesis of the Macrolide Antibiotic Tylosin. *Antimicrobial Agents and Chemotherapy* **20** (2): 214-225.

Barrett CL, Kim TY, Kim HU, Palsson BØ, Lee SY. 2006. Systems biology as a foundation for genome-scale synthetic biology. *Current Opinion in Biotechnology* **17** (5): 488-492.

Benson DA, Karsch-Mizrachi I, Lipman DJ, Ostell J, Sayers EW. 2009. GenBank. *Nucleic Acids Research* **37**D26-D31.

Birol G, Ündey C, Çinar A. 2002. A modular simulation package for fed-batch fermentation: penicillin production. *Computers & Chemical Engineering* **26** (11): 1553-1565.

Bolten CJ, Kiefer P, Letisse F, Portais JC, Wittmann C. 2007. Sampling for metabolome analysis of microorganisms. *Analytical Chemistry* **79** (10): 3843-3849.

Brakhage AA. 1998. Molecular regulation of β-lactam biosynthesis in filamentous fungi. *Microbiology and Molecular Biology Reviews* **62** (3): 547-585.

Brakhage AA, Browne P, Turner G. 1992. Regulation of *Aspergillus nidulans* Penicillin Biosynthesis and Penicillin Biosynthesis Genes *acvA* and *ipnA* by Glucose. *Journal of Bacteriology* **174** (11): 3789-3799.

Burgstaller W. 1997. Transport of small ions and molecules through the plasma membrane of filamentous fungi. *Critical Reviews in Microbiology* **23** (1): 1-46.

Burns M, van Dijck PWM. 2002. The development of the penicillin production process in Delft, The Netherlands, during World War II under Nazi occupation. *Advances in Applied Microbiology, Vol 51* **51**185-200.

Buscher JM, Czernik D, Ewald JC, Sauer U, Zamboni N. 2009. Cross-Platform Comparison of Methods for Quantitative Metabolomics of Primary Metabolism. *Analytical Chemistry* **81** (6): 2135-2143.

Canelas AB, Ras C, ten Pierick A, van Dam JC, Heijnen JJ, van Gulik WM. 2008a. Leakage-free rapid quenching technique for yeast metabolomics. *Metabolomics* **4** (3): 226-239.

Canelas AB, ten Pierick A, Ras C, Seifar RM, van Dam JC, van Gulik WM, Heijnen JJ. 2009. Quantitative Evaluation of Intracellular Metabolite Extraction Techniques for Yeast Metabolomics. *Analytical Chemistry* **81** (17): 7379-7389.

Canelas AB, van Gulik WM, Heijnen JJ. 2008b. Determination of the cytosolic free NAD/NADH ratio in *Saccharomyces cerevisiae* under steady-state and highly dynamic conditions. *Biotechnology and Bioengineering* **100** (4): 734-743.

Chain E, Florey HW, Adelaide MB, Gardner AD, Oxfd DM, Heatley NG, Jennings MA, Orr-Ewing J, Sanders AG. 1940. Penicillin as chemotherapeutic agent. *The Lancet* **236** (6104): 226-228.

Christensen LH, Henriksen CM, Nielsen J, Villadsen J, Egelmitani M. 1995. Continuous Cultivation of *Penicillium chrysogenum* - Growth on Glucose and Penicillin Production. *Journal of Biotechnology* **42** (2): 95-107.

Christensen LH, Mandrup G, Nielsen J, Villadsen J. 1994. A Robust Liquid-Chromatographic Method for Measurement of Medium Components During Penicillin Fermentations. *Analytica Chimica Acta* **296** (1): 51-62.

Clutterbuck PW, Lovell R, Raistrick H. 1932. The formation from glucose by members of the *Penicillium chrysogenum* series of a pigment, an alkali-soluble protein and penicillin - The antibacterial substance of fleming. *Biochemical Journal* **26** (6): 1907-1918.

Condon C, Squires C, Squires CL. 1995. Control of rRNA Transcription in *Escherichia coli*. *Microbiological Reviews* **59** (4): 623-645.

De Koning W, Van Dam K. 1992. A Method for the Determination of Changes of Glycolytic Metabolites in Yeast on A Subsecond Time Scale Using Extraction at Neutral pH. *Analytical Biochemistry* **204** (1): 118-123.

Demain AL, Elander RP. 1999. The β-lactam antibiotics: past, present, and future. *Antonie Van Leeuwenhoek International Journal of General and Molecular Microbiology* **75** (1-2): 5-19.

Douma RD, de Jonge LP, Jonker CTH, Seifar RM, Heijnen JJ, van Gulik WM. 2010a. Intracellular metabolite determination in the presence of extracellular abundance: application to the penicillin biosynthesis pathway in *Penicillium chrysogenum*. *Biotechnology and Bioengineering* **107** (1): 105-115.

Douma RD, Verheijen PJT, De Laat WTAM, Heijnen JJ, van Gulik WM. 2010b. Dynamic Gene Expression Regulation Model for Growth and Penicillin Production in *Penicillium chrysogenum*. *Biotechnology and Bioengineering* **106** (4): 608-618.

Dunn WB, Ellis DI. 2005. Metabolomics: Current analytical platforms and methodologies. *Trends in Analytical Chemistry* **24** (4): 285-294.

Elander RP. 1983. Strain improvement and preservation of beta-lactam producing microorganisms. In: Demain AL, Solomon N, editors. Antibiotics Containing the Beta-Lactam Structure I. New York: Springer-Verlag. p 97-146.

Eriksen SH, Soderblom TB, Jensen B, Olsen J. 1998. Uptake of phenylacetic acid by two strains of *Penicillium chrysogenum*. *Biotechnology and Bioengineering* **60** (3): 310-316.

Feng B, Friedlin E, Marzluf GA. 1994. A Reporter Gene Analysis of Penicillin Biosynthesis Gene-Expression in *Penicillium Chrysogenum* and Its Regulation by Nitrogen and Glucose Catabolite Repression. *Applied and Environmental Microbiology* **60** (12): 4432-4439.

Fernández-Cañón JM, Reglero A, Martínez-Blanco H, Ferrero MA, Luengo JM. 1989a. II. Phenylacetic Acid Transport-System in *Penicillium chrysogenum* Wis 54-1255: Molecular Specificity of Its Induction. *Journal of Antibiotics* **42** (9): 1410-1415.

Fernández-Cañón JM, Reglero A, Martínez-Blanco H, Luengo JM. 1989b. I. Uptake of Phenylacetic Acid by *Penicillium chrysogenum* Wis 54-1255: A Critical Regulatory Point in Benzylpenicillin Biosynthesis. *Journal of Antibiotics* **42** (9): 1398-1409.

Fierro F, Barredo JL, Díez B, Gutierrez S, Fernández FJ, Martín JF. 1995. The Penicillin Gene-Cluster Is Amplified in Tandem Repeats Linked by Conserved Hexanucleotide Sequences. *Proceedings of the National Academy of Sciences of the United States of America* **92** (13): 6200-6204.

Fleischmann RD, Adams MD, White O, Clayton RA, Kirkness EF, Kerlavage AR, Bult CJ, Tomb JF, Dougherty BA, Merrick JM, Mckenney K, Sutton G, Fitzhugh W, Fields C, Gocayne JD, Scott J, Shirley R, Liu LI, Glodek A, Kelley JM, Weidman JF, Phillips CA, Spriggs T, Hedblom E, Cotton MD, Utterback TR, Hanna MC, Nguyen DT, Saudek DM, Brandon RC, Fine LD, Fritchman JL, Fuhrmann JL, Geoghagen NSM, Gnehm CL, Mcdonald LA, Small KV, Fraser CM, Smith HO, Venter JC. 1995. Whole-Genome Random Sequencing and Assembly of *Haemophilus influenzae* Rd. *Science* **269** (5223): 496-512.

Fleming A. 1928. Antibacterial Action of Cultures of A Penicillium, with Special Reference to Their Use in the Isolation of *B. Influenza*. *British Journal of Experimental Pathology* **10**185-194.

Foster JW, Woodruff HB, McDaniel LE. 1943. Microbiological aspects of penicillin. *Journal of Bacteriology* **46** (5): 421-433.

Gidijala L, Kiel JAKW, Douma RD, Seifar RM, van Gulik WM, Bovenberg RAL, Veenhuis M, van der Klei IJ. 2009. An Engineered Yeast Efficiently Secreting Penicillin. *Plos One* **4** (12).

Gonzalez B, Francois J, Renaud M. 1997. A rapid and reliable method for metabolite extraction in yeast using boiling buffered ethanol. *Yeast* **13** (14): 1347-1355.

Gravius B, Bezmalinovic T, Hranueli D, Cullum J. 1993. Genetic Instability and Strain Degeneration in *Streptomyces rimosus*. *Applied and Environmental Microbiology* **59** (7): 2220-2228.

Gray PP, Bhuwapathanapun S. 1980. Production of the Macrolide Antibiotic Tylosin in Batch and Chemostat Cultures. *Biotechnology and Bioengineering* **22** (9): 1785-1804.

Greenbaum D, Colangelo C, Williams K, Gerstein M. 2003. Comparing protein abundance and mRNA expression levels on a genomic scale. *Genome Biology* **4** (9).

Griffin TJ, Gygi SP, Ideker T, Rist B, Eng J, Hood L, Aebersold R. 2002. Complementary profiling of gene expression at the transcriptome and proteome levels in Saccharomyces cerevisiae. *Molecular & Cellular Proteomics* **1** (4): 323-333.

Gunnarsson N, Eliasson A, Nielsen J. 2004. Control of fluxes towards antibiotics and the role of primary metabolism in production of antibiotics. *Advances in Biochemical Engineering / Biotechnology* **88**137-178.

Gutierrez S, Marcos AT, Casqueiro J, Kosalkova K, Fernandez FJ, Velasco J, Martin JF. 1999. Transcription of the pcbAB, pcbC and penDE genes of *Penicillium chrysogenum* AS-P-78 is repressed by glucose and the repression is not reversed by alkaline pHs. *Microbiology* **145**317-324.

Gutiérrez S, Marcos AT, Casqueiro J, Kosalková K, Fernández FJ, Velasco J, Martín JF. 1999. Transcription of the pcbAB, pcbC and penDE genes of *Penicillium chrysogenum* AS-P-78 is repressed by glucose and the repression is not reversed by alkaline pHs. *Microbiology* **145**317-324.

Harris DM, Diderich JA, van der Krogt ZA, Luttik MAH, Raamsdonk UM, Bovenberg RAL, van Gulik WM, van Dijken JP, Pronk JT. 2006. Enzymic analysis of NADPH metabolism in beta-lactam-producing *Penicillium chrysogenum*: Presence of a mitochondrial NADPH dehydrogenase. *Metabolic Engineering* **8** (2): 91-101.

Harris DM, van der Krogt ZA, Klaassen P, Raamsdonk LM, Hage S, van den Berg MA, Bovenberg RAL, Pronk JT, Daran JM. 2009. Exploring and dissecting genome-wide gene expression responses of *Penicillium chrysogenum* to phenylacetic acid consumption and penicillinG production. *Bmc Genomics* **10**.

Hazelwood LA, Tai SL, Boer VM, de Winde JH, Pronk JT, Daran JM. 2006. A new physiological role for Pdr12p in *Saccharomyces cerevisiae*: export of aromatic and branched-chain organic acids produced in amino acid catabolism. *Fems Yeast Research* **6** (6): 937-945.

Heijnen JJ, Roels JA, Stouthamer AH. 1979. Application of Balancing Methods in Modeling the Penicillin Fermentation. *Biotechnology and Bioengineering* **21** (12): 2175-2201.

Hillenga DJ, Versantvoort HJM, Driessen AJM, Konings WN. 1996a. Basic amino acid transport in plasma membrane vesicles of *Penicillium chrysogenum*. *Journal of Bacteriology* **178** (14): 3991-3995.

Hillenga DJ, Versantvoort HJM, Driessen AJM, Konings WN. 1996b. Sulfate transport in *Penicillium chrysogenum* plasma membranes. *Journal of Bacteriology* **178** (13): 3953-3956.

Hillenga DJ, Versantvoort HJM, Vandermolen S, Driessen AJM, Konings WN. 1995. *Penicillium chrysogenum* Takes Up the Penicillin-G Precursor Phenylacetic Acid by Passive Diffusion. *Applied and Environmental Microbiology* **61** (7): 2589-2595.

Ideker T, Thorsson V, Ranish JA, Christmas R, Buhler J, Eng JK, Bumgarner R, Goodlett DR, Aebersold R, Hood L. 2001. Integrated genomic and proteomic analyses of a systematically perturbed metabolic network. *Science* **292** (5518): 929-934.

Jaklitsch WM, Hampel W, Röhr M, Kubicek CP, Gamerith G. 1986. α-Aminoadipate pool concentration and penicillin biosynthesis in strains of *Penicillium chrysogenum*. *Canadian Journal of Microbiology* **32** (6): 473-480.

Jami M-S, Barreiro C, García-Estrada C, Martín J-F. 2010. Proteome Analysis of the Penicillin Producer *Penicillium chrysogenum*: characterization of protein changes during the industrial strain improvement. *Mol Cell Proteomics* **9** (6): 1182-1198.

Kiel JAKW, van den Berg MA, Fusetti F, Poolman B, Bovenberg RAL, Veenhuis M, van der Klei IJ. 2009. Matching the proteome to the genome: the microbody of penicillin-producing *Penicillium chrysogenum* cells. *Functional & Integrative Genomics* **9** (2): 167-184.

Kiel JAKW, van der Klei IJ, van den Berg MA, Bovenberg RAL, Veenhuis M. 2005. Overproduction of a single protein, Pc-Pex 11p, results in 2-fold enhanced penicillin production by *Penicillium chrysogenum*. *Fungal Genetics and Biology* **42** (2): 154-164.

Kitano H. 2002. Systems biology: A brief overview. *Science* **295** (5560): 1662-1664.

Kleijn RJ, Liu F, van Winden WA, van Gulik WM, Ras C, Heijnen JJ. 2007. Cytosolic NADPH metabolism in penicillin-G producing and non-producing chemostat cultures of *Penicillium chrysogenum*. *Metabolic Engineering* **9** (1): 112-123.

Kleijn RJ, van Winden WA, Ras C, van Gulik WM, Schipper D, Heijnen JJ. 2006. C-13-labeled gluconate tracing as a direct and accurate method for determining the pentose phosphate pathway split ratio in *Penicillium chrysogenum*. *Applied and Environmental Microbiology* **72** (7): 4743-4754.

Kresnowati MTAP, Suarez-Mendez C, Groothuizen MK, van Winden WA, Heijnen JJ. 2007. Measurement of fast dynamic intracellular pH in *Saccharomyces cerevisiae*, using benzoic acid pulse. *Biotechnology and Bioengineering* **97** (1): 86-98.

Kresnowati MTAP, van Winden WA, Almering MJH, ten Pierick A, Ras C, Knijnenburg TA, Daran-Lapujade P, Pronk JT, Heijnen JJ, Daran JM. 2006. When transcriptome meets metabolome: fast cellular responses of yeast to sudden relief of glucose limitation. *Molecular Systems Biology* **2** (49): 1-12.

Kresnowati MTAP, van Winden WA, van Gulik WM, Heijnen JJ. 2008. Energetic and metabolic transient response of *Saccharomyces cerevisiae* to benzoic acid. *Febs Journal* **275** (22): 5527-5541.

Krikken AM, Veenhuis M, van der Klei IJ. 2009. *Hansenula polymorpha pex11* cells are affected in peroxisome retention. *Febs Journal* **276** (5): 1429-1439.

Künkel W, Berger D, Risch S, Wittmannbresinsky B. 1992. Genetic Instability of Industrial Strains of *Penicillium chrysogenum*. *Applied Microbiology and Biotechnology* **36** (4): 499-502.

Lange HC, Eman M, van Zuijlen G, Visser D, van Dam JC, Frank J, de Mattos MJT, Heijnen JJ. 2001. Improved rapid sampling for in vivo kinetics of intracellular metabolites in *Saccharomyces cerevisiae*. *Biotechnology and Bioengineering* **75** (4): 406-415.

Legerton TL, Kanamori K, Weiss RL, Roberts JD. 1983a. Measurements of Cytoplasmic and Vacuolar pH in *Neurospora* Using N-15 Nuclear Magnetic-Resonance Spectroscopy. *Biochemistry* **22** (4): 899-903.

Legerton TL, Kanamori K, Weiss RL, Roberts JD. 1983b. Measurements of Cytoplasmic and Vacuolar pH in *Neurospora* Using Nitrogen-15 Nuclear Magnetic Resonance Spectroscopy. *Biochemistry* **22** (4): 899-903.

Legisa M, Kidric J. 1989. Initiation of Citric Acid Accumulation in the Early Stages of *Aspergillus niger* Growth. *Appl Microbiol Biotechnol* **31** (5-6): 453-457.

Lein J. 1986. The Panlabs penicillin strain improvement program. In: Vanek Z, Hostálek Z, editors. Overproduction of microbial metabolites. Boston: Butterworths. p 105-139.

Levin AM, de Vries RP, Conesa A, de Bekker C, Talon M, Menke HH, van Peij NNME, Wosten HAB. 2007a. Spatial differentiation in the vegetative mycelium of Aspergillus niger. *Eukaryotic Cell* **6** (12): 2311-2322.

Levin AM, de Vries RP, Wosten HAB. 2007b. Localization of protein secretion in fungal colonies using a novel culturing technique; the ring-plate system. *Journal of Microbiological Methods* **69** (2): 399-401.

Litzka O, Bergh KT, Van den Brulle J, Steidl S, Brakhage AA. 1999. Transcriptional control of expression of fungal β-lactam biosynthesis genes. *Antonie Van Leeuwenhoek International Journal of General and Molecular Microbiology* **75** (1-2): 95-105.

Lynch HC, Bushell ME. 1995. The physiology of erythromycin biosynthesis in cyclic fed batch culture. *Microbiology* **141**3105-3111.

Martin JF. 1992. Clusters of Genes for the Biosynthesis of Antibiotics - Regulatory Genes and Overproduction of Pharmaceuticals. *Journal of Industrial Microbiology* **9** (2): 73-90.

Martín JF, Casqueiro J, Kosalková K, Marcos AT, Gutiérrez S. 1999. Penicillin and cephalosporin biosynthesis: Mechanism of carbon catabolite regulation of penicillin production. *Antonie Van Leeuwenhoek International Journal of General and Molecular Microbiology* **75** (1-2): 21-31.

Martín JF, Casqueiro J, Liras P. 2005. Secretion systems for secondary metabolites: how producer cells send out messages of intercellular communication. *Current Opinion in Microbiology* **8** (3): 282-293.

Martin JF, Casqueiro J, Liras P. 2005. Secretion systems for secondary metabolites: how producer cells send out messages of intercellular communication. *Curr Opin Microbiol* **8** (3): 282-293.

Martín JF, Gutiérrez S. 1995. Genes for β-Lactam Antibiotic Biosynthesis. *Antonie Van Leeuwenhoek International Journal of General and Molecular Microbiology* **67** (2): 181-200.

Martínez-Blanco H, Reglero A, Ferrero MA, Fernández-Cañón JM, Luengo JM. 1989. Repression of Phenylacetic Acid Transport-System in *Penicillium chrysogenum* Wis 54-1255 by Free Amino-Acids and Ammonium-Salts. *Journal of Antibiotics* **42** (9): 1416-1423.

Mashego MR, Jansen MLA, Vinke JL, van Gulik WM, Heijnen JJ. 2005. Changes in the metabolome of *Saccharomyces cerevisiae* associated with evolution in aerobic glucose-limited chemostats. *Fems Yeast Research* **5** (4-5): 419-430.

Mashego MR, Rumbold K, de Mey M, Vandamme E, Soetaert W, Heijnen JJ. 2007. Microbial metabolomics: past, present and future methodologies. *Biotechnology Letters* **29**1-16.

Mashego MR, van Gulik WM, Vinke JL, Heijnen JJ. 2003. Critical evaluation of sampling techniques for residual glucose determination in carbon-limited chemostat culture of *Saccharomyces cerevisiae*. *Biotechnology and Bioengineering* **83** (4): 395-399.

Meijer WH, Gidijala L, Fekken S, Kiel JAKW, van den Berg M, Lascaris R, Bovenberg R, van der Klei IJ. 2010. Peroxisomes are required for efficient penicillin biosynthesis in *Penicillium chrysogenum*. *Applied and Environmental Microbiology* **76** (17): 5702-5709.

Menezes JC, Alves SS, Lemos JM, Deazevedo SF. 1994. Mathematical-Modeling of Industrial Pilot-Plant Penicillin-G Fed-Batch Fermentations. *Journal of Chemical Technology and Biotechnology* **61** (2): 123-138.

Miller JR, Ingolia TD. 1989. Cloning and Characterization of Beta-Lactam Biosynthetic Genes. *Molecular Microbiology* **3** (5): 689-695.

Moles CG, Mendes P, Banga JR. 2003. Parameter estimation in biochemical pathways: A comparison of global optimization methods. *Genome Research* **13** (11): 2467-2474.

Moyer AJ, Coghill RD. 1946a. Production of Penicillin in Surface Cultures. *Journal of Bacteriology* **51** (1): 57-78.

Moyer AJ, Coghill RD. 1946b. The Laboratory Scale Production of Penicillin in Submerged Cultures by *Penicillium notatum* Westling (NRRL 832). *Journal of Bacteriology* **51** (1): 79-93.

Moyer AJ, Coghill RD. 1947. The Effect of Phenylacetic Acid on Penicillin Production. *Journal of Bacteriology* **1947** (53): 3-329.

Nasution U. 2007. Mass balance analysis of the dynamic interactions between central metabolism and penicillin synthesis in *Penicillium chrysogenum*. In: PhD thesis: A dynamic and steady state metabolome study of central metabolism and its relation with the penicillin biosynthesis pathway.

Nasution U, van Gulik WM, Kleijn RJ, van Winden WA, Proell A, Heiinen JJ. 2006a. Measurement of intracellular metabolites of primary metabolism and adenine nucleotides in chemostat cultivated *Penicillium chrysogenum*. *Biotechnology and Bioengineering* **94** (1): 159-166.

Nasution U, van Gulik WM, Proell A, van Winden WA, Heijnen JJ. 2006b. Generating short-term kinetic responses of primary metabolism of *Penicillium chrysogenum* through glucose perturbation in the bioscope mini reactor. *Metabolic Engineering* **8** (5): 395-405.

Nasution U, van Gulik WM, Ras C, Proell A, Heijnen JJ. 2008. A metabolome study of the steady-state relation between central metabolism, amino acid biosynthesis and penicillin production in *Penicillium chrysogenum*. *Metabolic Engineering* **10** (1): 10-23.

Nelson DL, Cox MM. 2000. Lehninger Principles of Biochemistry Third Edition. New York, NY: Worth Publishers.

Newbert RW, Barton B, Greaves P, Harper J, Turner G. 1997. Analysis of a commercially improved *Penicillium chrysogenum* strain series: involvement of recombinogenic regions in amplification and deletion of the penicillin biosynthesis gene cluster. *Journal of Industrial Microbiology & Biotechnology* **19** (1): 18-27.

Nielsen J. 1997. Physiological Engineering Aspects of *Penicillium chrysogenum*. Singapore: World Scientific.

Nielsen J, Jørgensen HS. 1995. Metabolic Control Analysis of the Penicillin Biosynthetic-Pathway in A High-Yielding Strain of *Penicillium chrysogenum*. *Biotechnology Progress* **11** (3): 299-305.

Nijland JG, Kovalchuk A, van den Berg MA, Bovenberg RAL, Driessen AJM. 2008. Expression of the transporter encoded by the cefT gene of *Acremonium chrysogenum* increases cephalosporin production in *Penicillium chrysogenum*. *Fungal Genetics and Biology* **45** (10): 1415-1421.

Nikerel IE. 2009. Managing complexity of cellular systems: theoretical tools for dynamic modeling of metabolic reaction networks. Delft, The Netherlands: PhD thesis,Delft University of Technology.

Orij R, Postmus J, Ter Beek A, Brul S, Smits GJ. 2009. In vivo measurement of cytosolic and mitochondrial pH using a pH-sensitive GFP derivative in Saccharomyces cerevisiae reveals a relation between intracellular pH and growth. *Microbiology-Sgm* **155**268-278.

Packer HL, Keshavarz-Moore E, Lilly MD, Thomas CR. 1992a. Estimation of Cell Volume and Biomass of *Penicillium chrysogenum* Using Image-Analysis. *Biotechnology and Bioengineering* **39** (4): 384-391.

Packer HL, Keshavarzmoore E, Lilly MD, Thomas CR. 1992b. Estimation of Cell-Volume and Biomass of *Penicillium chrysogenum* Using Image-Analysis. *Biotechnol Bioeng* **39** (4): 384-391.

Peñalva MA, Rowlands RT, Turner G. 1998. The optimization of penicillin biosynthesis in fungi. *Trends in Biotechnology* **16** (11): 483-489.

Pilatus U, Techel D. 1991. ^{31}P-NMR-studies on Intracellular pH and Metabolite Concentrations in Relation to the Circadian Rhythm, Temperature and Nutrition in *Neurospora crassa*. *Biochimica et Biophysica Acta* **1091** (3): 349-355.

Pirt SJ. 1965. Maintenance Energy of Bacteria in Growing Cultures. *Proceedings of the Royal Society of London - Series B: Biological Sciences* **163** (991): 224-231.

Poelwijk FJ, Kiviet DJ, Weinreich DM, Tans SJ. 2007. Empirical fitness landscapes reveal accessible evolutionary paths. *Nature* **445**383-386.

Raper KB, Aexander DF, Coghill RD. 1944. Penicillin II. Natural varation and penicillin production in Penicillium notatum and allied species. *Journal of Bacteriology* **48** (6): 639-659.

Revilla G, Ramos FR, López-Nieto MJ, Alvarez E, Martín JF. 1986. Glucose Represses Formation of δ-(L-α-Aminoadipyl)-L-Cysteinyl-D-Valine and Isopenicillin N Synthase But Not Penicillin Acyltransferase in *Penicillium chrysogenum*. *Journal of Bacteriology* **168** (2): 947-952.

Righelato RC. 1976. Selection of Strains of *Penicillium chrysogenum* with Reduced Penicillin Yields in Continuous Cultures. *Journal of Applied Chemistry and Biotechnology* **26** (3): 153-159.

Roa Engel CA, Straathof AJJ, van Gulik WM, de Sandt EJAX, van der Does T, van der Wielen LAM. 2009. Conceptual Process Design of Integrated Fermentation, Deacylation, and Crystallization in the Production of β-Lactam Antibiotics. *Industrial & Engineering Chemistry Research* **48** (9): 4352-4364.

Robin J, Lettier G, McIntyre M, Noorman H, Nielsen J. 2003. Continuous cultivations of a *Penicillium chrysogenum* strain expressing the expandase gene from *Streptomyces clavuligerus*: Growth yields and morphological characterization. *Biotechnology and Bioengineering* **83** (3): 361-368.

Rodríguez-Sáiz M, Barredo JL, Moreno MA, Fernández-Cañón JM, Peñalva MA, Díez B. 2001. Reduced function of a phenylacetate-oxidizing cytochrome P450 caused strong genetic improvement in early phylogeny of penicillin-producing strains. *Journal of Bacteriology* **183** (19): 5465-5471.

Roels JA. 1983. Structured models of microbial growth and product formation. In: Energetics and kinetics in biotechnology. Amsterdam, The Netherlands: Elsevier biomedical press. p 259-303.

Ruijter GJG, Visser J. 1996. Determination of intermediary metabolites in *Aspergillus niger*. *Journal of Microbiological Methods* **25** (3): 295-302.

Sáez MJ, Lagunas R. 1976. Determination of Intermediary Metabolites in Yeast - Critical-Examination of Effect of Sampling Conditions and Recommendations for Obtaining True Levels. *Molecular and Cellular Biochemistry* **13** (2): 73-78.

Sanders D, Slayman CL. 1982. Control of Intracellular pH - Predominant Role of Oxidative Metabolism, Not Proton Transport, in the Eukaryotic Microorganism *Neurospora*. *Journal of General Physiology* **80** (3): 377-402.

Savinell JM, Palsson BO. 1992. Network Analysis of Intermediary Metabolism Using Linear Optimization .1. Development of Mathematical Formalism. *Journal of Theoretical Biology* **154** (4): 421-454.

Seifar RM, Zhao Z, van Dam J, van Winden W, van Gulik W, Heijnen JJ. 2008. Quantitative analysis of metabolites in complex biological samples using ion-pair reversed-phase liquid chromatography-isotope dilution tandem mass spectrometry. *Journal of Chromatography A* **1187** (1-2): 103-110.

Stephanopoulos GN, Aristidou AA, Nielsen J. 1998. Comprehensive Models for cellular reactions. In: Metabolic Engineering: Principles and Methodologies. San Diego: Academic Press. p 81-114.

Tan IKP, Fernández-Cañón JM, Reglero A, Luengo JM. 1993. Effect of Analogs of Phenylacetic Acid (Pa) on the Pa Transport-System in *Penicillium chrysogenum* Strains H1107 and M223. *Applied Microbiology and Biotechnology* **40** (1): 113-116.

Taymaz-Nikerel H, de Mey M, Ras C, ten Pierick A, Seifar RM, van Dam JC, Heijnen JJ, van Gulik WM. 2009. Development and application of a differential method for reliable metabolome analysis in Escherichia coli. *Analytical Biochemistry* **386** (1): 9-19.

Theilgaard HA, Nielsen J. 1999. Metabolic control analysis of the penicillin biosynthetic pathway: the influence of the LLD-ACV : bisACV ratio on the flux control. *Antonie Van Leeuwenhoek International Journal of General and Molecular Microbiology* **75** (1-2): 145-154.

Theilgaard HA, van den Berg MA, Mulder CA, Bovenberg RAL, Nielsen J. 2001. Quantitative analysis of *Penicillium chrysogenum* Wis54-1255 transformants overexpressing the penicillin biosynthetic genes. *Biotechnology and Bioengineering* **72** (4): 379-388.

Theobald U, Mailinger W, Reuss M, Rizzi M. 1993. *In Vivo* Analysis of Glucose-Induced Fast Changes in Yeast Adenine-Nucleotide Pool Applying A Rapid Sampling Technique. *Analytical Biochemistry* **214** (1): 31-37.

Thykaer J, Nielsen J. 2003. Metabolic engineering of beta-lactam production. *Metabolic Engineering* **5** (1): 56-69.

Thykaer J, Rueksomtawin K, Noorman H, Nielsen J. 2008. NADPH-dependent glutamate dehydrogenase in *Penicillium chrysogenum* is involved in regulation of beta-lactam production. *Microbiology-Sgm* **154**1242-1250.

Vallino JJ, Stephanopoulos G. 1993. Metabolic Flux Distributions in *Corynebacterium glutamicum* During Growth and Lysine Overproduction. *Biotechnology and Bioengineering* **41** (6): 633-646.

van Dam JC, Eman MR, Frank J, Lange HC, van Dedem GWK, Heijnen SJ. 2002. Analysis of glycolytic intermediates in *Saccharomyces cerevisiae* using anion exchange chromatography and electrospray ionization with tandem mass spectrometric detection. *Analytica Chimica Acta* **460** (2): 209-218.

van den Berg MA, Albang R, Albermann K, Badger JH, Daran JM, Driessen AJM, Garcia-Estrada C, Fedorova ND, Harris DM, Heijne WHM, Joardar V, Kiel JAKW, Kovalchuk A, Martín JF, Nierman WC, Nijland JG, Pronk JT, Roubos JA, van der Klei IJ, van Peij NNME, Veenhuis M, von Dohren H, Wagner C, Wortman J, Bovenberg RAL. 2008. Genome sequencing and analysis of the filamentous fungus *Penicillium chrysogenum*. *Nature Biotechnology* **26** (10): 1161-1168.

van den Berg, M. A., Bovenberg, R. A. L., Driessen, A. J. M., Konings, W. N., Schuurs, T. A., Nieboer, M., and Westerlaken, I. 2001a. Enhancing secretion of beta-lactam compounds from a micro-organism by enhancing adenosine triphosphate-binding cassette transporter activity, useful for producing e.g. penicillin and cephalosporins. WO2001/32904.

van den Berg, M. A., Bovenberg, R. A. L., Driessen, A. J. M., Konings, W. N., Schuurs, T. A., Nieboer, M., and Westerlaken, I. 2001b. Method for enhancing secretion of beta-lactam transport. PCT patent WO2001/32904.

van der Klei IJ, Veenhuis M. 2002. Peroxisomes: flexible and dynamic organelles. *Current Opinion in Cell Biology* **14** (4): 500-505.

van der Rest ME, Kamminga AH, Nakano A, Anraku Y, Poolman B, Konings WN. 1995. The Plasma Membrane of *Saccharomyces cerevisiae*: Structure, Function, and Biogenesis. *Microbiological Reviews* **59** (2): 304-322.

van Gulik WM, Antoniewicz MR, De Laat WTAM, Vinke JL, Heijnen JJ. 2001. Energetics of growth and penicillin production in a high-producing strain of *Penicillium chrysogenum*. *Biotechnology and Bioengineering* **72** (2): 185-193.

van Gulik WM, De Laat WTAM, Vinke JL, Heijnen JJ. 2000. Application of metabolic flux analysis for the identification of metabolic bottlenecks in the biosynthesis of penicillin-G. *Biotechnology and Bioengineering* **68** (6): 602-618.

van Gulik WM, Heijnen JJ. 1995. A Metabolic Network Stoichiometry Analysis of Microbial-Growth and Product Formation. *Biotechnology and Bioengineering* **48** (6): 681-698.

Veenstra AE, Vansolingen P, Bovenberg RAL, Vandervoort LHM. 1991. Strain Improvement of *Penicillium chrysogenum* by Recombinant DNA Techniques. *Journal of Biotechnology* **17** (1): 81-90.

Veses V, Richards A, Gow NAR. 2008. Vacuoles and fungal biology. *Current Opinion in Microbiology* **11** (6): 503-510.

Villas-Bôas SG, Højer-Pedersen J, Åkesson M, Smedsgaard J, Nielsen J. 2005a. Global metabolite analysis of yeast: evaluation of sample preparation methods. *Yeast* **22** (14): 1155-1169.

Villas-Bôas SG, Mas S, Åkesson M, Smedsgaard J, Nielsen J. 2005b. Mass spectrometry in metabolome analysis. *Mass Spectrometry Reviews* **24** (5): 613-646.

Weibel KE, Mor JR, Fiechter A. 1974. Rapid Sampling of Yeast-Cells and Automated Assays of Adenylate, Citrate, Pyruvate and Glucose-6-Phosphate Pools. *Analytical Biochemistry* **58** (1): 208-216.

Weuster-Botz D. 1997. Sampling tube device for monitoring intracellular metabolite dynamics. *Analytical Biochemistry* **246** (2): 225-233.

Winder CL, Dunn WB, Schuler S, Broadhurst D, Jarvis R, Stephens GM, Goodacre R. 2008. Global metabolic profiling of *Escherichia coli* cultures: An evaluation of methods for quenching and extraction of intracellular metabolites. *Analytical Chemistry* **80** (8): 2939-2948.

Wittmann C, Kromer JO, Kiefer P, Binz T, Heinzle E. 2004. Impact of the cold shock phenomenon on quantification of intracellular metabolites in bacteria. *Analytical Biochemistry* **327** (1): 135-139.

Wu L, Mashego MR, van Dam JC, Proell AM, Vinke JL, Ras C, van Winden WA, van Gulik WM, Heijnen JJ. 2005. Quantitative analysis of the microbial metabolome by isotope dilution mass spectrometry using uniformly C-13-labeled cell extracts as internal standards. *Analytical Biochemistry* **336** (2): 164-171.

Zangirolami TC, Johansen CL, Nielsen J, Jørgensen SB. 1997. Simulation of penicillin production in fed-batch cultivations using a morphologically structured model. *Biotechnology and Bioengineering* **56** (6): 593-604.

List of publications

Douma RD, Batista JIM, Touw KM, Kiel JAKW, Krikken AM, Zhao Z, Veiga dos Inocentes T, Klaassen P, Bovenberg RA, Daran J, Heijnen JJ, Van Gulik WM. Degeneration of penicillin production in ethanol limited chemostat cultivation of *Penicillium chrysogenum*: A systems biology approach (manuscript in preparation).

Van Gulik WM, Canelas AB, **Douma RD**, De Jonge LP, Heijnen JJ. Fast sampling of the cellular metabolome. In: Methods in Microbial Biology. Berlin: Springer (book chapter in preparation).

De Jonge LP, **Douma RD**, Heijnen JJ, Van Gulik WM. Prevention of metabolite leakage for quantitative metabolomics in *Penicillium chrysogenum* (manuscript in preparation).

Douma RD, Deshmukh AT, De Jonge LP, De Jong BW, Seifar RM, Heijnen JJ, Van Gulik WM. Novel insights in transport mechanisms and kinetics of phenylacetic acid and penicillin-G in *Penicillium chrysogenum* (submitted for publication).

Douma RD*, de Jonge LP*, Jonker CTH, Seifar RM, Heijnen JJ, van Gulik WM. 2010. Intracellular metabolite determination in the presence of extracellular abundance: application to the penicillin biosynthesis pathway in *Penicillium chrysogenum*. *Biotechnology and Bioengineering* **107** (1): 105-115.
* These authors contributed equally to this work.

Douma RD, Verheijen PJT, De Laat WTAM, Heijnen JJ, van Gulik WM. 2010. Dynamic Gene Expression Regulation Model for Growth and Penicillin Production in *Penicillium chrysogenum*. *Biotechnology and Bioengineering* **106** (4): 608-618.

Gidijala L, Kiel JA, **Douma RD**, Seifar RM, van Gulik WM, Bovenberg RA, Veenhuis M, van der Klei IJ. 2009. An engineered yeast efficiently secreting penicillin. **PLoS One 4** (12): e8317.

Cellmer T, **Douma R**, Huebner A, Prausnitz J, Blanch H. 2007. Kinetic studies of protein L aggregation and disaggregation. *Biophys Chem* **125** (2-3): 350-359.

Hoekema S, **Douma RD**, Janssen M, Tramper J, Wijffels RH. 2006. Controlling light-use by *Rhodobacter capsulatus* continuous cultures in a flat-panel photobioreactor. *Biotechnology and Bioengineering* **95** (4):613-626.

Curriculum vitae

Rutger Dirk Douma was born in Sittard, The Netherlands on the 4th of November of 1981. After completing his gymnasium high school education at Trevianum Gymnasium in Sittard in 2000, he started with the BSc and MSc Biotechnology program at Wageningen University, the Netherlands. He performed a 5 months BSc thesis project at the organic chemistry department on “YEH-catalyzed epoxide hydrolysis towards the synthesis of enantiopure lactones” under supervision of dr. C.A.G.M. Weijers and dr. M.C.R. Franssen. During the MSc program he specialized in process engineering and obtained international experience by performing a 5 months internship on “Kinetic studies of protein L aggregation and disaggregation” at the Department of Chemical Engineering of UC Berkeley, USA under Supervision of dr. T.L. Cellmer, prof. dr. H.W. Blanch and prof. dr. J.M. Prausnitz. He conducted his 6 months MSc thesis project on "Optimization of hydrogen production in a flat plate photobioreactor" at the Food- and Bioprocess Engineering Group under Supervision of ir. S. Hoekema, prof. dr. ir. R.H. Wijffels and prof. dr. ir. J. Tramper.

After receiving his MSc diploma in 2005, he started as a PhD student in the bioprocess technology group of dr. W.M. van Gulik and prof. dr. ir. J.J. Heijnen at Delft University of Technology, the Netherlands in 2006. He studied regulation, degeneration and transport aspects of penicillin biosynthesis in *Penicillium chrysogenum*. The most interesting results of this project can be found in this thesis.

In September 2010, Rutger started working as scientist for fermentation process development at Novozymes in Bagsværd, Denmark.

Acknowledgements

After all these years of hard and persistent work it is a pleasure to finally write this last (and probably most-read) chapter of my thesis. I realize that I would never have made it to this chapter without the help and support of many others, which makes it even nicer to write it.

First of all, I would like to thank Sef, my promotor. You are such a friendly and pleasant person to work with and I really appreciate your eternal patience and dedication to your students. It is very rewarding to work with a supervisor who regards the scientific development of the student as the main product of his supervision, rather than the number of produced papers. I learned a lot from you and enjoyed the scientific freedom you gave me. Secondly, I would like to thank Walter, my copromotor, for the very nice cooperation during these last 4 years. Your critical and systematic view greatly improved my work and my manuscripts. I admire the quality of your writing-style and hope that one day I'll be able to write like that as well. My gratitude also goes out to Peter for all the on- and off-science discussions we had together and the help you offered me with parameter estimation for my regulation model. I really like your way to put things in perspective (on- and off-science). Furthermore I would like to thank Wouter, who was initially involved as staff member of the BPT group and later as industrial partner via DSM. I find it remarkable how easily you come up with valuable comments and tips every time you saw one of my presentations.

Very stimulating in performing this project was the presence of critical mass in the form of other PhD students working with *Penicillium chrysogenum*, the 'pen-clan'. Lodewijk and Zheng, thanks for the numerous discussions we had about our beloved (and sometimes behated) fungus and all the fun time we spent! Very memorable was our two week road-trip in Mexico, which was by far the most scientific vacation I ever had and it was interesting to find out that the tequila factory we visited does not have a strain improvement program, room for improvement! Furthermore, I want to thank Roelco for being my unofficial mentor in my first year and Amit for the pleasant cooperation we had on the transport paper. André, you were officially not involved with *Penicillium*, but you seemed to be

involved with every project which was going on within 200 m of your office. Thanks for all practical and theoretical advice!

Part of the work presented in this thesis was performed by some excellent and very motivated students. In order of appearance I would like to thank Joana, Caspar, Kai, Bouke, Maurice and Sijbren for your contributions to this booklet and the pleasant cooperation we had.

A very nice aspect of working with an industrial partner was the possibility to discuss our results with experts from DSM, the University of Groningen and the Industrial Microbiology Group of TU Delft. It's always interesting to get comments from coworkers with a different background and this offered me a different perspective on my work. Concrete examples of what this cooperation led to were the measurements of intracellular metabolites in penicillin producing *Hansenula polymorpha* and the measurement of pen enzyme amounts and pen cluster copy numbers in my degenerating cultures. I want to thank Denise, Najat, Paul, Rémon, Roel and Wouter from DSM, Andriy, Annemarie, Arnold, Hazrat, Ida, Jan, Jeroen, Loknath, Łukasz, Magda, Marta and Marten from the University of Groningen and Andreas, Diana, Ishtar, Jack, Jean-Marc, Marta, Tânia and Zita from IMB for all input, discussions and meetings! Martijn, thanks for the help with the pen-proteomics. Hopefully our data can be used some day!

Key in all the successes of our lab is the quality of our analytical team. I want to thank Angie, Cor, Jan, Johan and Zhen for handling the vast flow of samples which were sent to you. I especially want to thank Reza for the numerous pen samples you analyzed for me scheduled or unscheduled. Susan, thanks for helping me to start working in the lab and Dirk, Mario and Rob for making sure that I could keep working in the lab. A special thanks goes out to the 'aio-hamer' for maintaining a continuous motivation to keep a high quality standard in my lab work; without you I would still be stuck in experiment number 1! Also I really appreciate all the help from Apilena and Astrid to get my media and reactors sterile, all the help with pH and DO probes and for providing me with all kind of back-up materials when we ran out of stock. And certainly I should thank Sjaak. Without you the Kluyver building would simply not function!

A very successful collaboration was the one with Carol, Jean-Paul, Joost, Sander, Yang and Zheng on organizing the Biotour to China. Next to the great scientific and non-scientific

time we spent in China, I had a lot of fun organizing it and the term ‘survival of the fittest’ got a complete new meaning to me while eating with chop sticks in Chinese restaurants!

Not only was the BPT group a great place to work in on the scientific level, also on a personal level I always had a great time. I want to thank Aljoscha, Amit, André, Annette, Angie, Bouke, Cor, Daphne, Dirk, Domenico, Caspar, Chiara, Elaheh, Emrah, Frederik, Hilal, Jan, Jenifer, Jenny, Joana, Johan, Kai, Katelijne, Klaas, Kristel, Lodewijk, Luísa, Marco, María, Marilia, Mario, Marjan, Mehmet, Michiel, Mlawule, Nanette, Nathalie, Penia, Peter, Reza, Rob, Rob, Roeland, Roelco, Sef, Sergio, Stefan, Susan, Tjerko, Uly, Walter, Wouter, Zhen, Zheng and everybody I forgot for all scientific advise, the companionship and the fun we had!

Except for my first week I spent my entire PhD career in one single office, simply because it was so nice! Aljoscha, Elaheh, Marija, Marjan, Nannette, Penia, Rob, Roelco and Sreekanth thanks for sharing the office with me! A nice aspect of our office was that it is so close to the coffee room. Adrie, Aljoscha, Camilo, Çağri, Carol, Corjan, Elaheh, Erica, Katelijne, Kawieta, Lodewijk, María, Marija, Marjan, Marloes, Nannette, Penia, Peter, Rob, Roelco, Rosario thanks for keeping my mental health on an (at least for me) acceptable level by providing some nonsense in between the science! Furthermore I want to thank all the “football for nerds” lads for our outstanding sportive performances and all the “flush it in” poker players for their steady contributions to my financial situation! A special thanks goes out to Carol for all the support and care throughout these years.

The Kluyver lab has an exceptionally nice environment. Next to the already-mentioned, I want to thank Arjan, Arjen, Arno, Beckley, Eline, Erik, Esteban, Geert, Ger, Gini, Han, Hans, Herman, Ines, Jasper, Janine, Jolanda, Joost, Jos, Katja, Kedar, Leon, Leonie, Lies, Loesje, Lucie, Marcel, Margarida, Mark, Marlies, Max, Merle, Mervin, Peter, Raymon, Rintze, Robert, Ronald, Stef, Stefan, Tangir, Ton, Victor, Wouter, Wouter and Xiaonan for creating this!

Although I know you think it’s ridiculous to end up in these acknowledgements I do want to thank all my family for all the love and support. Also thanks to all my friends for being my friends! A special thanks goes out to Joris for designing the cover. Lastly, I want to thank Carla. I can’t imagine having done this without you, just as I can’t imagine a life without you. Thanks for all the care, love, support and companionship during these years. Now on to our next adventure: Copenhagen!